



UNIVERSITÀ DI FOGGIA
*Dipartimento di Scienze Agrarie,
degli Alimenti e dell'Ambiente*

*Doctoral Thesis in
Management of Innovation in the Agricultural and Food
Systems of the Mediterranean Region
– XXVI cycle –*

**Use of Titanium Oxide (TiO₂) to
Decompose Ethylene During
Storage of Horticultural Crops**

Candidate:

Maria Lucia Valeria de Chiara

Tutor:

Prof. Giancarlo Colelli



UNIVERSITÀ DI FOGGIA
*Dipartimento di Scienze Agrarie, degli
Alimenti e dell'Ambiente*

***Doctorate Course in 'Management of Innovation in the
Agricultural and Food Systems of the Mediterranean
Region' – XXVI cycle –***

**Doctoral thesis on 'Use of Titanium Oxide (TiO₂) to
Decompose Ethylene During Storage of Horticultural
Crops', discussed at the Università di Foggia, April 11, 2014**

Candidate:

Maria Lucia Valeria de Chiara

Tutor:

Prof. Giancarlo Colelli (*Università di Foggia, Italy*)

Committee members:

Dott. Domenico Carlucci (*Università degli Studi di Bari, Dip.to di
Scienze Agro-Ambientali e Territoriali, Italy*)

Prof. Salvador Castillo García (*Universidad Miguel Hernández,
Spain*)

Prof. Kevin D. Sinclair (*University of Nottingham, School of
Biosciences, United Kingdom*)

Use of Titanium Oxide (TiO₂) to Decompose Ethylene during Storage of Horticultural Crops

Contents

Abstract	8
Part One - General	
1. Ethylene (C ₂ H ₄)	11
1.1. Ethylene effect on fruit and vegetable	16
1.2. Ethylene in postharvest technology	21
1.3. Strategies to prevent ethylene effects	22
1.3.1. Inhibition of synthesis (AVG, AOA)	24
1.3.2. Inhibition of action (1-MCP)	24
1.3.3. Removal	26
1.3.3.a) Chemical methods	27
- <i>Potassium permanganate (KMnO₄)</i>	27
- <i>Palladium (Pd)</i>	28
1.3.3.b) Physical methods	29
- <i>Catalytic oxidizers</i>	29
- <i>Adsorption</i>	30
1.3.4. Photocatalysis	31
1.3.4.1. Types of photocatalysis	31
- <i>Homogeneous photocatalysis</i>	31
- <i>Heterogeneous photocatalysis</i>	32
2. Titanium Oxide (TiO ₂) photocatalysis	34
2.1. Mechanism of action	35
2.1.1. Photocatalytic degradation of organic compounds	38
2.1.2. Antimicrobial activity	40
Part Two - Experimental	
1. Introduction	43

1.1.	Use of titanium oxide during storage of horticultural crops	43
1.2.	Photocatalytic materials	44
1.3.	Fluidized bed photoreactor	45
2.	General objectives	47
3.	Materials and Methods	49
3.1.	Design of photocatalytic reactor in laboratory scale	49
3.2.	TiO ₂ powder synthesis	49
3.3.	Ethylene detection	50
3.4.	Evaluation of photocatalytic activity	50
3.5.	Experimental setup	50
3.6.	Statistical analysis	51
4.	Comparison of photocatalytic properties of different titanium oxide-based materials	52
4.1.	Materials and Methods	52
4.2.	Experimental setup	52
4.3.	Results and Discussions	53
5.	Study of mesoporous mixed SiO ₂ /TiO ₂ nanocomposites photocatalytic activity	62
5.1.	Materials and Methods	62
5.2.	Experimental setup	63
5.3.	Results and Discussions	64
6.	Ethylene reduction efficacy of photocatalytic mixed SiO ₂ /TiO ₂ nanocomposites and effects on ripening of mature-green tomatoes	72
6.1.	Materials and Methods	72
6.2.	Experimental setup	73
6.3.	Results and Discussions	74
7.	Design of a fluidized bed photoreactor for ethylene oxidation on mesoporous mixed SiO ₂ /TiO ₂ nanocomposites under UV-A illumination	81
7.1.	Fluidized bed photoreactor and fluidization regimes	81
7.2.	Materials and Methods	83
7.2.1.	Design of fluidized bed reactor prototype	83
7.2.2.	Fluidization tests	87

7.2.3.	Fluidized bed photoreactor activity evaluation	87
7.3.	Results and Discussion	88
8.	General conclusions	93
	<i>References</i>	96

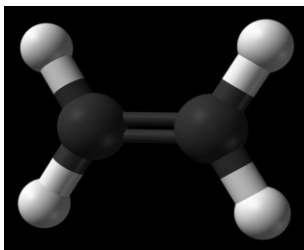
Abstract

Ethylene (C_2H_4) is a naturally occurring substance that acts as plant hormone on many horticultural and ornamental crops. It accelerates senescence, stimulates chlorophyll loss, enhances excessive softening, promotes discoloration and browning. These effects could be beneficial or detrimental, depending on the degree of quality changes on fruits and vegetables tissues. Among the techniques used to remove or inhibit ethylene action during postharvest handling of fresh products (potassium-based system, high temperature catalytic oxidation, inhibition of ethylene receptor), the use of titanium oxide (TiO_2)-based materials with photocatalytic activity under UV light is one of the most promising. Use of TiO_2 may represent an innovation in the postharvest field, due to its high oxidizing capacity, low cost and non-toxicity. In this study several materials were synthesized and tested for photocatalytic activity, and mesoporous mixed SiO_2/TiO_2 nanocomposite (80% of TiO_2 and 20% of SiO_2) showed the best light-dependent oxidant activity resulting in its complete elimination from the atmosphere in a closed system. Ethylene reduction rate increased when the contact time between C_2H_4 and the photocatalyst was prolonged. Mature green tomatoes were exposed to ethylene-enriched atmosphere mixture treated or not with SiO_2/TiO_2 and UV light. Photocatalytical destruction of ethylene by titanium oxide resulted in a slower ripening trend of the tomato berries as showed by pericarp reduced color evolution. The developed material would be suitable for postharvest handling of whole or fresh-cut fruits and vegetables in order to prolong their shelf-life. To decompose ethylene in storage room atmosphere, a fluidized bed photoreactor was designed and the relative prototype was manufactured. Its functionality was tested with different support material and actual photocatalytic activity was tested using SiO_2/TiO_2 -coated alumina microspheres. A reduction of about 70% of ethylene concentration in the tested gas mixture was observed. However, the fluidization regime caused strong collisions between the coated microparticles causing a tendency of the coated powdered photocatalytic material to separate from its support that causing a progressive partial blocking of the reactor filters which resulted in a reduced flow rate and lower bed height. Hence a need to better refine photoreactor efficiency, in order to make it suitable for use in presence of possibly high quantity of powder separating from its support due to unavoidable collisions during the fluidization state.

Part one - General

1. Ethylene

Ethylene is a naturally occurring plant growth substance that has numerous effects on many horticultural and ornamental crops at part-per-million (ppm) and part-per-billion (ppb) concentrations (1 ppm equals 6.5×10^9 M at 25 °C). It is a hydrocarbon with the formula C_2H_4 or $H_2C=CH_2$. It is a colorless flammable gas with a "sweet and musky" odor when pure (Booth and Campbell, 1926). Ethylene is the simplest alkene (a hydrocarbon with carbon-carbon double bonds), and the simplest unsaturated hydrocarbon after acetylene (C_2H_2). It is widely used in chemical industry, and its worldwide production exceeds that of any other organic compound. This hydrocarbon has four hydrogen atoms bound to a pair of carbon atoms that are connected by a double bond. All six atoms that comprise ethylene are coplanar. The H-C-H angle is 117.4° , close to the 120° for ideal sp^2 hybridized carbon. The molecule is also relatively rigid: rotation about the C-C bond is a high energy process that requires breaking the π -bond. The π -bond in the ethylene molecule is responsible for its useful reactivity. The double bond is a region of high electron density, thus it is susceptible to attack by electrophiles. Many reactions of ethylene are catalyzed by transition metals, which bind transiently to the ethylene using both the π and π^* orbitals. Being a simple molecule, ethylene is spectroscopically simple.



Ethylene structure

In higher vascular plants, the biosynthetic pathway that produces C₂H₄ takes origin from “Yang” cycle (Figure 1.1). The biochemistry and regulation of ethylene biosynthesis as well as its perception and signaling have been subjects of intensive study in plant hormone physiology during the last decades (Kende, 1993; Solano and Ecker, 1998; Stepanova and Ecker, 2000; Argueso *et al.*, 2007; Stepanova and Alonso, 2009). Major breakthroughs in the ethylene synthesis pathway were the establishment of *S*-adenosylmethionine and 1-amino-cyclopropane carboxylic acid (ACC) as the precursors of ethylene by Yang and Hoffman (1984). Subsequently, the enzymes that catalyze these reactions (ACC synthase and ACC oxidase) were characterized and purified using biochemistry approaches. The molecular cloning of the ACC synthase (Sato and Theologis, 1989) and ACC oxidase (ACO) (Hamilton *et al.*, 1991; Spanu *et al.*, 1994) genes led to the demonstration that these enzymes belong to a multigene family and are regulated by a complex network of developmental and environmental signals responding to both internal and external stimuli (Johnson and Ecker, 1998; Wang *et al.*, 2002). These discoveries have led to a growing understanding of the mechanisms of action and regulation of ethylene. Both the synthesis and action of C₂H₄ involve complicated metabolic processes.

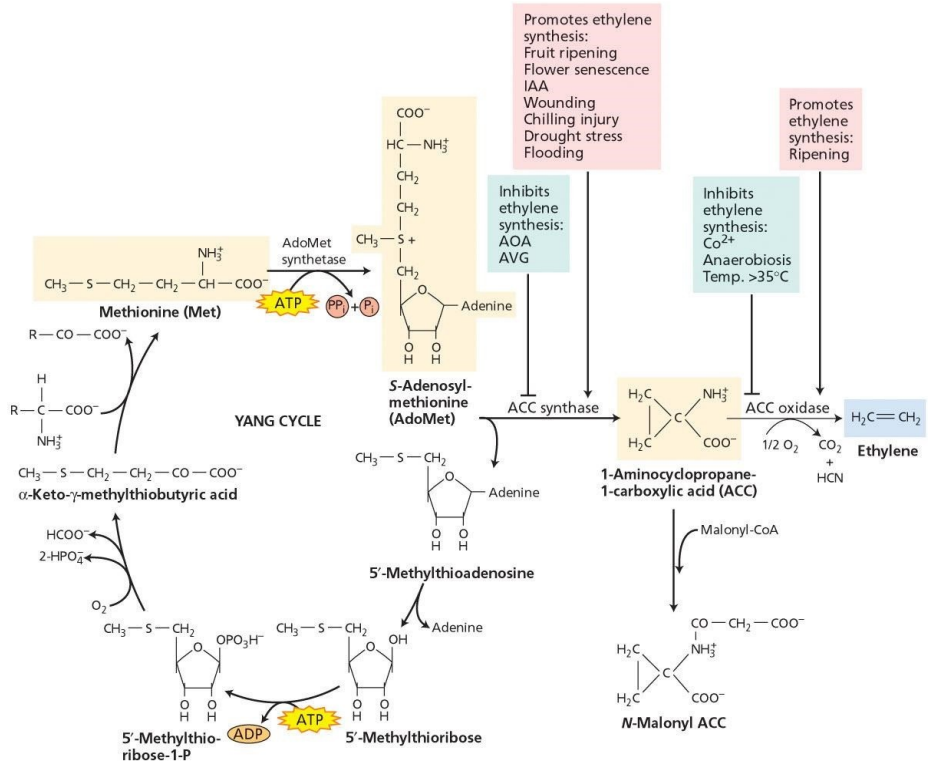


Figure 1.1. Biosynthesis of ethylene in higher vascular plants (“Yang cycle”). Some of the intrinsic and extrinsic factors that promote or inhibit ethylene synthesis. (from Tiaz and Zeiger, 2002).

The amino acid methionine (Met) is the starting point for synthesis. It is converted to *S*-adenosyl methionine (AdoMet) by the addition of adenine, and AdoMet is then converted to 1-amino-cyclopropane carboxylic acid by the enzyme ACC synthase. ACC synthase belongs to a family of proteins that require pyridoxal-5'-phosphate (PLP) as cofactors, known as PLP-dependent enzymes (Argueso *et al.*, 2007). ACC synthase converts AdoMet into ACC through a β,γ carbon elimination reaction (Li *et al.*, 2005). The production of ACC is often the controlling step for C₂H₄ synthesis. A number of intrinsic (e.g. developmental stage) and extrinsic (e.g. wounding) factors influence this pathway (Yang, 1987). The pool of ACC available for C₂H₄ production can be increased by factors which increase ACC synthase activity, reduced by application of growth regulators (e.g. daminozide), or reduced

by a side reaction which forms the relatively biologically inert malonyl-amino-cyclopropane carboxylic acid (*N*-Malonyl ACC). In the final step, ACC is oxidized by the enzyme ACC oxidase (ACO) to form C₂H₄. Ethylene synthesis is inhibited (negative feed-back inhibition) by C₂H₄ in vegetative and immature climacteric and non-climacteric reproductive tissue and is promoted (positive feed-back promotion, or autocatalytic) by C₂H₄ in reproductive climacteric tissue. (Saltveit, 1999; Wang *et al.*, 2002). This oxidation reaction requires the presence of oxygen, and low levels of carbon dioxide activate ACC oxidase. While the level of ACC oxidase activity is usually in excess of what is needed in most tissues, it can show a dramatic increase in activity in ripening fruit and in response to C₂H₄ exposure. In conditions of high ethylene production, such as ripening fruit, ACO is often the rate-limiting step in biosynthesis. ACO belongs to a family of mononuclear, non-heme iron enzymes (Hegg and Que, 1997). ACC is converted to ethylene by a modification of carbons C-2 and C-3 of ACC, whereas C-1 is converted to cyanide, and the carboxyl group is converted into carbon dioxide (Peiser *et al.*, 1984). There are two classes of horticultural produce in terms of respiration and ethylene production patterns during maturation and ripening. There are climacteric products, mainly represented by fruit that produce a burst of ethylene as they ripen, as well an increase in respiration, and there are the non-climacteric products that do not increase ethylene production when they ripen. Climacteric fruits typically ripen by softening significantly (Haji *et al.*, 2003; Hiwasa *et al.*, 2003), by changing color (Flores *et al.*, 2002) and by becoming sweeter producing aromas (Rupasinghe *et al.*, 2000; Alexander and Grierson, 2002; Flores *et al.*, 2002). All these changes are strongly dependent on C₂H₄ production; examples are bananas and nectarines. Conversely, non-climacteric fruits do not change significantly after harvest. Horticultural commodities classified according to their ethylene production rates are reported in Table 1.1. There is no consistent relationship between the C₂H₄ production capacity of a given commodity and its perishability; however, exposure of most commodities to ethylene accelerates their senescence (Kader, 2002).

Table 1.1. Classification of horticultural commodities according to ethylene production rates
(from Kader, 2002)

<i>Class</i>	<i>Range at 20°C ($\mu\text{l/kg hr}$)</i>	<i>Commodities</i>
Very low	Less than 0.1	Artichoke, asparagus, cauliflower, cherry, citrus fruits, grape, jujube, strawberry, pomegranate, leafy vegetables, root vegetables, potato, most cut flower
Low	0.1-1.0	Blackberry, blueberry, casaba melon, cranberry, cucumber, eggplant, okra, olive, pepper, persimmon, pineapple, pumpkin, raspberry, tamarillo, watermelon
Moderate	1.0-10.0	Banana, fig, guava, honeydew melon, lychee, mango, plantain, tomato
High	10.0-100.0	Apple, apricot, avocado, cantaloupe, feijoa, kiwifruit (ripe), nectarine, papaya, peach, pear, plum
Very high	More than 100.0	Cherimoya, mammee apple, passion fruit, sapote

For these products, two distinct ethylene biosynthesis systems have been described. *System 1* corresponds to low ethylene production in the pre-climacteric period of climacteric fruit and is also present throughout the development and ripening of non-climacteric fruit. Conversely, *system 2* refers to an auto-stimulated massive ethylene production, called ‘autocatalytic’ synthesis (Barry *et al.*, 2000; Giovannoni, 2001; Alexander and Grierson; 2002; Argueso *et al.*, 2007) and is specific to climacteric fruit. This positive feedback loop for ethylene biosynthesis is proposed to integrate ripening of the entire fruit once it has started. It is promoted by the ethylene synthesized by the cell. Therefore, the major differences related to ethylene between climacteric and non-climacteric fruit are the presence or absence of autocatalytic ethylene production (Bouzayen *et al.*, 2009, Bapat *et al.*, 2010). Apart from increases in ethylene production associated with the traumas of harvesting or processing for fresh-cut, endogenous ethylene levels are maintained at low levels by negative feedback, and endogenously produced ethylene probably has minimal effect on the postharvest quality of vegetables and non-climacteric fruit (Saltveit, 2005).

1.1 Ethylene effects on fruit and vegetables

Ethylene regulates many aspects of growth, development and storage life of fresh produce (Abeles *et al.*, 1992). There are some significant interactions between the plant and its environment that are important in understanding how C_2H_4 exerts its action on plant tissues (Figure 1.1.1). Abiotic and biotic stresses, as well as the same C_2H_4 biosynthesis and the atmospheric ethylene from smoke, exhaust gases, pollution, compressed C_2H_4 gas, C_2H_4 releasing chemicals (e.g. ethephon), catalytic production of C_2H_4 from ethanol, and C_2H_4 analogues produced by a variety of processes (Saltveit, 1999) can stimulate vegetal tissues to synthesize ethylene and cause plant response.

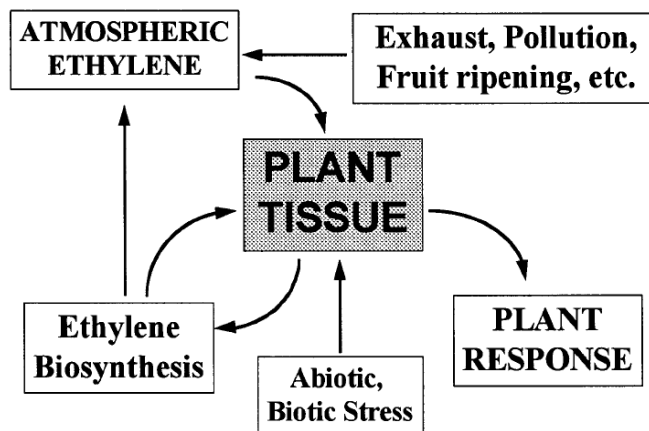


Figure 1.1.1. Ethylene interactions with the plant and its environment (from Saltveit, 1999).

Plant sensitivity to endogenous C_2H_4 changes during its development, as does its rate of synthesis and loss by diffusion from the plant. In terms of growth, ethylene is associated with the regulation of cell size, often restricting cell elongation, but it can also regulate cell division. Instead, in terms of development ethylene is most commonly considered an ‘aging’ hormone, as it accelerates and is required for such processes as ripening, senescence, and abscission. However, ethylene has regulatory roles on development throughout the life cycle of the plant. It stimulates root

initiation in many plant species, controls the formation of root nodules in legumes, inhibits the formation of such storage organs as tubers and bulbs, promotes flowering in some species (but inhibits it in others), and induces the production of female rather than male flowers in cucurbits (Schaller, 2012).

Fruit ripening is characterized by several metabolic and physiological processes that cause softening of the fruit flesh, changes in the synthesis and excretion of surface waxes, change in color (loss of chlorophyll and synthesis of yellow and red pigments), changes in aroma and flavor (conversion of starch to sugar, decreases in acidity, production of aroma and flavor volatiles, polymerization of tannins) (Reid, 2002) and ethylene has variable effects on each of these changes.

Much of what is known about the effects of C_2H_4 on the ripening and quality of fresh fruits and vegetables has been slowly amassed since the 1920s, and needs constant updating. Considerable evidences at the physiological, biochemical, and molecular levels have been accumulated, indicated ethylene mediated regulation of ripening at different levels. This includes ethylene biosynthesis and its perception by the target cells through receptors (ETRs), signal transduction cascade involving both positive and negative regulators (CTR, EIN2, EIN3 etc.) and finally regulation of target gene expression by transcription factors such as ethylene response factors (ERFs) (Bapat *et al.*, 2010). This mechanism has been depicted in Figure 1.1.2. The target gene or set of genes which control fruit firmness, taste, color and aroma are regulated by specific set of genes which in turn may be regulated by a single or set of transcription factors (Nath *et al.*, 2007).

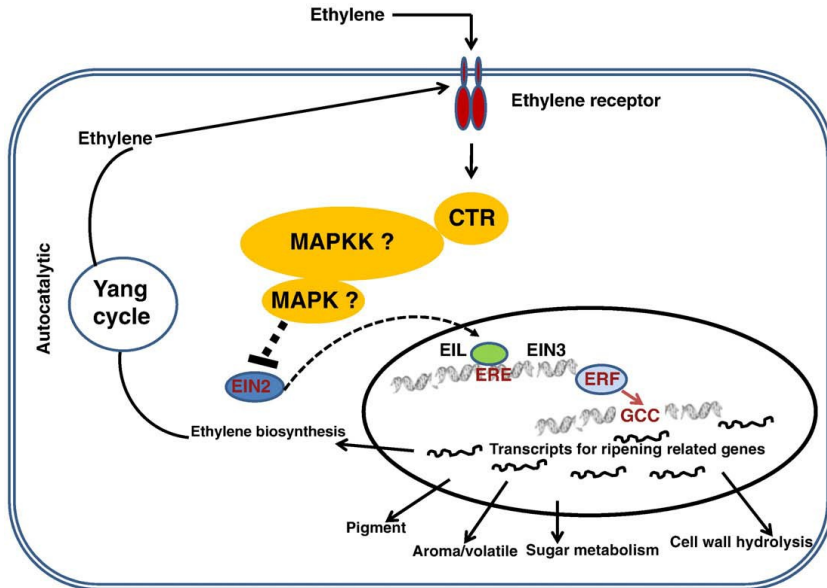


Figure 1.1.2. Ethylene reception pathway (from Bapat *et al.*, 2010).

Table 1.1.1. Plant responses to ethylene (from Saltveit, 1999)

Ethylene stimulates

Synthesis of C₂H₄ in ripening climacteric fruit.

Ripening of fruit.

Pigment (e.g. anthocyanin) synthesis.

Chlorophyll destruction and yellowing.

Seed germination.

Adventitious root formation.

Respiration.

Phenylpropanoid metabolism.

Flowering of bromeliads.

Abscission.

Senescence.

Ethylene inhibits

Ethylene synthesis in vegetative tissue and non-climacteric fruit.

Flower development in most plants.

Auxin transport.

Shoot and root elongation (growth).

Normal orientation of cell wall microfibrils.

The responses to endogenously produced or exogenously applied C₂H₄ are therefore numerous and varied, and they are reported in Table 1.1.1.

Depending on the extent of fruits and vegetables quality changes and on the type of product effects could be beneficial or detrimental (Table 1.1.2). For example, effects that are viewed as beneficial include the promotion of flowering in pineapple (*Ananas comosus*) and the hastening of ripening in tomato (*Lycopersicon esculentum*) and melons (*Cucumis melo*). Effects that are viewed as deleterious include the abortion of flowers and the development of russet spotting in lettuce (*Lactuca sativa*). Often the same response (e.g. acceleration of chlorophyll loss, promotion of ripening, or stimulation of phenylpropanoid metabolism) is viewed as beneficial in some crops (e.g. de-greening of citrus, ripening of climacteric fruit, and stimulating defenses against pathogens) and detrimental in others (e.g. yellowing of green vegetables, excessive softening of fruit, or browning of lettuce; Table 1.1.2).

Table 1.1.2. Examples of how the same ethylene response can be beneficial in one system and detrimental in another (from Saltveit, 1999)

<i>Example of benefit</i>	<i>Ethylene response</i>	<i>Example of detriment</i>
Degreening of citrus	Accelerates chlorophyll loss	Yellowing of green vegetables
Ripening of climacteric fruit	Promotes ripening	Overly soft and mealy fruit
Defense against pathogens	Stimulates phenylpropanoid metabolism	Browning and bitter taste

The introduction of new cultural practices, cultivars, harvest and handling methods, postharvest treatments, consumer products and packaging influence the effect that C₂H₄ could have on quality attributes. Continued research in these areas, provides the foundation upon which the commercial agricultural use of C₂H₄ is based.

On the basis of this knowledge it is clear that exposure of plant tissues to ethylene causes changes in their physiology. Harvested fruits and vegetables may be intentionally or unintentionally exposed to biologically active levels of ethylene.

Both endogenous and exogenous sources of ethylene contribute to its biological activity. Ethylene synthesis and sensitivity are enhanced during certain stages of plant development, as well as by a number of biotic and abiotic stresses. Exposure may occur inadvertently in storage or transit from atmospheric pollution or from ethylene produced by adjacent crops. Intentional exposure is primarily used to ripen harvested fruit. Once the ripening of climacteric fruit has started, the internal C₂H₄ concentration quickly increases and exogenous application of C₂H₄ has no further effect in promoting ripening. Similarly, reducing the external concentration of C₂H₄ around bulky fruit (e.g. apples (*Malus domestica*), bananas (*Musa* spp.), melons and tomatoes) has almost no effect on reducing the internal concentration in these ripening climacteric fruit because of the large diffusion resistance of their skin and flesh. In these fruit, the rate of production exceeds the rate of diffusive losses until a quite high level is reached. Internal C₂H₄ concentration can exceed 100 µl l⁻¹, even when the external concentration is zero (Saltveit, 1999). Other gaseous chemicals are analogs of C₂H₄ (propylene, carbon monoxide, acetylene, 1-butene) and can elicit the same physiological effects as C₂H₄, but often much higher concentrations are required to produce the same effect (Abeles *et al.*, 1992). The response of the tissue to C₂H₄ exposure depends on the sensitivity of the tissue, concentration of C₂H₄, composition of the atmosphere, duration of exposure, and temperature.

Ethylene production is promoted by stresses such as chilling (Wang, 1990) and wounding (Abeles *et al.*, 1992), and this stress-induced C₂H₄ can enhance fruit ripening. However, these stresses also induce other physiological changes (e.g. enhanced respiration and phenylpropanoid metabolism) and it is not easy to understand whether it is the stress per se or one of the stress-induced changes (e.g. stimulated C₂H₄ production) that is producing the effect. In the case of lettuce, and probably in most vegetative tissues, sub-lethal levels of stress only induce transitory increases in C₂H₄ production, which have minimal lasting effects. In climacteric fruit tissue, stress-induced C₂H₄ can have a significant and protracted effect.

1.2 Ethylene in postharvest technology

Ethylene is frequently used in pre- and postharvest technology, due to the utility of this growth regulator in regulate and standardize growth, development and ripening phases of many horticultural crops. An example could be the wide range of approved uses for Ethephon (an ethylene-releasing chemical) in agriculture to promote several benefits such as fruit thinning (apples, cherries), fruit loosening prior to harvest (nuts), color development (apples), postharvest de-greening of citrus, flower induction (pineapples) and it can stimulate lateral branching in potted plants (azaleas and geraniums) taking advantage of the C₂H₄ various effects such as fruit ripening, fruit removal, defoliation, fruit loosening, maturity or color development, de-greening, dehiscence, leaf curing, flower induction, sex expression, flower bud development, plant height control, stimulate lateral branching (Reid, 2002). Fruit ripening is by far the largest application of ethylene gas in postharvest technology (Reid, 2002). The application of ethylene at a controlled rate means that these products can be presented to the customer as “ready to eat”. Stimulation of ripening by ethylene of fruit picked mature but unripe is commercially practiced for a number of fruit including avocado (*Persea Americana* Mill.), banana, pear and tomato (Gross *et al.*, 2004). The postharvest life of these fruit is greatly extended by harvest prior to the tree-ripe stage as unripe fruit, allowing them to react to commercial harvest, handling, storage and distribution systems much better than tree-ripe fruit (Forney *et al.*, 2009). Fruit and fruit type vegetables are ripened artificially in specially built rooms that must be gas tight, have systems for controlling temperature and relative humidity. Ethylene concentration inside the ripening room should be maintained at 100 to 150 ppm with sufficient air circulation. The flow-thru system is the most efficient and economical method for initiating ripening (Dhall, 2013). This kind of ripening rooms are often used for tomatoes, citrus fruits and bananas. In these cases the use of diluted ethylene gas mixtures is safer than using pure ethylene which is explosive and flammable at concentrations of 3% or higher. For example, for tomatoes,

technical grade ethylene gas is introduced into the room at a concentration of about 100 ppm for about 48 hours (Kitinoja and Kader, 2002).

However, the presence of ethylene is not always beneficial in terms of postharvest life of whole or minimally processed fruits and vegetables. In fact, as previously reported, C₂H₄ is responsible for a variety of effects. It accelerates senescence, stimulates chlorophyll loss, enhances excessive softening, stimulates sprouting, promotes abscission of leaves and flowers, stimulates phenylpropanoid metabolism, promotes discoloration and browning and hastens toughening (Saltveit, 1999). All the reported effects are not desirable during postharvest handling and should be avoided.

Furthermore, fresh and minimally processed produce are usually stored at low temperatures. This could enhance chilling injury (CI) development (Megías *et al.*, 2014). The involvement of ethylene in CI is not clear but in several climacteric and non-climacteric fruits, external treatments with either ethylene or ethylene inhibitor are able to induce or alleviate, respectively, CI in pineapples (Selvarajah *et al.*, 2001), avocado (Pesis *et al.*, 2002), loquat (Cai *et al.*, 2006) and plum (Candan *et al.*, 2008).

Several chemical and/or physical methods could be used to prevent C₂H₄ negative effects. Following, a brief description of the main strategies used to prevent ethylene effects during storage of whole or minimally processed horticultural products.

1.3 Strategies to prevent ethylene effects

Commercial strategies and best practices for the management of fresh horticultural products are based on avoiding exposure to ethylene and attempting to minimize ethylene production and action during ripening, harvest, storage, transport and handling by temperature and atmosphere control (Watkins, 2002). The control of ethylene is an important component in postharvest management and the strategies used to protect fruits and vegetables from the negative outcomes of ethylene are based on avoidance, removal, and inhibition of its biosynthesis and/or action.

Removing the source of C_2H_4 from enclosed spaces such as cold room for postharvest storage of horticultural commodities is the best way to eliminate it. However, often this is impossible or uneconomical. In these cases dilution of C_2H_4 by adequate ventilation with clean outside air can minimize its effects. Where the air outside storage and handling areas is not polluted, ventilation can reduce ethylene concentrations without onerous costs. An exchange rate of one air change per hour can readily be provided by installing an intake fan and a passive exhaust (Reid, 2002). Ethylene production strongly depends on environmental conditions (temperature, O_2 and CO_2 concentrations surrounding the stored crops) (Schotsmans *et al.*, 2009). Since C_2H_4 exerts its effects through metabolic reactions, the use of modified or controlled atmospheres could be useful. Keeping the exposed tissue at their lowest recommended storage temperature will reduce the response to C_2H_4 . Following the Arrhenius model (Bisswanger, 2002), low temperatures slow down the activity of ACC synthase and oxidase. Similarly, reducing metabolism by reducing the oxygen concentration will mitigate the effects of exposure, as will keeping the duration of exposure to a minimum and adding C_2H_4 antagonists like carbon dioxide to the atmosphere (Lougheed, 1987). It is demonstrated that modified atmospheres (MA; usually represented by use of low oxygen and high carbon dioxide concentrations) generally reduce the respiration rate (Hertog *et al.*, 1998) and inhibit the onset of the autocatalytical increase of ethylene production (Kader, 1995). Low oxygen concentrations might reduce ethylene formation regulating its synthesis at the level of ACC oxidase, which requires oxygen to work (Kader, 1995). High carbon dioxide also reduces ethylene production. It possibly also acts by affecting the conversion from ACC to ethylene by ACC oxidase (de Wild *et al.*, 2003).

1.3.1. Inhibition of synthesis (AVG, AOA)

Inhibitors of ethylene synthesis such as aminoethoxyvinylglycine (AVG) and aminoxyacetic acid (AOA) could be used to avoid its negative effects on stored horticultural crops. These compounds effectively delay senescence of climacteric products by inhibiting the action of 1-aminocyclopropane-1-carboxylate synthase (ACCS). 1-aminocyclopropane-1-carboxylic acid synthase (ACC synthase, ACCS) (EC 4.4.1.14) is the enzyme that catalyzes the synthesis of 1-aminocyclopropane-1-carboxylic acid (ACC), a precursor for ethylene (Capitani *et al.*, 1999; Huai *et al.*, 2001; Zhang *et al.*, 2004). Therefore, ACC-synthase is the rate limiting step in ethylene synthesis. The mode of action by which an inhibitor of ethylene synthesis (e.g., AVG; [S]-*trans*-2-amino-4-(2-aminoethoxy)-3-butenoic acid hydrochloride) reduces the ripening of climacteric fruit is obvious since elevated internal levels of ethylene, produced by autocatalytic ethylene synthesis, are necessary for ripening of these fruit (Burg *et al.*, 1971; Abeles *et al.*, 1992; Saltveit, 1999; Saltveit, 2005). AVG is frequently used as a specific inhibitor of ethylene biosynthesis to determine the affects of ethylene on plant growth, development, and response to stress (Abeles *et al.*, 1992). Aminoxyacetic acid also can inhibit 1-aminocyclopropane-1-carboxylate synthase preventing ethylene synthesis, which can increase the vase life of cut flowers (Broun and Mayak, 1981; Zuliana *et al.*, 2008).

1.3.2. Inhibition of action

A new strategy for controlling ethylene and thus ripening and senescence of fruit, especially climacteric ones, as well as senescence of vegetative tissues, has emerged with the discovery and commercialization of the inhibitor of ethylene perception, 1-methylcyclopropene (1-MCP) (Watkins, 2006). It was shown to be a very effective inhibitor of ethylene action in ornamentals, fruits and vegetables (Reid, 2002). 1-MCP is a low-molecular-weight unsaturated hydrocarbon gas that readily diffuses through plant tissues. Plant tissues exposed to 1-MCP lose the capacity to respond to ethylene possibly due to a direct interaction between 1-MCP and ethylene

receptors (Sisler and Serek, 1997, 2003). 1-MCP is a cyclic alkene able to block ethylene action (Sisler and Serek, 1999, 2003; Sisler, 2006). 1-MCP interacts with ethylene receptors and thereby prevent ethylene-dependent responses in plant tissues (Sisler and Blankenship, 1996; Sisler and Serek, 1997, 2003). This gaseous inhibitor of ethylene perception is able to delay ripening and senescence of many horticultural products (Blankenship and Dole, 2003; Watkins, 2006; Huber, 2008). Some example: 1-MCP inhibits ethylene production, softening, and other ripening characteristics of apples during air and controlled atmosphere (CA) storage (Fan *et al.*, 1999; Rupasinghe *et al.*, 2000; Watkins *et al.*, 2000; Bai *et al.*, 2005); it is effective in delaying further ripening of partially ripe bananas (Pelayo *et al.*, 2003), also as fresh-cut produce (Vilas-Boas and Kader, 2006). 1-methylcyclopropene also affects, slowing it, softening of fresh-cut kiwifruit, mango and persimmon slices (Vilas-Boas and Kader, 2007). In minimally processed pineapple, 1-MCP decreased respiration, browning and hydrolysis of ascorbic acid (Buda and Joyce, 2003). Exposure to 1-methylcyclopropene extended the shelf life, reducing postharvest deterioration, retarding chlorophyll degradation, and delaying visual quality loss and flowering of fresh-cut broccoli raab florets (Cefola *et al.*, 2010). Effects of 1-MCP in delaying ripening of tomatoes was also studied (Colelli *et al.*, 2003; Amodio *et al.*, 2005; Cornacchia *et al.*, 2007).

The use of cyclopropenes to inhibit ethylene action was patented by Sisler and Blankenship in 1996 and a commercial breakthrough in 1-MCP application technology resulted from the formulation of 1-MCP as a stable powder in which it is complexed with γ -cyclodextrin. In this way, 1-MCP is easily released as a gas when the powder is dissolved in water. 1-MCP was approved by the Environmental Protection Agency (EPA) in 1999 for use on ornamentals, and was marketed as EthylBloc® by Floralife, Inc. (Walterboro, SC), while AgroFresh, Inc., a subsidiary of Rohm and Haas (Springhouse, PA), subsequently developed 1-MCP under the trade name SmartFresh™ and have global use rights for edible horticultural products. 1-MCP has a non-toxic mode of action, negligible residue and is active at very low concentrations, and by 2005 food use registration for the chemical had been obtained in 41 countries around the world including Argentina, Australia,

Brazil, Canada, France, Israel, Italy, Mexico, the Netherlands, South Africa, UK, and the US. Registered crops, which are specific to countries, include apple, apricot, avocado, kiwifruit, mango, melon, nectarine, papaya, peach, pear, pepper, persimmon, pineapple, plantain, plum, squash, tomatoes and tulip bulbs. To date, 1-MCP marketed as SmartFresh™ has had the most commercial impact on the apple industry (Mattheis, 2008; Watkins, 2008).

Ethylene is an important factor also in the postharvest life of cut flowers (Joyce and Poole, 1993; Elgar *et al.*, 1999; Han and Miller, 2003), as it accelerates flower abscission and leaf yellowing (Joyce and Poole, 1993; Cameron and Reid, 2001; Celikel *et al.*, 2002). For the management of cut flowers silver thiosulphate (STS) is commonly used as inhibitor of ethylene action. It is used more in postharvest treatment of ornamental crops. Silver ions in the form of silver thiosulphate, have the capacity to delay carnation flower senescence, and to block the ethylene receptor site, and also inhibit autocatalytic ethylene production (Veen, 1979; Wawrzyńczak and Goszczyńska, 2003). Different studies demonstrated that treatments with anti-ethylene compounds (STS or 1-MCP) protect flowers against exogenous ethylene (Serek *et al.*, 1995; Serek and Trolle, 2000; Redman *et al.*, 2002; Hunter *et al.*, 2004). Although STS could be an essential tool for the delay of senescence of climacteric flowers, it contains a heavy metals that is a harmful environmental pollutant.

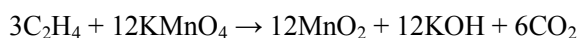
1.3.3. Removal

As previously mentioned, C₂H₄ complete elimination from storage room atmosphere is the best technique to prevent its negative effects on quality of fresh produce. This can be achieved through chemical or physical methods. These methods exploit the ability of some substances or treatment to oxidize, decompose or adsorb gaseous ethylene, via different mechanisms. Following, most common methods and the related bases that cause chemical or physical elimination of ethylene will be discussed.

1.3.3.a) Chemical methods

-Potassium permanganate ($KMnO_4$)

Potassium permanganate ($KMnO_4$) is a stable purple solid that is a strong oxidizing agent and readily decomposes ethylene via a series of reactions to acetaldehyde and then acetic acid, which, in turn, can be further oxidized to CO_2 and H_2O :



The ability of potassium permanganate to reduce ethylene concentration in the atmosphere around horticultural produce was first demonstrated by Forsyth *et al.* (1967) on apples. The requirements to enhance high activity of this material are a high surface area coated with the permanganate and ready permeability to gases (Reid, 2002). This has been achieved by the absorption of $KMnO_4$ onto porous inert minerals such as celite (Forsyth *et al.*, 1967), vermiculite (Scott *et al.*, 1970), alumina (Jaymaran and Raju, 1992), zeolite (Oh *et al.*, 1996) and clay (Picon *et al.*, 1993). For removing ethylene from room air, the absorber should be spread out in shallow trays, or air should be drawn through the absorber system (Reid, 2002). The reduction in ethylene caused by use of potassium permanganate was subsequently found to delay the ripening of many climacteric fruit such as banana (Scott *et al.*, 1970), kiwifruit (Scott *et al.*, 1984), mango (Esguerra *et al.*, 1978) and avocado (Hatton and Reeder, 1972). Fewer studies have been conducted with non climacteric produce but potassium permanganate has been found to extend postharvest life by retarding loss of green color and microbial contamination of lemon (Wild *et al.*, 1976) and lettuce (Kim and Wills, 1995) and inhibiting rotting of strawberry (Wills and Kim, 1995). Given the effectiveness of potassium permanganate in oxidizing ethylene molecule it has been also used for the preparation of active packaging (Arvanotoyannis and Oikonomou, 2012).

A range of commercial potassium permanganate products is now available with a common carrier being alumina beads (e.g., Purafil (Purafil, Doraville, Ga.), Circul-Aire (Circul-Aire, Montreal), Ethysorb (Molecular Products, Thaxted, Essex) and Bloomfresh (Ausdel, Cheltenham, Victoria)) (Wills and Warton, 2004). However,

the disadvantage of the use of potassium permanganate during storage of horticultural crops is the discontinuity of the treatment. In fact, regeneration of KMnO_4 -beads is not possible and therefore scrubbers must be checked frequently and spent beads replaced (Hoehn *et al.*, 2009). In addition, due to the chemical properties of potassium permanganate, precautions must be taken to prevent contamination of food products and waste disposal may be an additional issue (Peiser and Suslow, 1998). KMnO_4 supported on activated alumina spheres has limited long-term efficacy in environments with high relative humidity (e.g. cold stores) (Terry *et al.*, 2007).

- Palladium

Palladium (Pd) is a chemical element, and its largest use today is in catalytic converters. When it is finely divided, such as in palladium on carbon, palladium forms a versatile catalyst and speeds up hydrogenation and dehydrogenation reactions. A large number of carbon-carbon bond forming reactions in organic chemistry (such as the Heck reaction and Suzuki coupling) are facilitated by catalysis with palladium compounds. In addition, palladium, when dispersed on conductive materials, proves to be an excellent electrocatalyst for oxidation of primary alcohols in alkaline media (Tsuji, 2004). In 2010, palladium-catalyzed organic reactions were recognized by the Nobel Prize in Chemistry. It is also a versatile metal for homogeneous catalysis. A 2008 study showed that palladium is an effective catalyst for making carbon-fluoride bonds (Drahl, 2008). The use of a novel palladium promoted material with a significant ethylene adsorption capacity at room temperature was firstly studied by Johnson Matthey scientists (Ilkenhans *et al.*, 2007, Smith *et al.*, 2009). Pd gave by far the best performance of the promoter metals tested. The material is a palladium-impregnated zeolite giving finely dispersed palladium particles. Ethylene adsorption capacity measurements were carried out at room temperature (21°C). Ethylene uptake capacity was measured using a simple 'breakthrough' measurement, in which the total integrated ethylene removal was determined after the outlet ethylene concentration from the reactor had

reached the inlet ethylene concentration, showing that the adsorber was saturated with ethylene (Terry *et al.*, 2007). It is clear, however, that the palladium-based material is acting largely as an adsorber rather than as a catalyst (Smith *et al.*, 2009). Also Martinez-Romero *et al.* (2009) reported that the efficacy of activated carbon–1% Pd to eliminate the accumulated ethylene was approximately 60% over time, while the application of heat pulses to the device increased the efficacy up to 95–97%, leading to ethylene concentrations below 0.1×10^{-4} kPa, considered the limit to avoid detrimental effects of ethylene in climacteric fruit such as tomato (Warton *et al.*, 2001; Wills *et al.*, 2001).

1.3.3.b) Physical methods

- Catalytic oxidizers

If ethylene and oxygen are combined at high temperature in the presence of a catalyst such as platinized asbestos, ethylene will be oxidized. They are very efficient reducing the ethylene concentration in the air to 1% of the input concentration. Because of the small air volume they process, they are most suited to small spaces or long term CA storage systems (Reid, 2002). Ethylene scrubbers using this technology are now commercially available. The catalytic reactors studied for reducing the concentration of ethylene and volatile odorous products are usually used inside normal and/or controlled atmosphere storage cells. An example is represented by Swingtherm that allows to maintain in refrigerated rooms for apples ethylene concentrations lower than 1-5 ppm, in citrus, pear and vegetable cells 0,05-0,1 ppm, in kiwi cells lower than 0,02 ppm. The process consists of cyclically reversing the gas flow direction through a platinum catalyst bed maintained at a temperature of 180-250 °C. The average temperature difference between inlet and outlet gas ranges from 10 °C to 15 °C but may reach 30 °C. This results in heat input into the storage room, which must be compensated by additional refrigeration (Hoehn *et al.*, 2009).

- Adsorption

Adsorption is the adhesion of atoms, ions, or molecules from a gas, liquid, or dissolved solid to a surface (U.S. EPA, 2009). Physical adsorption is caused by van der Waals force between the molecules (Ponec *et al.*, 1974) of the adsorbent and the adsorbate. Physical adsorbents with mesopores can adsorb different and consecutive layers of adsorbate, while those with micropores, have the volume of the pores filled with the adsorbate. Physical adsorbents develop the selectivity to the adsorbate after the former undergo specific treatments, like react under a gas stream or with certain agents. The kind of treatment will depend on the type of sorbents (Zhang, 1989) (Wang *et al.*, 2009). The common physical adsorbents are activated carbon, activated carbon fibre, silica gel and zeolite (Wang *et al.*, 2009). Ethylene adsorption can be regarded as a benchmark study in order to investigate the interaction involving olefin and solid surfaces and ethylene interaction with solid surface plays an important role in many kinds of technological, industrial and also environmental applications such as separation of light olefins from paraffins and various industrial transformations of hydrocarbons in the chemical industries (Elridge, 1993; Busca *et al.*, 1986), production of clean transportation fuels (Cheng *et al.*, 2009), and degradation of various harmful volatile organic compounds (VOCs) derived from ethylene (Yamazaki *et al.*, 2001; Shukri and Kasai, 2014). For use in postharvest handling of fruits and vegetables a suitable material chemically stable, that possesses ethylene adsorption capacity and has received much attention is zeolite (Abe and Watada, 1991; Suslow, 1997; Faubion and Kader, 1996; Peiser and Suslow, 1998). Zeolite is a crystalline aluminosilicate of alkali and alkaline earth which is composed of SiO_4 and AlO_4 in a framework structure (Dyer, 1988; Breck, 1984). Many kinds of zeolite have been reported to have ethylene adsorption properties (Patdhanagul *et al.*, 2010).

1.3.4 Photocatalysis

A recent development in postharvest management of ethylene-sensitive crops is the use of photocatalytic materials or packaging films illuminated with ultraviolet light to remove C_2H_4 through light-promoted oxidation mechanism. During the last decades photocatalysis has been the focus of considerable attention being used in a variety of products across a wide range of research areas, including especially environmental and energy-related fields (Fujishima *et al.*, 2000a,b; Hashimoto *et al.*, 2005; Fujishima *et al.*, 2008; Nakata and Fujishima, 2012). Photocatalysis is generally thought of as the catalysis of a photochemical reaction at a solid surface, usually a semiconductor (Nakata and Fujishima, 2012). It is, practically, the acceleration of a photoreaction in the presence of a substance that acts as a catalyst. In catalysed photolysis, light is absorbed by an adsorbed substrate. In photogenerated catalysis, the photocatalytic activity depends on the ability of the catalyst to create electron-hole pairs, which generate free radicals (e.g. hydroxyl radicals: $\cdot OH$) able to undergo secondary reactions. Its practical application was made possible by the discovery of water electrolysis by means of titanium dioxide, which will be discussed below.

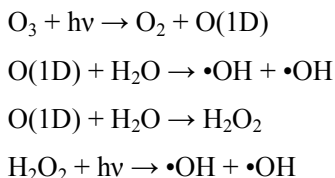
1.3.4.1 Types of photocatalysis

The basic principles about photocatalysis and photocatalytic materials are reported. Two different kinds of photocatalysis were studied, on the basis of the phase in which photocatalytic material and reagent exist.

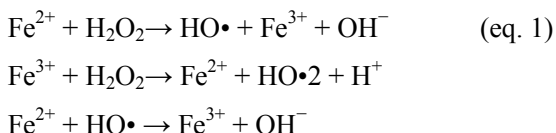
- Homogeneous photocatalysis

In homogeneous photocatalysis, photocatalysts and reactants exist in the same phase. The most commonly used homogeneous photocatalysts include ozone, transition metal oxide and photo-Fenton systems (Fe^+ and Fe^+/H_2O_2). The

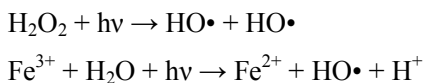
mechanism of the reactive species (hydroxyl radical) production by ozone can follow the two reported paths (Wu and Chang, 2006).



The mechanism of the Fenton's process is quite complex but it can be summarized by the following steps: a mixture of H_2O_2 and ferrous iron in acidic solution generates the hydroxyl radicals (eq. 1), which will subsequently attack the organic compounds present in the solution (Peternel *et al.*, 2007; Herney-Ramirez *et al.*, 2010):



In photo-Fenton type processes, additional sources of OH radicals should be considered: through photolysis of H_2O_2 , and through reduction of Fe^{3+} ions under UV light:

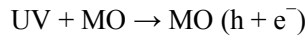


- *Heterogeneous photocatalysis*

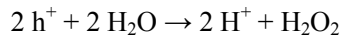
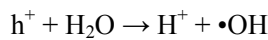
Heterogeneous catalysis has the catalyst in a different phase from the reactants. It includes a wide variety of reactions such as mild or total oxidations, dehydrogenation, hydrogen transfer, water detoxification, gaseous pollutant removal. Most common heterogeneous photocatalysts are semiconductors, which

possess a void energy region where no energy levels are available to promote recombination of an electron and hole produced by photoactivation in the solid. This region, which extends from the top of the filled valence band to the bottom of the vacant conduction band, is called the band gap (Linsebigler *et al.*, 1995). When a photon with energy equal to or greater than the materials band gap is absorbed by the semiconductor, an electron is excited from the valence band to the conduction band, generating a positive hole in the valence band. The excited electron and hole can recombine and release the energy gained from the excitation of the electron as heat. The ultimate goal of the process is to have a reaction between the excited electrons with an oxidant to produce a reduced product, and also a reaction between the generated holes with a reductant to produce an oxidized product. Due to the generation of positive holes and electrons, red-ox reactions take place at the surface of semiconductors. In the oxidative reaction, the positive holes react with the moisture present on the surface and produce a hydroxyl radical.

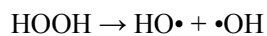
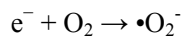
Oxidative reactions due to photocatalytic effect:



Where MO stands for metal oxide.



The reductive reaction due to photocatalytic effect:



The hydroxyl radicals are generated in both the reactions. This reactive species is very oxidative in nature and non selective with redox potential equal to $E_0 = +3.06$ V (Daneshvar *et al.*, 2004).

Photocatalysis has recently become a common word and various products using photocatalytic functions have been commercialized. Of the many different photocatalysts, titanium oxide (TiO_2) has been the most widely studied and used in many applications because of its strong oxidizing abilities (Hoffmann *et al.*, 1995; Nosaka *et al.*, 2002; Nosaka *et al.*, 2003a; Nosaka *et al.*, 2003b; Nosaka *et al.*, 2004; Jańczyk *et al.*, 2006) for the decomposition of organic pollutants (Fujishima and Zhang, 2006; Fujishima *et al.*, 2007), superhydrophilicity (Wang *et al.*, 1997), chemical stability, long durability, nontoxicity, low cost, and transparency to visible light. TiO_2 is almost the only material suitable for industrial use at present and also probably in the future. It has been used as a white pigment from ancient times, and thus, its safety to humans and the environment is guaranteed by history. It has been approved by the American Food and Drug Administration (FDA) for use in human food, drugs, cosmetics and compounded in food contact materials such as cutting board and other surfaces in contact with unprotected food. An anticipated use is as a new material technology for future requirements in the hygienic design of food processing facilities (Maneerat and Hayata, 2006).

2. Titanium oxide (TiO_2) photocatalysis

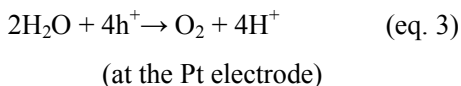
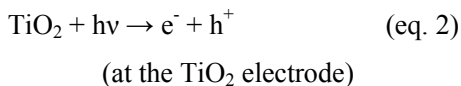
Following on from the water splitting breakthrough reported by Fujishima and Honda in 1972, the photocatalytic properties of different materials have been used to convert light energy into chemical energy to oxidize or reduce materials and obtain useful materials including hydrogen (Fujishima and Honda, 1972; Kudo and Miseki, 2009; Ryu, 2010; Maeda, 2011) and hydrocarbons (Inoue *et al.*, 1979), and to remove pollutants and bacteria on wall surfaces and in air and water (Nakata and Fujishima, 2012). There are two types of photochemical reaction proceeding on a TiO_2 surface when irradiated with ultraviolet light. One includes the photo-induced

redox reactions of adsorbed substances, and the other is the photo-induced hydrophilic conversion of TiO₂ itself. The former type has been known since the early part of the 20th century, but the latter was found only at the end of the century. The combination of these two functions has opened up various novel applications of TiO₂, particularly in the field of building materials (Hashimoto *et al.*, 2005). The chemical stability of TiO₂ holds only in the dark. Instead, it is active under UV light irradiation, inducing some chemical reactions. Such activity under sunlight was known from the flaking of paints and the degradation of fabrics incorporating TiO₂ (Keidel, 1929). Scientific studies on such photoactivity of TiO₂ have been reported since the early part of the 20th century. For example, there was a report on the photobleaching of dyes by TiO₂ both in vacuo and in oxygen in 1938 (Doodeve and Kitchener). It was reported that UV absorption produces active oxygen species on the TiO₂ surface, causing the photobleaching of dyes. It is equivocal when and who started utilizing first such a photochemical power of TiO₂ to induce chemical reactions actively, but at least in Japan, there were a series of reports by Mashio *et al.*, from 1956, entitled “Autooxidation by TiO₂ as a photocatalyst” (Kato and Mashio, 1956). They dispersed TiO₂ powders into various organic solvents such as alcohols and hydrocarbons followed by the UV irradiation and observed the oxidation of solvents and the simultaneous formation of H₂O₂ under ambient conditions. It is interesting to note that they had already compared the photocatalytic activities of various TiO₂ powders using twelve types of commercial anatase and three types of rutile, and concluded that the anatase activity of the autooxidation is much higher than that of rutile, suggesting a fairly high degree of progress of the research (Kat and Masuo, 1964).

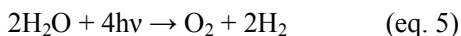
2.1 Mechanism of action

The discovery of the TiO₂ photocatalytic mechanism of action started in the late 1960s when the investigation about the photoelectrolysis of water began. The first studies were carried out using a single crystal n-type TiO₂ (rutile) semiconductor electrode, because it has a sufficiently positive valence band edge to oxidize water

to oxygen. It is also an extremely stable material even in the presence of aqueous electrolyte solutions. The existence of photoelectrolysis under solar light was firstly demonstrated in 1969 with a system which was exposed to near-UV light, and was connected to a platinum black counter electrode through an electrical load (Fujishima *et al.*, 1969). Then, this electrochemical photolysis of water was reported in Nature by analogy with a natural photosynthesis in 1972 (Fujishima and Honda). The scientists demonstrated that when the surface of the rutile TiO₂ electrode was irradiated with light consisting of wavelengths shorter than its band gap, about 415 nm (3.0 eV), photocurrent flowed from the platinum counter electrode to the TiO₂ electrode through the external circuit. The direction of the current revealed that the oxidation reaction (oxygen evolution) occurs at the TiO₂ electrode and the reduction reaction (hydrogen evolution) at the Pt electrode. This observation shows that water can be decomposed, using UV light, into oxygen and hydrogen, without the application of an external voltage, according to the following scheme:



The overall reaction is:



Subsequently studies demonstrated that the photocatalytic properties of TiO₂ derive from the formation of photogenerated charge carriers (hole and electron) which occurs upon the absorption of ultraviolet (UV) light corresponding to the band gap (Sakai *et al.*, 1995; Ikeda *et al.*, 1997; Fujishima *et al.*, 1999; Fujishima *et al.*, 2000b; Fujishima *et al.*, 2008). The basic mechanism of TiO₂ photocatalysis is shown

in Figure 2.1.1. In general, UV irradiation induces the photogeneration of electron-hole pairs, whose charge carriers react with chemical species such as H_2O , OH^- , and O_2 to produce hydroxyl radicals ($\bullet\text{OH}$), meanwhile, electrons in the conduction band participate in reduction processes, reacting with molecular oxygen in the air to produce superoxide radical anions ($\text{O}_2^{\bullet-}$), and H_2O_2 contributes to decomposition of organics at the TiO_2 surface (Fujishima *et al.*, 2008; Ochiai and Fujishima, 2012). The majority of the holes are subsequently consumed by reacting directly with adsorbed organic species or adsorbed water, producing $\bullet\text{OH}$ radicals as described above. However, a small proportion of the holes is trapped at lattice oxygen sites and may react with TiO_2 itself, which weakens the bonds between the lattice titanium and oxygen ions. Water molecules can then interrupt these bonds, forming new hydroxyl groups. The singly coordinated OH groups produced by UV-light irradiation are thermodynamically less stable and have high surface energy, which leads to the formation of a superhydrophilic surface (Nakata and Fujishima, 2012).

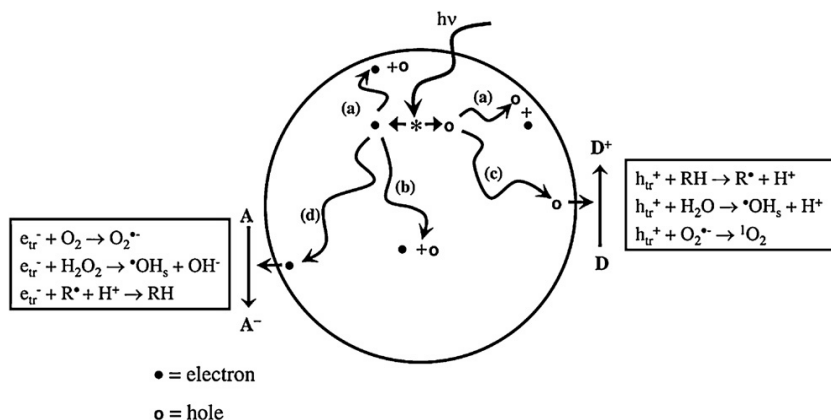


Figure 2.1.1. Processes occurring on bare TiO_2 particles after UV excitation (from Fujishima *et al.*, 2008).

2.1.1 Photocatalytic degradation of organic compounds

The application of photocatalytic reactions to water and air decontamination has been widely studied. In particular TiO₂ presents an interesting property that is the unselectivity in oxidation reactions. Very few compounds are known that cannot be degraded by TiO₂ irradiated by UV-light (Gulyas *et al.*, 1994; Watanabe *et al.*, 2005; Garcia-Lopez *et al.*, 2007; Augugliaro *et al.*, 2012). In particular, TiO₂ ability in oxidizing organics under UV irradiation, could have important applications in cleaning indoor and outdoor air. Given that there is a sufficient supply of O₂ and UV illumination, gaseous contaminants can be completely degraded into CO₂, H₂O, and mineral acids on a TiO₂ surface. Mo *et al.* (2009) summarized kinetic models of photocatalytic oxidation reactions involving adsorption steps. In the case of the photocatalytic oxidation of an unimolecular reactant (called R) on TiO₂, the rate of R degradation, r , could be expressed by unimolecular type Langmuir–Hinshelwood (L–H) model (Peral and Ollis, 1992; Sauer and Ollis, 1994; Biard *et al.*, 2007; Shiraishi *et al.*, 2007; Yang *et al.*, 2007; Ochiai and Fujishima, 2012):

$$r = k\theta_R = k(K[R])/(1+K[R]) \quad (\text{eq. 6})$$

where k is the reaction constant (dependent on temperature, UV intensity, etc.), θ_R represents the fractional coverage of R adsorbed to the TiO₂ surface, and K is the adsorption equilibrium coefficient. This model could be used in many practical studies for decomposition of formaldehyde (Noguchi *et al.*, 1998; Yang *et al.*, 2007), acetaldehyde (Obuchi *et al.*, 1999; Noguchi *et al.*, 1998), acetone (Alberici and Jardim, 1997; Zorn *et al.*, 1999), benzene (Zhang *et al.*, 2007; Zhong *et al.*, 2007), and other organic compounds. The removal rate is obviously influenced by numerous parameters: UV light intensity, substrate concentration, O₂ partial pressure, humidity, substrate type, and so on (Ochiai and Fujishima, 2012).

Because of the described high oxidative activity of TiO₂-based materials, the research shifted to the utilization of its strong photoproducted oxidation power for the destruction of pollutants, starting from 1970s. The first such reports were those

of Frank and Bard in 1977, in which they described the decomposition of cyanide in the presence of aqueous TiO₂ suspensions. Subsequently, detoxications of various harmful compounds in both water and air were demonstrated using powdered TiO₂ actively as potential purification methods of waste water and polluted air. (Fox and Dulay, 1993; Hoffman *et al.*, 1995).

For the purpose of easy handling of photocatalysts, the immobilization of TiO₂ powders on supports was carried out in the late 1980s (Matthews, 1987). Although many research studies were on the purification of wastewater and polluted air, TiO₂ photocatalysis could not be developed to the stage of a real industrial technology in the 1980s.

TiO₂-based photooxidation is also effective against ethylene. It is seen as an interesting and promising alternative to the other most conventional processes used to degrade ethylene and has attracted increasing attention over the last years (Obee and Hay, 1997; Tibbitts *et al.*, 1998; Park *et al.*, 1999; Surajit *et al.*, 2005). If compared to the other techniques the major advantage of this technology is the complete decomposition of ethylene to CO₂ and H₂O (Ye *et al.*, 2009, 2013). The development of a TiO₂ photocatalyst supported on materials with a large surface area would be of very important to decontaminate environment of storage facilities where the ethylene concentration is dilute under conditions of high relative humidity and low temperature (Ye *et al.*, 2009). Recently, literature concerning the effect of titanium dioxide on prolong quality of fruits and vegetables during storage is growing (Maneerat and Hayata, 1996; Maneerat *et al.*, 2003; Chawengkijwanich and Hayata, 2008; Bodaghi *et al.*, 2013). The use of TiO₂ for the elimination of ethylene and pathogen during postharvest handling of fresh and minimally processed produce, may therefore represent an innovation compared to the previously mentioned used technologies.

2.1.2 Antimicrobial activity

A photocatalytic decomposition reaction can be applicable also to microorganisms.

Hydroxyl radicals ($\bullet\text{OH}$)

and reactive oxygen species (ROS) generated on the illuminated TiO_2 surface play a role in inactivating microorganisms by oxidizing the polyunsaturated phospholipid component of the cell membrane of microbes (Saito *et al.*, 1992; Fujishima *et al.*, 1999; Maness *et al.*, 1999; Huang *et al.*, 2000; Kuhn *et al.*, 2003; Cho *et al.*, 2004, Chawengkijwanich and Hayata, 2008). Sunada *et al.* (1998) reported that *Escherichia coli* cells can completely disappear on TiO_2 under UV irradiation of 1 mW/cm^2 . The anti-bacterial function of a TiO_2 photocatalyst is markedly enhanced even with weak UV light, using a fluorescent lamp and the aid of either silver or copper (Sunada *et al.*, 2003).

The cell deactivation, when metals are present, proceeds as follows (Figure 2.1.2.1(a)(b)(c)). The first step is that the reactive species generated by the TiO_2 photocatalyst attacks the outer membrane (Figure 2.1.2.1(b)). The second step is the effective uptake of the copper ions into the cytoplasmic membrane (Figure 2.1.2.1(c)). In this case, the TiO_2 photocatalytic reaction assists the intrusion of the copper ions into the cell, which causes the destruction of the *E. coli* cells on a Cu/TiO_2 film even under very weak UV light (Sunada *et al.*, 2003) It has been reported that the copper species photodeposited on the TiO_2 film is a mixture of metallic copper (Cu^0) and copper ions (Cu^+ and Cu^{2+}). When this Cu/TiO_2 film is irradiated, the copper ions can be reduced to metallic copper and metallic copper can be oxidized to copper ions by photogenerated electrons and holes, respectively. Although the oxidation state of copper might change under UV light irradiation, copper ions (Cu^{2+}) exist on the Cu/TiO_2 film (Sunada *et al.*, 2003; Hashimoto *et al.*, 2005). The enhancement of the antibacterial effect under UV-A light was also observed on the silver-deposited TiO_2 . The antibacterial ceramic tile coated with photocatalytic TiO_2 containing Cu and/or Ag started full-scale manufacturing by TOTO Ltd. in 1995, and its technology was exported to Western countries widely.

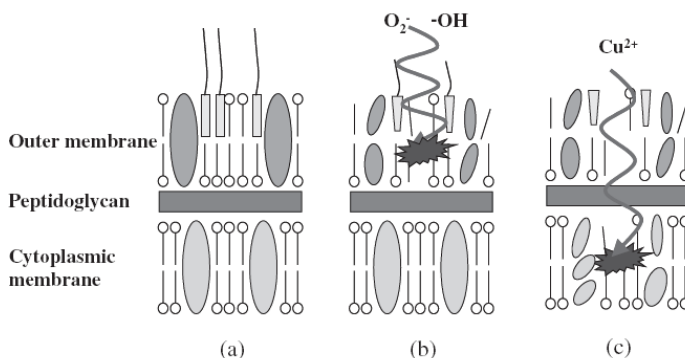


Figure 2.1.2.1(a)(b)(c). Schematic illustrations of bactericidal process for copper-resistant *E. coli* cells on Cu/TiO₂ thin film under weak UV light irradiation (from Hashimoto *et al.*, 2005).

Currently there is considerable interest in the self-disinfecting property of TiO₂ for meeting hygienic design requirements in food processing and packaging surfaces. Bactericidal and fungicidal effects of TiO₂ on *E. coli*, *Salmonella choleraesuis*, *Vibrio parahaemolyticus*, *Listeria monocytogenes*, *Pseudomonas aeruginosa*, *Staphylococcus aureus*, *Diaporthe actinidiae* and *Penicillium expansum* have been reported in many studies over the years. Numerous applications to control food and postharvest pathogens, *E. coli* endotoxin decomposition by TiO₂ powder, TiO₂ slurry and TiO₂ thin film surface have been reported (Matsunaga *et al.*, 1985, 1988; Wei *et al.*, 1994; Kikuchi *et al.*, 1997; Horie *et al.*, 1998; Sunada *et al.*, 1998; Maness *et al.*, 1999; Choi and Kim, 2000; Wist *et al.*, 2002; Kim *et al.*, 2003; Cho *et al.*, 2004; Hur *et al.*, 2005; Maneerat and Hayata, 2006). Application of TiO₂ photocatalytic disinfection for drinking water production was also investigated (Wist *et al.*, 2002). In the last years, the development of TiO₂-coated or incorporated food packaging and food preparing equipment has also received attention. (Chawengkijwanich and Hayata, 2008, Xing *et al.*, 2012).

Part two - Experimental

1. Introduction

As widely described in the first part of this thesis ethylene plays a key-role during pre- and postharvest management of fruits and vegetables due to its effects as a plant hormone. In the management of the postharvest life of fruit and vegetables such effect may be more or less desirable. Omitting its relevant use as regulator in the growth, development and ripening phases of many horticultural crops, here we focus on the strategies used to prevent ethylene effects during storage of fresh produce. Methods to inhibit ethylene synthesis and action or to remove it from storage rooms atmosphere were previously described. However, most of them are expensive and uneconomical or discontinuous. Among the new technologies for its removal fits the photocatalytic oxidation of ethylene on titanium dioxide (TiO₂).

1.1. Use of titanium oxide during storage of horticultural crops

As previously mentioned, titanium oxide is a material studied and used as a photocatalyst for the degradation of organic or inorganic compounds. Briefly, when activated by UV light, it generates hydroxyl radicals and superoxide ions at its surface. The hydroxyl radical acts as a powerful oxidizing agent to convert organic pollutants absorbed on the TiO₂ catalytic surface into CO₂ and water vapor (Akiyama and Togeda, 2000; Maneerat *et al.*, 2003). The contaminant degradation is realized in the form of heterogeneous photocatalysis. In the last decades, this field was broadly studied. Its main applications were those correlated to the use of light and a solid catalyst to degrade liquid and gas-phase pollutants (Hoffmann *et al.*, 1995; Augugliaro *et al.*, 2006; Moa *et al.*, 2009). The application of photocatalytic reactions to water and air decontamination was extensively studied. In particular TiO₂ presents a precious property that is the unselectivity in oxidation reactions. Very few compounds are known that cannot be degraded by TiO₂ irradiated by UV-light (Gulyas *et al.*, 1994; Watanabe *et al.*, 2005; Garcia-Lopez *et al.*, 2007; Augugliaro *et al.*, 2012). The ability to promote chemical changes and act as a photocatalyst makes TiO₂ very interesting for applications in the field of

environmental clean-up to improve quality of air or water (Suzuki, 1993; Obee and Hay, 1997; Horie *et al.*, 1998; Choi and Kim, 2000; Muggli and Ding, 2001). This activity is also exerted against ethylene, commonly found in postharvest storage room atmosphere. Park and co-workers (1999) demonstrated that ethylene can be completely oxidized into CO₂ on the powdered TiO₂ photocatalysts. The decomposition rate depending on the nature of the catalysts, and the photocatalytic oxidation of C₂H₄ can be enhanced by the coexistence of H₂O vapor in the reaction system. Subsequently, other studies were performed to assess the efficacy of titanium oxide in the decomposition of ethylene (Sirisuk *et al.*, 1999; Kumar *et al.*, 2005; Ye *et al.*, 2009; 2013). TiO₂-coated materials or packaging films illuminated with ultraviolet light are able to remove ethylene during storage of whole and fresh-cut produce. Maneerat *et al.* (2003) demonstrated that ethylene can be photocatalytically oxidized using TiO₂-coated glass beads in closed and open system in laboratory scale. This activity is exerted also under high humidity and at both room and low temperatures, and under both normal air and modified atmosphere conditions. Also in the fruit ripening test the photocatalytic reaction of titanium oxide delayed the ripening of green mature tomatoes, without inducing symptoms of disorder in fruits.

Besides the effect on ethylene is also shown the effectiveness of this catalyst to inactivate pathogenic microorganisms. The antimicrobial activity could be interesting in order to eliminate pathogen or spoilage bacteria that cause deterioration of fresh produce during shelf-life. In recent literature studies on the effect of titanium dioxide during postharvest handling are reported, showing its efficacy in prolonging shelf-life of products (Maneerat and Hayata, 2006; Chawengkijwanich and Hayata, 2008; Hu *et al.*, 2011; Bodaghi *et al.*, 2013).

1.2. Photocatalytic materials

The construction of TiO₂-based nano- or micro-structures with different and interesting morphologies and properties has attracted considerable attention (Chen and Mao, 2006) and many TiO₂ nanostructural materials, such as spheres, nanorods,

fibers, tubes, sheets, and interconnected architectures, have been fabricated and tested (Nakata and Fujishima, 2012). Many factors can have significant influence on photocatalytic activity of the material, including the size, specific surface area, pore volume, pore structure, crystalline phase, and the exposed surface facets. The development of performance improvements by adjusting these factors is the main objective of photocatalysis research. Nano- or micro-structured TiO₂ spheres are the most widely studied and used in TiO₂-related materials because a sphere with zero dimensionality has a high specific surface area, resulting in a higher rate of photocatalytic decomposition of organic pollutants (Liu *et al.*, 2011). Choosing TiO₂ materials with the correct dimensionalities allows to obtain the greatest benefits from this materials (Nakata and Fujishima, 2012). For an easy handling of photocatalysts and a cost-effective separation of it from the systems, the immobilization of TiO₂ nanoparticles on solid supports was also investigated from the late 1980s (Fujishima *et al.*, 2000a-b; Ryu, 2010; Maeda, 2011).

1.3. *Fluidized bed photoreactor*

The use of fluidized bed for photocatalysts to obtain both uniform light distribution and an immobilizing support has been firstly proposed and studied by Yue and Khan (1983). Fluidized bed photocatalytic reactor systems have several advantages over conventional immobilized or slurry-type photocatalytic reactors (Lim and Kim, 2002, 2004). The particular photoreactor configuration provides a good exposure of photocatalyst to UV light and good penetration of the light into the photocatalyst bed that allows more contact between photocatalyst and gas (Lim and Kim, 2004). Also, UV light can be more uniformly distributed within the given catalyst bed.

TiO₂, as a photocatalyst, has been used in different forms in photocatalytic oxidation reactors (PCO reactors) (Vincent *et al.*, 2007; Mo *et al.*, 2009; An *et al.*, 2012). Photocatalytic reactors can be employed to eliminate pollutants from water and air streams. Coating of TiO₂ on walls of the reactor as a thin film and on the bed particles (e.g., silica gel, activated carbon, and alumina) are two common forms

of TiO₂ handling in reactors. The reactors which use TiO₂ coated particles can be categorized into two separate classes; packed and fluidized bed reactors. Since exposing of photocatalyst with UV light and good contact between reactants and photocatalyst are vital factors in the PCO reactions, the fluidized bed reactor is preferred to the packed bed one (Nelson *et al.*, 2007) (Dashliborun *et al.*, 2013).

2. General objectives

This thesis is part of the project “OFRALSER - *High-Convenience Fruits and Vegetables: New Technologies for Quality and New Products*” (PON01-01435), that includes activities aimed to improve quality of existing products, and to develop new products/technologies. Among the new technologies to prolong fruit and vegetables shelf-life the use of titanium oxide-based photocatalytic activity is one of the most promising. The applications of photocatalytic activity of TiO₂-based materials, may therefore represent an innovation compared to the commercially used technologies (potassium-based system, high temperature catalytic oxidation, inhibition of ethylene receptor). The innovation will be reflected in the development of TiO₂-based materials able to prolong postharvest life of fresh products, and in the development of a fluidized bed reactor for the photocatalytic oxidation of ethylene in the atmosphere of cold storage rooms.

General aim of this work is the use of photocatalytic titanium oxide to decompose ethylene during storage of horticultural crops. Use of TiO₂ as an innovative technology to preserve fresh produce from detrimental effects of ethylene requires preliminary stage of development and study of materials. First objective of this work is the production of a lighting system in laboratory scale for the assessment of photocatalytic activity of the developed materials. TiO₂-coated glass beads, alumina-based and mesoporous mixed SiO₂/TiO₂ materials will be investigated in order to select the most effective in reducing ethylene from storage room atmosphere. The materials will be developed through coating of supports with TiO₂ powder, or development of sol-gel method to obtain mesoporous photocatalytic resources supported on alumina and silica. Materials photoactivity will be compared to traditional technology (such as KMnO₄). Different C₂H₄ concentration (from 0.1 up to 50 ppm), and/or ethylene-enriched mixture flow-rate (0.5-5 mL min⁻¹) will be tested. To better understand the photocatalytic behavior, trials with and without light exposition will be carried out. The selected material will be then used in a biological assay to verify its actual ability to delay ripening of plant tissues. For this purpose, exogenous ethylene will be treated through passage in the photocatalytic

reactor, reaching then the fruits. The last part concerns the design and development phases of a prototype of fluidizing bed photoreactor, with the aim of technological transfer of innovation to companies.

3. Materials and Methods

3.1. Design of photocatalytic reactor in laboratory scale

Photocatalytic materials were positioned inside glass cylinders (height=24.5 cm, internal diameter= 4 cm, volume=0.3 l) with input and output holes to allow transit of ethylene-enriched air. The gaseous mixture was obtained diluting ethylene (initial concentration 100 ppm) with air to obtain the desired final concentration. The photocatalytic reaction occurred within cold rooms illuminated under black light lamps as UV-A source (OSRAM L18/73 SUPRABLACK™, UV-A: 400-315 nm). The light intensity was measured with a digital luxmeter (ASITA LX350).

3.2. TiO₂ powder synthesis

TiO₂ powders were synthesized in aqueous solution by using pluronic F127 (EO₁₀₆ PO₇₀ EO₁₀₆), a non-ionic triblock copolymer, as a sacrificing template in order to get the ordered mesopores. The sample is denoted as T-SBA 10 (TiO₂=100%). Total metal oxide content in the solution was maintained to the equivalent amount of 12.256 g. To prepare the solution, first 28 g of F127 (Sigma-Aldrich) was dissolved in 150 g of water and 600 g of 2M HCl and stirred until it fully dissolved. Then equivalent amount of titanium isopropoxide (TTIP, Sigma-Aldrich) was dropwise added to the above acidified polymeric aqueous solution. At this moment the precipitate of titanium hydroxides was observed which turned into a clear sol after stirring of about 1 h. Then 8.498 g of TEOS (Tetraethoxysilane, Sigma-Aldrich) was added dropwise and stirring was continued to another 1 h. Then the obtained solution was placed in a polypropylene bottle with closed cap and heated for 24 h in an oven at 100 °C with static condition. After this step a solid product was obtained which was subjected to heat treatment 550 °C for 6 h with the increasing and decreasing ramp of 8h to remove the polymer template. After this step pure white powder was obtained.

3.3. Ethylene detection

The detection of the concentrations of ethylene was performed through a gas chromatograph Agilent, model 7890 A, with a flame ionization detector (FID). Detector temperature was set at 300 °C, with a hydrogen flow of 45 mL min⁻¹ and air flow of 400 mL min⁻¹. For the separation of ethylene a packed column 19091J - 413 (Agilent) was used, and Helium as carrier gas (pressure 15 psi). Oven temperature was 120 °C.

3.4. Evaluation of photocatalytic activity

The photocatalytic activity of the tested materials was expressed as percentage of ethylene reduction. The percentage of ethylene degradation was expressed as the difference between ethylene concentration in input and output at each sampling time. The following formula was applied:

$$\left(\frac{\text{ppm } C_2H_4\text{in} - \text{ppm } C_2H_4\text{out}}{\text{ppm } C_2H_4\text{in}} \right) * 100$$

3.5. Experimental setup

Several experimental trials was carried out, varying photocatalytic material, ethylene concentration of treated mixture and flow-rate. The figure below (Figure 3.5.1 (a)(b)) reports the experimental settings. Known concentration of gaseous C₂H₄ was flushed at a constant rate inside photocatalytic cylinders, exposed or not to ultra violet light. *In* and *out* gas samples were analyzed by injecting in gas chromatograph for ethylene detection (GC-FID) (Figure 3.5.1(a). Flow-through system). Concerning the closed setup (Figure 3.5.1(b)), after flush the mixture inside the cylinders for the time required to replace the original air, the flow was stopped and the system closed to leave the gas mixture in contact with the active surface of the photocatalytic material.

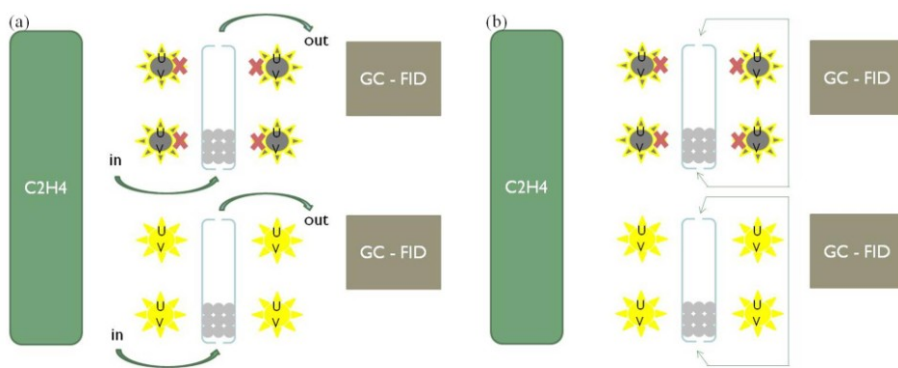


Figure 3.5.1. Experimental setup carried out during the trials. (a). Flow-through system. (b). Closed system.

3.6. Statistical analysis

The effect of treatments was tested by performing a one-way ANOVA using StatGraphics Centurion XVI.I (StatPoint Technologies, Inc., USA), and mean values within each sampling were separated applying Tukey test with significant difference when $P \leq 0.05$. Analysis of variance was performed separately for each sampling time.

4. Comparison of photocatalytic properties of different titanium oxide-based materials

4.1. Materials and Methods

The photocatalytic reactor (as described at point 3.1. *Design of photocatalytic reactor in laboratory scale*) was created to test different photocatalytic materials and different experimental conditions (C_2H_4 concentrations, flow rate, UV exposition). Photocatalytic material consisted of glass beads (diameter 6 mm) (denoted as “*TiO₂-coated glass beads-UniFg*”), previously washed with denatured alcohol and dried in a stove overnight at 105 °C. Titanium oxide powder, obtained from the Department of Engineering of University of Salento (Lecce, Italy) as reported in subparagraph 3.2., was fixed on the support by immersion in ethanolic suspension of TiO_2 (≈ 0.1 g TiO_2 /100ml ethanol) (Maneerat *et al.*, 2003) and subsequent drying by evaporation of the solvent at room temperature. The amount of TiO_2 powder effectively "anchored" to the beads was evaluated by the difference in weight of the beads before and after the dipping. Alternatively were used media provided by *Salentec* srl (Lecce, Italy), consisting of glass beads with a diameter of 6 mm with titanium powder coating fixed at high temperatures (300 °C) (“*TiO₂-coated glass beads-Salentec*”). In the last experiment photocatalytic material consisted of alumina-based titanium oxide (called “*Alumina-TiO₂*”). The TiO_2 microspheres were fixed on the substrate by heat treatment at 400 °C. This material contained higher content of active photocatalytic titanium oxide.

4.2. Experimental setup

Several preliminary trials were performed, according to general settings described at point 3.5.

In Table 4.2.1, setups for each conducted experiment are described.

Table 4.2.1. Detail of experimental settings.

	Photocatalytic material	Ethylene (ppm)	System-type	Flow-rate (mL min⁻¹)
<i>exp1</i>	<i>TiO₂-coated glass beads- UniFg</i>	0.1 and 2	Flow-through	5
<i>exp2</i>	<i>TiO₂-coated glass beads- UniFg</i>	50	Flow-through	2.5
<i>exp3</i>	<i>TiO₂.coated glass beads- Salentec</i>	10	Flow-through	1.5
<i>exp4</i>	<i>Alumina-TiO₂</i>	2.5	Flow-through	1.5
<i>exp5</i>	<i>Alumina-TiO₂</i>	2.5	Flow-through	1.5
<i>exp6</i>	<i>Alumina-TiO₂</i>	2	Flow-through	0.5
<i>exp7</i>	<i>Alumina-TiO₂</i>	2	Closed	//

4.3. Results and Discussions

TiO₂ microspheres, usually possess a high specific surface area and a high pore volume size, and these properties increase the accessible surface area and the rate of mass transfer for pollutant adsorption, resulting in better photocatalytic performance (Li *et al.*, 2007; Zheng *et al.*, 2009; 2010; Liu *et al.*, 2010a-b; Xiang *et al.*, 2011). The white photocatalytic powder was positioned on different support, in order to characterize the most efficient one and easily manage it.

In the first phase titanium oxide was fixed on 6 mm diameter glass beads, as described in materials and methods section. The obtained outside layer was of 0.00037 mg_{TiO₂}/mm². To verify the quality of titanium oxide coating on glass beads different images were acquired. After dipping in ethanolic suspension beads were photographed at different levels of enlargement (Figure 4.3.1).

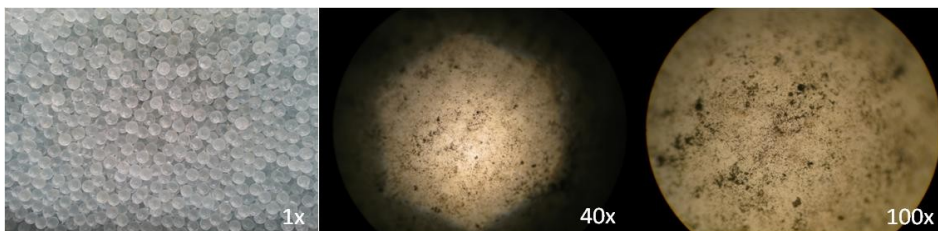


Figure 4.3.1. Photocatalytic material at different levels of enlargement.

The picture shows how the thin layer of TiO_2 powder is not regular and uniform on the whole surface of the glass marbles. Microscopic holes represented as black points in the picture (more evident in 100X enlargement), corresponding to titanium oxide microparticles.

Preliminary test on TiO_2 -coated glass beads (*exp1* and *exp2*) was performed using two different ethylene concentration and air flow rate of 5 mL min^{-1} , temperature: $5 \text{ }^\circ\text{C} \pm 1 \text{ }^\circ\text{C}$ and light intensity of about 80 lux. Final C_2H_4 quantity was monitored up to 180 and 240 minutes. First experimental evidence, reported in Figure 4.3.2, did not show any reduction of ethylene between cylinder input and output. This experiment was triplicated and the same results were obtained (data not shown).

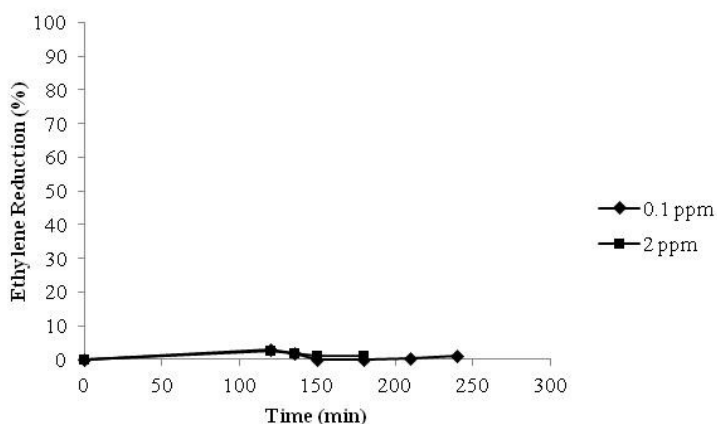


Figure 4.3.2. *Exp1*. Ethylene degradation percentage over time (UV lights = ON). Photocatalytic material: TiO_2 -coated glass beads-*UniFg* (ϕ 6 mm), flow rate: 5 mL min^{-1} ; $[\text{C}_2\text{H}_4]$: 0.1 ppm and 2 ppm.

A possible explanation of this trend was that mixture flow rate was too high to allow the correct contact time between photocatalyst surface and gaseous pollutant. Since the photocatalytic activity is based on chemical reactions on the surface of the catalyst, probably the contact time should be as longer as possible. For this reason, the gas flow rate was reduced. In addition, in order to promote and facilitate the collision between contaminant and the active sites of the photocatalyst, C₂H₄ concentration was increased, up to 50 ppm. The graphs below show some of the results obtained from the experiments that were carried out. Figure 4.3.3 reports the trend of percentage reduction of ethylene over 480 minutes.

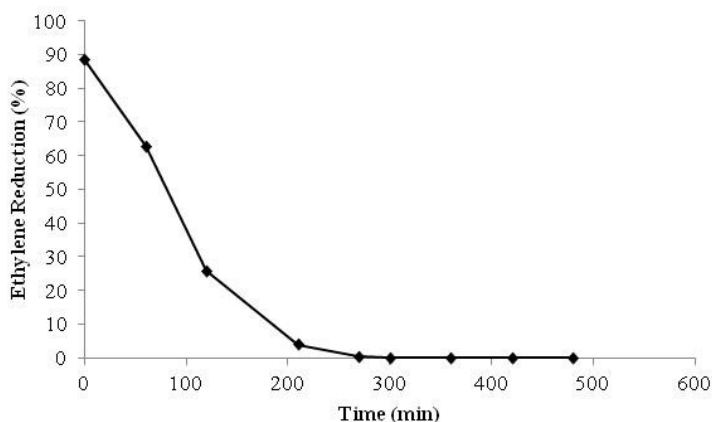


Figure 4.3.3. *Exp2*. Ethylene degradation percentage over time (UV lights = ON). Photocatalytic material: *TiO₂-coated glass beads-UniFg* (ø 6 mm), flow rate: 2.5 mL min⁻¹; [C₂H₄]: 50 ppm.

High initial reduction, which slowly decreases, was due to the initial filling of the cylinder. In fact, to remove 95% of the original gaseous mixture in cylinder is applicable the following formula:

$$t = 2.9965 \left(\frac{V}{F} \right)$$

where:

V = volume of the cylinder (250 ml, not considering the area occupied by the glass beads)

F = inlet flow (about 2,5 ml/min)

So, in this case:

$$t = 2.9957 * 100 = 299.57 \text{ minutes}$$

After about 5 hours of UV-A exposure was not observed more reduction in ethylene concentration.

Further tests (*exp3*) were carried out using a photocatalytic material provided by *Salentec* s.r.l. (Lecce, Italy), consisting of glass beads with a diameter of 6 mm with TiO₂-coating applied through high temperature treatment. High temperature should enhance cohesion between the powder and the surface of the sphere, avoiding loss of material. The performed trial, using the same conditions of *exp1* and *exp 2* showed no reduction of ethylene (data not shown). In subsequent experiments UV lights were turned on after the air inside the cylinder has reached the desired final C₂H₄ concentration. Moreover, the ethylene-enriched air was dehumidified through a passage into silica gel, in order to assess if air humidity could impact photocatalytic activity of glass beads. In this case, as show in Figure 4.3.4, a slight initial reduction of ethylene in the outgoing flow was observed due to the dilution of the gaseous mixture with the residual air present in the cylinder. Subsequently, after about one hour, no appreciable reduction was further observed. Water content of the gaseous mixture did not affect titanium oxide photoactivity. Rather, in some work it is demonstrated that the photocatalytic oxidation of C₂H₄ is enhanced by the coexistence of H₂O vapor in the reaction system (Park *et al.*, 1999). For this reason, all subsequent tests were conducted under high humidity conditions.

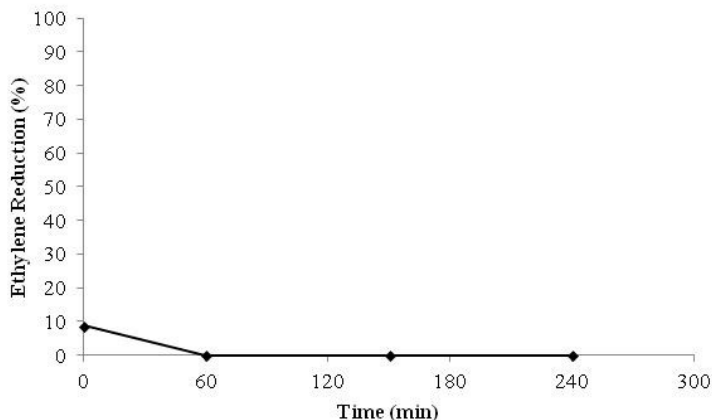


Figure 4.3.4. *Exp3*. Ethylene degradation percentage over time (UV lights = ON). Photocatalytic material: TiO_2 -coated glass beads-Salentec (\varnothing 6 mm), dehumidified flow rate: 1.5 mL min^{-1} , $[C_2H_4]$: 10 ppm.

The TiO_2 -coated glass beads used in this trials were not effective in reducing ethylene in gaseous mixture, probably because of the low efficiency of coating techniques. As previously showed in the coated-support image, small quantities of TiO_2 powder were attached on the support, due to its spherical surface.

The material used for *exp4* was *Alumina-TiO₂*. The powder (1 g) was placed within the glass cylinders previously described. In order to evaluate also the effect of UV-A light two cylinders were exposed to UV radiation (4 black light lamps, sample is denoted in the graph as UV-A ON), while the others were completely shielded from any light source (UV-A OFF). Air flow rate containing 2.5 ppm of C_2H_4 crossed cylinders for 210 minutes at a rate of about 1.5 mL min^{-1} . Compared to the other tests flow rate was further reduced, in order to allow even greater contact time. The temperature inside the photocatalytic room was maintained around $15 \text{ }^\circ\text{C}$. The lamps were turned on after the complete filling of the cylinder with the mixture. Figure 4.3.5 shows the trend of percentage reduction of ethylene over time. It is possible to observe a slight increase in reduction during the time, indicating that reaction time influenced the material activity. The cylinders exposed to light showed a faintly higher reduction, however, no statistically significant differences were found compared to setup not exposed to UV-A light. The reached

decomposition was about 20% after 210 minutes. Final measured C_2H_4 content in the gaseous mixture was 2 ppm.

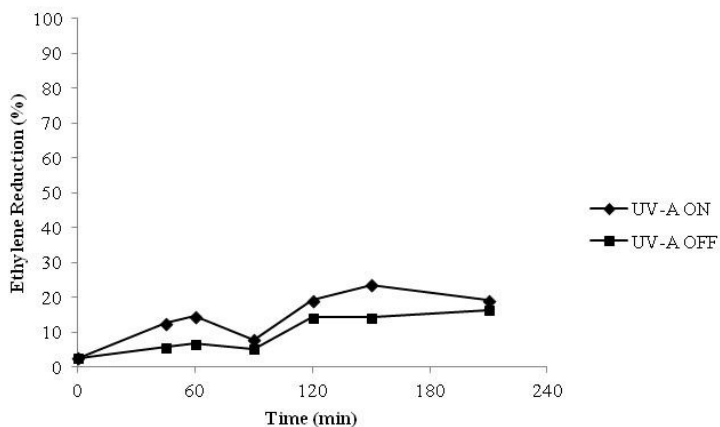


Figure 4.3.5. *Exp4*. Trend of ethylene degradation percentage over time. Photocatalytic material: *Alumina-TiO₂*, flow rate: 1.5 mL min^{-1} ; $[C_2H_4]$: 2.5 ppm. UV-A ON: cylinders containing 1 g alumina-based TiO_2 exposed to UV-A light (80 lux). UV-A OFF: cylinders containing 1 g alumina-based TiO_2 not exposed to UV-A light.

The same setup was performed comparing the alumina- TiO_2 samples to a control cylinder. The results are represented in Figure 4.3.6, showing ethylene reduction trend in mixtures flushed through the cylinder containing the alumina-based material and exposed or not to ultraviolet radiation (UV-A ON, UV-A OFF) and the control (CTRL: empty cylinder, not exposed to ultra violet light) (*exp5*).

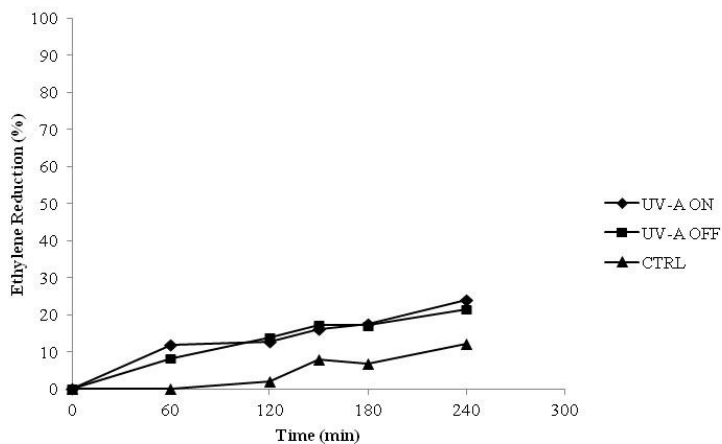


Figure 4.3.6. *Exp5*. Ethylene degradation percentage over time. Photocatalytic material: *Alumina-TiO₂*, flow rate: 1.5 mL min⁻¹; [C₂H₄]: 2.5 ppm. UV-A ON: cylinders containing 1 g alumina-based TiO₂ exposed to UV-A light. UV-A OFF: cylinders containing 1 g alumina-based TiO₂ not exposed to UV-A light.

After 240 minutes the same reduction percentage in ethylene content in UV-A ON and UV-A OFF cylinders occurs. During 4 hours of treatment the ethylene reduction percentage gradually increase. As in the previous experiment the maximum reached reduction was about 20%. This reduction was higher than that observed in the control cylinder. Control sample reached final percentage reduction of 10%. However, no significant differences between sample exposed or not to the light was observed.

In further tests we proceeded with more reduction of the flow-rate of the gaseous mixtures fluxed in the cylinders: from 1.5 mL min⁻¹ to 0.5 mL min⁻¹. Figure 4.3.7 reports the trend of ethylene decomposition over the treatment time (*exp6*). At the end of the treatment one half of the initial content of ethylene in the mixture was observed. Even in this case, the effect of UV exposure appears to be not significant, instead the control differs significantly from samples containing TiO₂ (UV-A ON and UV-A OFF) after 240 minutes. As already established the higher the reaction time, the higher the reduction: constant increase in percentage reduction was observed during the time. Moreover, reducing flow-rate the reduction was higher,

due to the longer contact time. At the end of the trial, 50% of the initial ethylene concentration was reached.

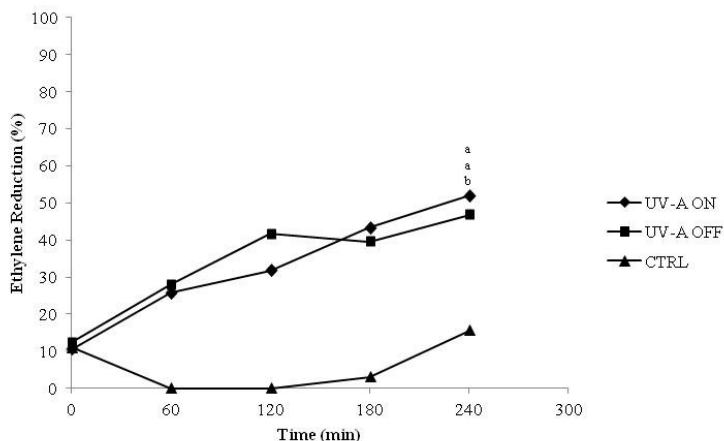


Figure 4.3.7. *Exp6*. Ethylene degradation percentage over time. Photocatalytic material: *Alumina-TiO₂*, flow rate: 0.5 mL min⁻¹; [C₂H₄]: 2 ppm. UV-A ON: cylinders containing 1 g alumina-based TiO₂ exposed to UV-A light (4 x 18W). UV-A OFF: cylinders containing 1 g alumina-based TiO₂ not exposed to UV-A light. CTRL: cylinders not containing TiO₂ and not exposed to UV-A light. Means with different letters during the same sample time are significantly different according to the Tukey test (P value ≤ 0.05).

Tests were also carried out in closed system (*exp7*). Results are shown in the graph in Figure 4.3.8. As in previous case, UV exposure had no significant effect on the reduction of ethylene, while after 240 and 300 minutes ethylene content in the control cylinder was significantly different from the TiO₂ treated gaseous mixture. As can be seen in the figure the greater the contact time the greater the reduction. Similar trend was observed for UV-exposed and UV-not exposed samples. The reduction rate showed the same slope in both cases. After 5 hours 60% of the initial ethylene was destroyed, reaching final ethylene concentration of 0.8 ppm. Compared with flow-through system it is possible to observe a larger reduction, due, also in this case, to the higher contact duration.

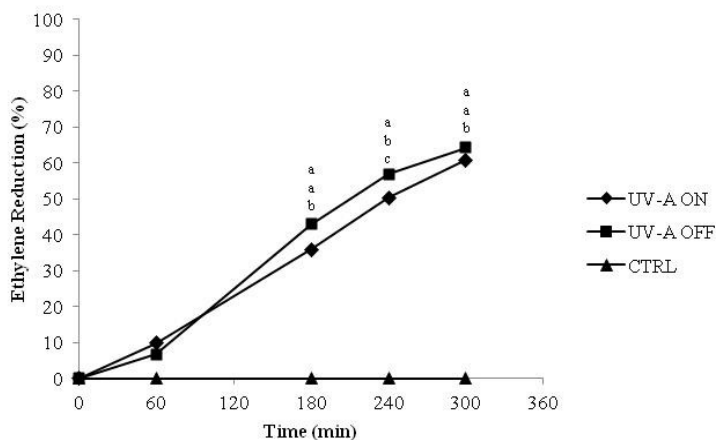


Figure 4.3.8. *Exp7*. Ethylene degradation percentage over time. Photocatalytic material: *Alumina-TiO₂*; closed system; [C₂H₄]: 2 ppm. UV-A ON: cylinders containing 1 g alumina-based TiO₂ not exposed to UV-A light (4 x 18W). UV-A OFF: cylinders containing 1 g alumina-based TiO₂ not exposed to UV-A light. CTRL: cylinders not containing TiO₂ and not exposed to UV-A light. Means with different letters during the same sample time are significantly different according to the Tukey test (P value ≤ 0.05).

Given the absence of significant influences of ultraviolet radiation on the percentage reduction of ethylene we can assume that such a reduction is caused by the alumina-based photocatalytic support rather than by the activation of the titanium oxide due to the ultra violet radiation. Aluminum oxide (or alumina) is generally useful as a drying agent and adsorbent for organic substances. It has high porosity (pore sizes ranging from 1.5 to 6 nm) that gives a high specific surface and a large adsorption capacity per unit weight (Srivastava and Eames, 1998). These experiments show that these particular type of photocatalytic materials supported on alumina are able to remove ethylene by means of adsorption rather than photocatalytic activity. As described for the reported results adsorption capacity is dependent by contact time between the used material and the ethylene. Extending this time the possibility that ethylene is adsorbed by alumina increases. Closed system represents the best technique to reduce C₂H₄ atmosphere concentration as it allows the greatest contact time.

5. Study of mesoporous mixed SiO₂/TiO₂ nanocomposites photocatalytic activity

5.1. Materials and Methods

- Mesoporous mixed SiO₂/TiO₂ nanocomposites synthesis

Mesoporous mixed SiO₂/TiO₂ nanocomposites were synthesized in aqueous solution by using pluronic F127 (EO₁₀₆ PO₇₀ EO₁₀₆), a nonionic triblock copolymer, as a sacrificing template in order to get the ordered mesopores. Four samples with different TiO₂/SiO₂ weight percentage were prepared in order to see the effect of SiO₂ on the structure and photocatalytic efficiency of the nanocomposites. The samples are denoted as T-SBA 10, T-SBA 91, T-SBA 82, T-SBA 73 and T-SBA 01 (where for T-SBA 10: TiO₂=100% and SiO₂=0%, for T-SBA 91: TiO₂=90% and SiO₂=10%, for T-SBA 82: TiO₂=80% and SiO₂=20%, for T-SBA 73: TiO₂=70% and SiO₂=30% and for T-SBA 01: TiO₂=0% and SiO₂=100%). In each case total metal oxide content in the solution was maintained to the equivalent amount of 12,256 g. To prepare the solution, first 28 g of F127 (Sigma-Aldrich) was dissolved in 150 g of water and 600 g of 2M HCl and stirred until it fully dissolved. Then equivalent amount of titanium isopropoxide (TTIP, Sigma-Aldrich, 34.88 g for T-SBA 82 sample) was added dropwise to the above acidified polymeric aqueous solution. At this moment the precipitate of titanium hydroxides was observed which turned into a clear sol after stirring of about 1 h. Then 8.498 g of TEOS (Tetraethoxysilane, Sigma-Aldrich) was added dropwise and stirring was continued to another 1 h. Then the obtained solution was placed in a polypropylene bottle with closed cap and heated for 24 h in an oven at 100 °C with static condition. After this step a solid product was obtained which was subjected to heat treatment 550 °C for 6 h with the increasing and decreasing ramp of 8h to remove the polymer template. After this step pure white powders were obtained.

5.1.2. Experimental setup

Three different experimental plans were carried out in order to evaluate photocatalytic activity of mesoporous mixed SiO₂/TiO₂ nanocomposites.

- Trial 1

The first experiment concerned the comparison between the synthesized materials to select the most active. Photocatalytic reactors, represented by glass cylinders as described at point 3.1, were filled with 0.5 g of each material (T-SBA-10, T-SBA-91, T-SBA-82, T-SBA-73, T-SBA-01). Empty cylinder shielded from UV-light was used as control (CTRL). Gaseous ethylene at 1.5 ppm concentration was flushed across the photoreactors at 1 mL min⁻¹. All the samples were exposed to UV-A light provided by four black light lamps (OSRAM L18/73 SUPRABLACK™). The same setting was used to perform a trial in a closed system.

- Trial 2

The most effective material selected from trial 1 was used to carry out further experiments. Its photocatalytic efficiency against ethylene was compared to the oxidant activity of a commercial formulate based on potassium permanganate (Purafil®, Doraville, USA) as positive control and empty and not illuminated cylinder as negative one. Also SiO₂ adsorption activity (T-SBA 01 sample) was monitored. To evaluate the effect of light exposure, the photocatalytic material was exposed (UV ON) or not (UV OFF) to black light lamps. Ethylene concentration in mixture was fixed at 2.5 ppm, at 0.5 mL min⁻¹. Temperature in the room was about 15 °C.

The five treatments are summarized below:

1. T-SBA 82 (UV ON) 0.5 g
2. T-SBA 82 (UV OFF) 0.5 g
3. T-SBA 01 0.5 g
4. PURAFIL 50 g
5. CTRL (no photocatalytic material, no UV light)

This setup was evaluated also as closed system, using an initial concentration of C_2H_4 of 1 ppm.

- Trial 3

In this test, photocatalytic activity of 0.5 g T-SBA 82 exposed or not to UV light, was monitored over time. After three hours of exposure, UV ON sample was shielded from light for two hours, and illuminated again for further two hours, in order to better investigate the impact of ultra violet light exposure on photocatalytic activity of silica-based TiO_2 material. Ethylene content of gaseous mixture was 8 ppm. Flow rate was maintained at 0.5 mL min^{-1} .

5.2. Results and Discussions

- Trial 1

Composite photocatalytic materials were designed by immobilization of titanium oxide on support with large surface areas in order to condense gaseous ethylene and to enhance the photocatalytic activity (Wang *et al.*, 2009). Using mesoporous mixed SiO_2/TiO_2 nanocomposites, ethylene reduction (expressed as percentage difference between input and output mixture) was monitored after 1, 3, 20 and 24 hours of continuous flow under UV-A light. Figure 5.2.1 shows the obtained results. The maximum reduction of ethylene (80%) was observed for the cylinder containing T-SBA 73 and T-SBA 82 photocatalytic powders. Already after 3 hours T-SBA 73 sample was able to decompose 74% of initial gaseous ethylene, while T-SBA 82 powder reached this result at the 20th hour of treatment (75%). This reduction rate was maintained up to 24 hours. These materials showed the best performances during the trial, allowing to reach low concentration of ethylene in the outgoing mixture (about 0.3 ppm). The other materials showed instead significantly lower photocatalytic activity. T-SBA 91 material, containing 90% of active titanium oxide, ranged between reductions percentage of 40 and 60%. TiO_2 powder alone (T-SBA 10) presented instead the lowest photooxidation capacity among the titanium-based materials. After 24 hours the maximum reduction was 48%, with a

final C₂H₄ concentration equal to 0.8 ppm. It is possible to observe that the higher the TiO₂ content, the smaller the reduction of C₂H₄. This behavior is probably due to the adsorption capacity of silica (Wang *et al.*, 2009). In fact, while the content of titanium oxide in the powder increases, the silica decreases, exerting smaller adsorption action. On the contrary, decomposition activity of the 100% TiO₂ material is exclusively due to its light-dependent activity, and therefore is lower. Silica 100% nanocomposite (T-SBA 01) was able to reduce ethylene of about 40%, being significantly different from the photocatalytic samples. It is possible to assimilate adsorption capacity of silica with that of activated carbon. It has been reported (Wang *et al.*, 2009) that TiO₂ supported on activated carbon shows synergistic effect based on the ability of activated carbon to adsorb pollutants and the photocatalytic activity of titanium oxide. (Baek *et al.*, 2013). This effect is due to the presence of a common contact interface created between the solids (Matos *et al.*, 2001; Ao *et al.*, 2008). In literature is reported that the adsorption could generally enhance the photocatalytic rate, but if the adsorption rate is much faster than the photocatalytic rate, the over-adsorbed molecules could inhibit photocatalytic reactions (Baek *et al.*, 2013). In this case it is possible to confirm the general behavior of composite materials reported by Baek and co-workers. When the silica amount increased, a higher reduction percentage was observed. inversely with respect to the titanium content. Since the reduction increased steadily, in this trial, no inhibition of photocatalytic activity of titanium oxide occurred.

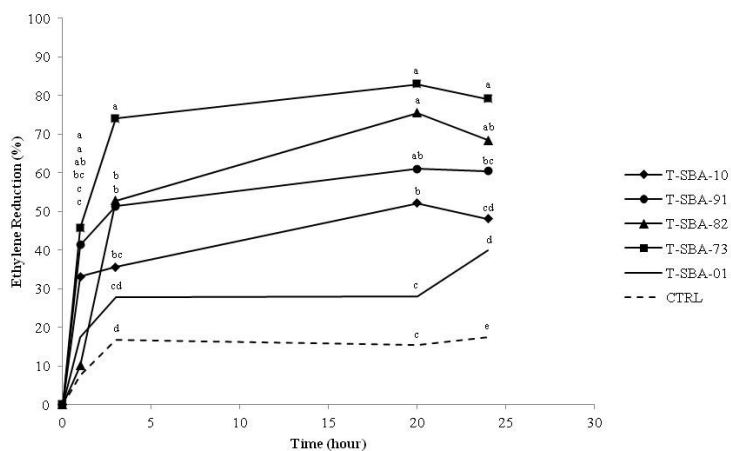


Figure 5.2.1. *Trial 1*. Ethylene degradation percentage over time. Photocatalytic material: mesoporous mixed $\text{SiO}_2/\text{TiO}_2$ nanocomposites; flow rate: 1 mL min^{-1} ; $[\text{C}_2\text{H}_4]$: 1.5 ppm. T-SBA 10: cylinders containing 0.5 g TiO_2 100% exposed to UV-A light, T-SBA 91: cylinders containing 0.5 g TiO_2 90%/ SiO_2 10% exposed to UV-A light, T-SBA 82: cylinders containing 0.5 g TiO_2 80%/ SiO_2 20% exposed to UV-A light, T-SBA 73: cylinders containing 0.5 g TiO_2 70%/ SiO_2 30% exposed to UV-A light, T-SBA 73: cylinders containing 0.5 g SiO_2 100% exposed to UV-A light, CTRL: cylinders not containing $\text{TiO}_2/\text{SiO}_2$ and not exposed to UV-A light. Means with different letters during the same sample time are significantly different according to the Tukey test ($P \text{ value} \leq 0.05$).

Concerning the closed system test (data not shown), after 16 hours, all the samples containing TiO_2 completely decompose ethylene under UV illumination, with no difference due to the actually titanium oxide amount in the mesoporous material. T-SBA 01 sample (100 % silica) showed a maximum percentage reduction equal to 80%, probably due to the saturation of the adsorption capacity of the powder. 0.5 g of silica were able to adsorb about 1.6 ppm of gaseous ethylene.

On the basis of the obtained results the selected sample for the subsequent tests was the T-SBA 82 containing 80% of TiO_2 and 20% of SiO_2 . It showed, like the T-SBA 73 sample, the highest photooxidation activity reducing ethylene up to 80% of the initial concentration.

- Trial 2

The described experiments was performed in order to assess the light-depending catalytic activity of mesoporous mixed $\text{SiO}_2/\text{TiO}_2$ nanocomposites composed by 80% titanium oxide and 20% silica. Also a comparison with silica adsorbption capacity and potassium permanganate oxidant activity were tested. Figure 5.2.2 shows the evolution of ethylene degradation in a dynamic system. The glass cylinder containing T-SBA 82 and exposed to light (T-SBA 82 UV ON) demonstrated the ability to completely destroy ethylene after 120 minutes of treatment up to 300 minutes. Also potassium permanganate-based formulate (PURAFIL) totally eliminate ethylene after one hour. As expected, photocatalytic sample not exposed to UV light (denoted in the graph as T-SBA 82 UV OFF) showed the same reduction capacity of silica alone. Their reduction capacity increased during time reaching a final percentage of about 70%. This result confirmed the previous one (Trial 1, closed system). 1.6 ppm of C_2H_4 were adsorbed by 0.5 g of silica. When ultra violet light did not activate the photocatalytic material it is demonstrated that the ethylene reduction was given only by adsorbtion capacity of silica.

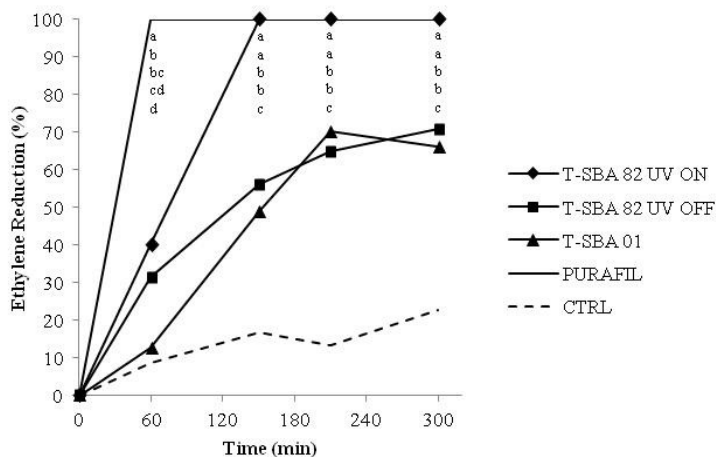


Figure 5.2.2. *Trial 2*. Ethylene degradation percentage over time. Photocatalytic material: *Mesoporous mixed SiO₂/TiO₂ nanocomposites*, flow rate: 0.5 mL min⁻¹; [C₂H₄]: 2.5 ppm. T-SBA 82 UV ON: cylinders containing 0.5 g T-SBA 82 exposed to UV-A light (4 x 18W), T-SBA UV OFF: cylinders containing 0.5 g T-SBA 82 not exposed to UV-A light, T-SBA 01: cylinders containing 0.5 g T-SBA01 (silica 100%), PURAFIL: cylinders containing 50 g potassium permanganate, CTRL: cylinders not containing SiO₂/TiO₂ material and not exposed to UV-A light. Means with different letters during the same sample time are significantly different according to the Tukey test (P value ≤ 0.05).

The same trend was observed in closed-system trial (Figure 5.2.3). Silica-based TiO₂ illuminated by 4 black light lamp and KMnO₄-based material had the best activity and T-SBA 82 not exposed to UV and silica performed similarly during all the experiment, showing no statistically significant differences. Moreover, it is possible to observe that reducing ethylene concentration the light-exposed material reduced it faster. Also the use of closed system, increasing contact time between pollutant and adsorbing active sites, enhanced this elimination of ethylene from the atmosphere. In fact, starting from 1 ppm of gaseous C₂H₄ in the mixture a final concentration of 0.15 ppm was reached, showing a reduction activity higher than the previous test.

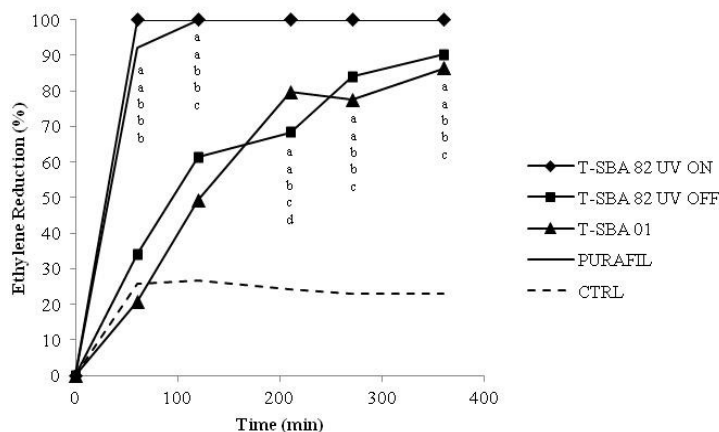


Figure 5.2.3. *Trial 2*. Ethylene degradation percentage over time. Photocatalytic material: *Mesoporous mixed SiO₂/TiO₂ nanocomposites*, closed system, [C₂H₄]: 1 ppm. T-SBA 82 UV ON: cylinders containing 0.5 g T-SBA 82 exposed to UV-A light, T-SBA 82 UV OFF: cylinders containing 0.5 g T-SBA 82 not exposed to UV-A light, T-SBA 01: cylinders containing 0.5 g T-SBA 01 (silica 100%), PURAFIL: cylinders containing 50 g potassium permanganate, CTRL: cylinders not containing SiO₂/TiO₂ material and not exposed to UV-A light. Means with different letters during the same sample time are significantly different according to the Tukey test (P value ≤ 0.05).

- *Trial 3*

In the last part of this section, the behavior of T-SBA 82 nanocomposite material interrupting the light exposure (*UV off* phase in the graph) and lighting up again was tested. In this case C₂H₄ concentration was incremented in order to slow its decomposition and better monitoring it. The lowest flow was maintained to allow the highest contact time between the photocatalyst and ethylene-enriched atmosphere. The graph below (Figure 5.2.4) shows the evolution of percentage reduction of ethylene during the time. It is possible to note that, when the cylinder was exposed to the lamps, the photocatalytic material exerted its activity against ethylene (reducing it up to 80%, final measured content 1.4 ppm). After two hours without ultra violet light, this activity significantly decreased reaching the one of T-SBA 82 UV OFF treatment, and started once again as soon as it was exposed again

to light. After 7 hours almost all ethylene was destroyed by UV-exposed T-SBA 82. Shielded cylinder reduction activity significantly differed from the light exposed one at each sample time, showing a slight increasing trend during the trial. Maximum reached ethylene reduction was about 50%.

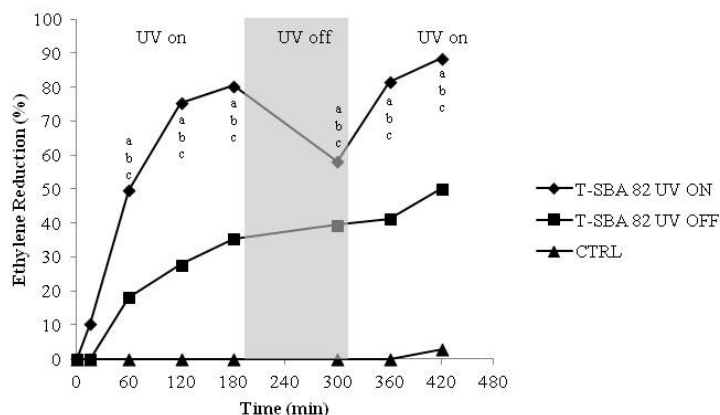


Figure 5.2.4. *Trial 3*. Ethylene degradation percentage over time. Photocatalytic material: mesoporous mixed SiO₂/TiO₂ nanocomposites, flow rate: 0.5 mL min⁻¹; [C₂H₄]: 8 ppm. T-SBA 82 UV ON: cylinders containing 0.5 g T-SBA 82 exposed to UV-A light (2 x 18W), T-SBA 82 UV OFF: cylinders containing 0.5 g T-SBA 82 not exposed to UV-A light, CTRL: cylinders not containing photocatalytic material and not exposed to UV-A light (4 x 18W). Means with different letters during the same sample time are significantly different according to the Tukey test (P value ≤ 0.05).

These results demonstrated that the synthesized materials possessed a powerful photocatalytic activity, being able to completely destroy ethylene in gaseous mixture that passes through them. Increasing C₂H₄ concentration in the mixture allowed to reduce photocatalytic destruction rate, as well as reducing gas flow-rate or closing the system enhanced ethylene decomposition. Since the difference between silica adsorption capacity and the photocatalytic oxidation of TiO₂-containing materials against ethylene was high and significant, the best choice for further experiments resulted to be the composite materials. The enhanced capacity to eliminate ethylene from storage rooms could be useful for postharvest industry.

For this reason, these materials could be suitable to develop SiO₂/TiO₂-doped packaging material for fresh fruit and vegetable and photocatalytic equipments for fluidized bed photoreactor. Further trials (at section 6. *Ethylene reduction efficacy of photocatalytic mixed SiO₂/TiO₂ nanocomposites and effects on ripening of mature-green tomatoes*) were performed to test the effect of this activity on plant tissues.

6. Ethylene reduction efficacy of photocatalytic mixed SiO₂/TiO₂ nanocomposites and effects on ripening of mature-green tomatoes

6.1. Materials and Methods

- Plant material

For biological test of photocatalytic activity of SiO₂/TiO₂ nanocomposites, mature green tomatoes were chosen due to its high ethylene sensitivity, and because ripening evolution could be easily monitored by observing the color changes of the external surface. Mature green tomatoes will ripen after harvesting in the same fashion as they would on the plant, and ethylene in storage atmosphere strongly influences ripening rate. Tomato fruits were harvested from organic greenhouses in Valenzano (Bari, Italy) and transferred to the Postharvest laboratory of the Dept. SAFE, at University of Foggia. Tomatoes were stored at 15 °C until use. Damaged or overmature fruit were discarded. Four tomatoes for each treatment were used, the single fruit represented a replicate.

- Ripening evaluation

The effect of ethylene on ripening rate of tomatoes was evaluated through the change of color of the epicarp from green to red. Color change was measured elaborating the images acquired with a Spectral scanner (DV SRL, Italia). The external surface of the tomatoes were scanned. The areas to be analyzed were manually selected. On these regions, color in CIE L*a* b* scale was measured. From the primary L*, a*, and b* values the following indexes were calculated:

- Hue angle $h^\circ = \arctan \frac{b^*}{a^*}$
- Chroma $C = \sqrt{a^{*2} + b^{*2}}$
- Global color variation $\Delta E = \sqrt{(L_0^* - L_t^*)^2 + (a_0^* - a_t^*)^2 + (b_0^* - b_t^*)^2}$

6.1.2. Experimental setup

Tomatoes were treated with three different gaseous mixture, according to the setup reported in Figure 6.1.2.1. Four green tomatoes were placed in 5 L plastic containers for flow-through treatment. C₂H₄ sample was flushed with 2 ppm ethylene at 2 mL min⁻¹ for three days. As for C₂H₄TiO₂ sample, it was processed with the same ethylene mixture previously flushed inside photocatalytic glass cylinder containing 0.5 g of T-SBA 82 powder and exposed to UV-A light. Photocatalytic material was obtained as described at point 5.1. Control sample (CTRL) was treated with air. Tomatoes were then stored in air at 15 °C for further 11 days, in order to follow the ripening evolution over time. Images and color parameters of fruits surface were acquired at initial time, and after 3, 7 and 14 days of storage.

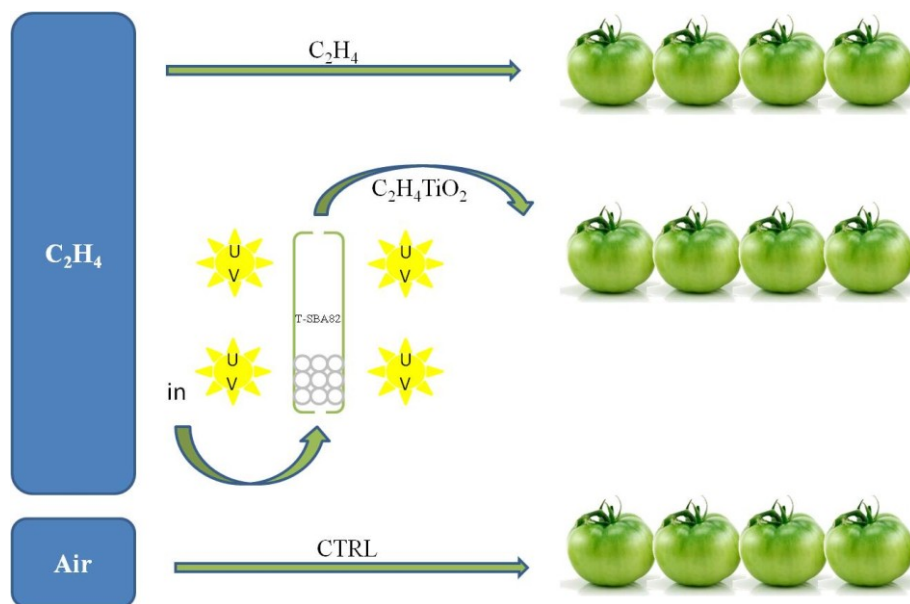


Figure 6.1.2.1. Experimental setting to evaluate effects of photocatalytic mixed SiO₂/TiO₂ nanocomposites on ripening of green mature tomatoes.

6.2. Results and Discussions

Ripening is a process of fruit development, which can be described as a result of biochemical and physiological changes leading to a ripe stage that culminates in changes in colour, texture, and flavour. Tomato is a climacteric fruit, and its ripening process is associated with a climacteric peak during the veraison phase. Among the physiological changes occurring during ripening of red-fleshed tomatoes, color evolution is the most evident to identify fruit maturity stages, and their corresponding characteristics. Tomato colour is the first external peculiarity which determines consumers acceptance. Colour changes verify at various stages of tomato development in terms of chlorophyll (green colour), β -carotene (orange colour) and lycopene (red colour) contents. The most visible changes are associated with chlorophyll loss (green colour) and gradual accumulation of lycopene (red colour), where plastids such as chloroplasts present in the mature-green fruit are transformed into chromoplasts. Transformation of chloroplasts to chromoplasts normally occurs simultaneously with other ripening changes such as cell wall softening (Bathgate *et al.*, 1985). USDA classified ripeness stages of tomatoes according to epicarp color (Figure 6.2.1).

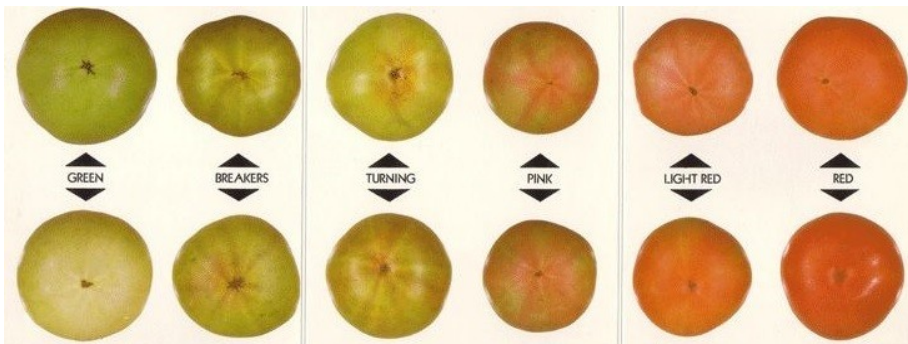


Figure 6.2.1. Color chart of maturity stages of tomatoes (adapted from USDA, 1991)

Surface color description for each stages is reported below (USDA, 1991):

- *Green*: surface is completely green; the shade of green may vary from light to dark.
- *Breaker*: there is a definite break in color from green to tannish-yellow, pink or red on not more than 10% of the surface.
- *Turning*: 10% to 30% of the surface is not green; in the aggregate, shows a definite change from green to tannish-yellow, pink, red, or a combination thereof.
- *Pink*: 30% to 60% of the surface is not green; in the aggregate, shows pink or red color.
- *Light red*: 60% to 90% of the surface is not green; in the aggregate, shows pinkish-red or red.
- *Red*: more than 90% of the surface is not green; in the aggregate, shows red color.

As shown in Figure 6.2.2, mature green tomatoes had different ripening trend. After the first three days, in which the fruits were treated with the three different gaseous mixture, no difference were observed in visual appearance of the external surfaces. Subsequently, as expected, C_2H_4 treated sample showed a faster and more uniform ripening during storage time as shown by color changes. “Turning” maturity stage was in fact reached after seven days. Conversely, CTRL and $C_2H_4TiO_2$ samples were at “breakers” stage and did not show the same color uniformity. These differences were maintained until the last day of storage (*day 14*). At the end of the trial ethylene plus titanium oxide-treated tomatoes did not reach “red” stage, showing less ripening occurrence compared to ethylene-treated samples. Air-flushed tomatoes showed instead an irregular ripening evolution, as it is possible to observe tomatoes at turning, pink and light red maturity stages. Only tomatoes treated with 2 ppm of ethylene achieved uniform red stage. In any case no symptoms of disorders were observed. These differences was the first evidence of the effect of photocatalytic oxidation of C_2H_4 by T-SBA 82.



Figure 6.2.2. Ripening evolution of tomatoes during the storage time. CTRL: sample air-treated, C2H4TiO2: tomatoes treated with ethylene ($2 \text{ ppm mL min}^{-1}$) and 0.5 g of photocatalytic powder T-SBA 82 for 3 days, C2H4: tomatoes treated with $2 \text{ ppm mL min}^{-1}$ for three days.

In order to confirm differences in color visually evaluated, measured color parameters was analyzed. Also in this case it is possible to observe that CTRL and C2H4TiO2 samples followed the same maturation trends. Figure 6.2.3(a) reports the evolution of a^* value of tomatoes surface. On day 3 and day 7 this parameter was similar for all the samples. Only at the last sampling day the C_2H_4 -treated sample differed in a statistically significant way from the other samples.. Positive a^* values represent the red index in the CIE $L^*a^*b^*$ scale, and higher values indicates riper fruits. As expected, ethylene-treated tomatoes showed significant higher a^* value than the other samples, reaching an average final value of 31.3, compared to about 23 of the other analyzed tomatoes. The same difference was observed regarding the global color variation value ΔE (reported in Figure 6.2.3(b)). The significant difference between C2H4 sample and C2H4TiO2 and CTRL indicates an appreciable color difference of the fruits. Tomatoes processed with 2

ppm of ethylene showed a greater color variation compared to day 0. Since this change was accompanied by a higher a^* index, it can be concluded that these tomatoes, at the end of storage time, were statistically more red and, hence, more mature.

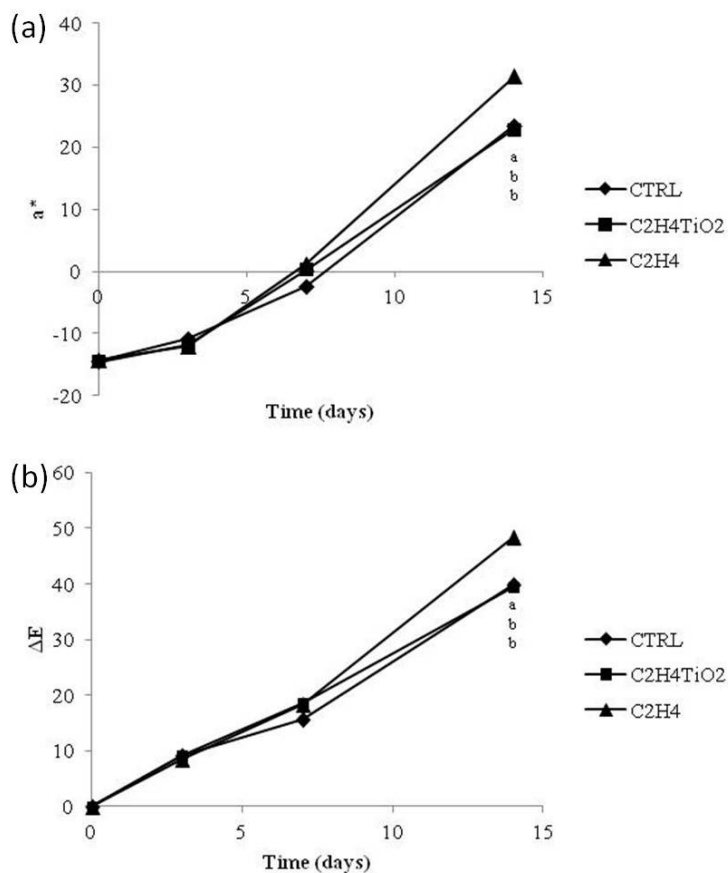


Figure 6.2.3(a)(b). Color parameters evolution of tomatoes surface during the time. CTRL: sample air-treated, C2H4TiO2: tomatoes treated with ethylene (2 ppm mL min⁻¹) and 0.5 g of photocatalytic powder T-SBA 82 for 3 days, C2H4: tomatoes treated with 2 ppm mL min⁻¹ for three days. Means with different letters during the same sample time are significantly different according to the Tukey test (P value \leq 0.05).

Chroma value represents the color intensity and the saturation of the tomatoes epicarp. Also concerning the evolution of this parameter, (Figure 6.2.4), significant differences occurred between control and TiO₂-treated samples compared to ethylene-treated fruit during the time. At the end of the trial the latter showed higher Chroma value (50.1), compared to about 44 of the other treatments, indicating fruits more red and more uniform, as can be seen also in the picture. In this case slight differences were observed also at the previous sampling time, and ethylene-treated berries showed higher Chroma values during all storage, while air and ethylene/TiO₂ samples followed a more irregular trend.

Moreover, C₂H₄ tomatoes reached a significantly lower final mean Hue angle value (Figure 6.2.5), indicating also in this case, more red surfaces of the product. Hue angle higher than 90°, in the second quadrant of L*a*b* color space, indicates green color, and represented the starting condition of tomatoes surface. During ripening, this value decreased up to 50° for ethylene-treated tomatoes and 60° for the other samples, positioning in the first quadrant, corresponding to red color. The lower the Hue angle, the more ripen the fruits. Significant differences occurred on day 14 of storage, while previously the three treatment did not show any difference for this parameter.

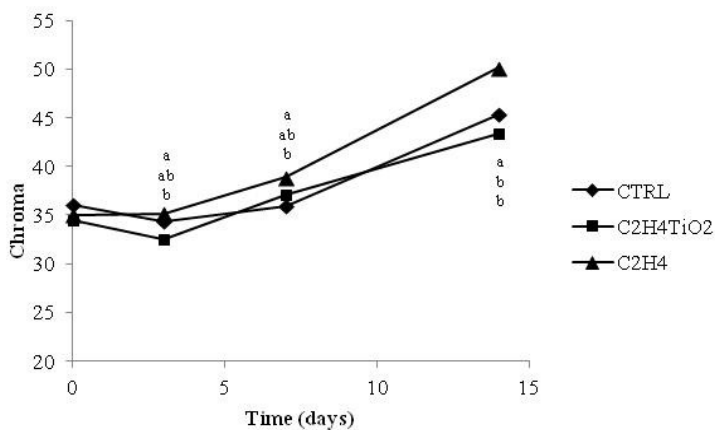


Figure 6.2.4. Evolution of Chroma value of tomatoes epicarp during storage time. CTRL: sample air-treated, C2H4TiO2: tomatoes treated with ethylene (2 ppm mL min⁻¹) and 0.5 g of photocatalytic powder T-SBA 82 for 3 days, C2H4: tomatoes treated with 2 ppm mL min⁻¹ for three days. Means with different letters during the same sample time are significantly different according to the Tukey test (P value ≤ 0.05).

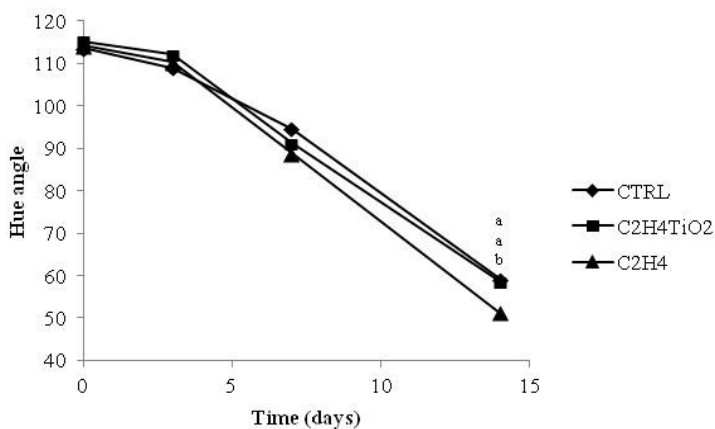


Figure 6.2.5. Evolution of Hue angle value of tomatoes epicarp during storage time. CTRL: sample air-treated, C2H4TiO2: tomatoes treated with ethylene (2 ppm mL min⁻¹) and 0.5 g of photocatalytic powder T-SBA 82 for 3 days, C2H4: tomatoes treated with 2 ppm mL min⁻¹ for three days. Means with different letters during the same sample time are significantly different according to the Tukey test (P value ≤ 0.05).

Given the obtained results it is possible to conclude that mixed $\text{SiO}_2/\text{TiO}_2$ nanocomposites containing 80% TiO_2 and 20% SiO_2 (T-SBA 82) is effective in reducing the concentration of ethylene in the atmosphere surrounding the product, thus delaying ripening of tomatoes. Its photocatalytic activity was exerted versus exogenous ethylene, resulting in its complete elimination from the atmosphere. Tomato fruits showed high sensitivity to this variation, and tissues response was strongly influenced by the presence of the photocatalyst.

7. Design of a fluidized bed photoreactor for ethylene oxidation on mesoporous mixed $\text{SiO}_2/\text{TiO}_2$ nanocomposites under UV-A illumination

7.1. Fluidized bed photoreactor and fluidization regimes

As previously described (section 1.3), fluidized bed photoreactor (FBP) could represent an innovative technology to remove ethylene in postharvest storage room atmosphere. It has many advantages such as the possibility to treat continuously the polluted gaseous mixture, to work at room temperature, while having low energy requirements. Titanium oxide-based materials are suitable for use in fluidized bed photoreactor to exert its photooxidation action against ethylene. FBP provides, in fact, good mixing of catalyst and pollutants, TiO_2 surface exposure to UV radiation due to catalyst circulation, and low mass transfer resistance (Nelson *et al.*, 2007; Imoberdorf *et al.*, 2008; Vega *et al.*, 2011; Baek *et al.*, 2013). However, TiO_2 powder is classified into Geldart C group having a poor fluidization behavior (Lim *et al.*, 2000a-b). It is necessary to choose an UV-transparent material to support titanium oxide for its use in the reactor. The configuration of the FBP should allow to easily insert an adequate number of UV lamps that produce a uniform and diffuse radiation on active sites of the photocatalyst surface in order to achieve a high mass transfer coefficient between the gas phase and the catalytic surface of the supported TiO_2 . Both of these aspects (high accessibility to ethylene of catalytically active sites and intense irradiation of the reaction volume) should contribute to increase the efficiency of the reactor compared to other configurations.

Generally, fluidization occurs when solid microparticles are suspended in an upward-flowing stream of fluid. Reactions in fluidized beds are described by the Kunii-Levenspiel bubbling-bed model. As the reactant gases form ascending bubbles, mass transfer takes place as they flow in and out the mass of solid particles, thus enhancing the photocatalytic reaction. The rate at which the reactants and products transfer in and out of the bubble affects the conversion, as does the time it takes for the bubble to pass through the bed (Fogler and Gürmen, 2008).

Yang (2003) considered six different fluidization behaviors for gas-solid fluidized beds: fixed bed, bubbling fluidization, slugging fluidization, turbulent fluidization, fast fluidization, and pneumatic conveying. Figure 7.1.1 shows images of the existent fluidization regimes. In the fixed bed regime the air flowing across the particle does not have enough energy to move the microparticles. As the superficial gas velocity increases, the system reaches the bubbling fluidization regime. In this regime, bubbles start to form and combine causing solid mixing; the velocity at which bubbles appeared is known as the minimum bubbling velocity. The slugging regime appears in beds where the bed height (H) over the bed diameter (D) is larger than 2. This ensures that bubbles have the time to coalesce in bigger bubbles (slugs); when the bubbles grow to $2/3$ of the bed diameter the system enters to a slugging regime.

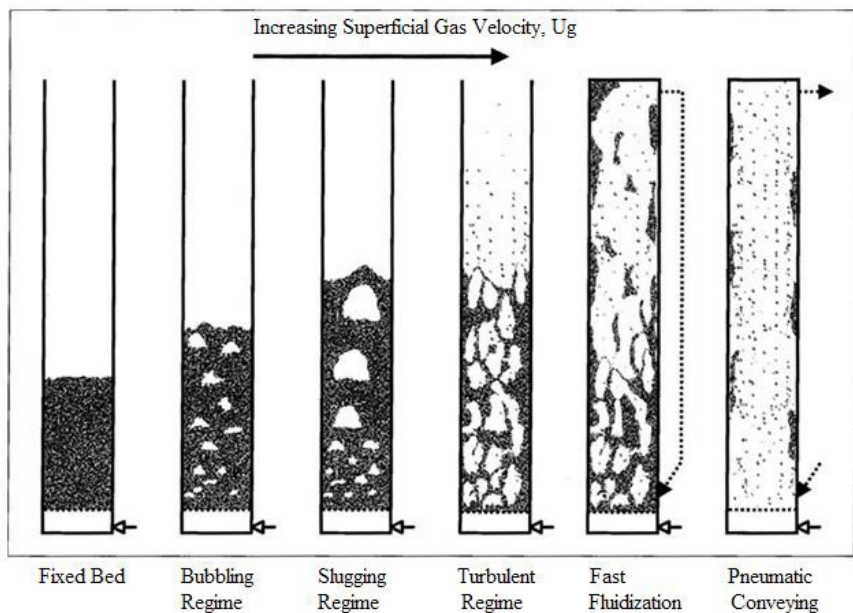


Figure 7.1.1. Fluidization regimes in a gas-solid fluidized bed (from Crowe, 2006).

Furthermore, Crowe (2006) said that turbulent fluidization occurs when, as the superficial gas velocity increased, a point is reached where the slugs begin to break down. If velocity increases a fast fluidization regime is then reached. In this

regime, solid particles exit from the reactor. Finally, the pneumatic conveying regime is reached when the superficial gas velocity is much higher than the transport velocity; this regime is characterized by the particle being transported out of the bed in a dilute phase.

7.2. *Materials and Methods*

7.2.1. *Design of fluidized bed reactor prototype*

The design and production phases of the FBP prototype were conducted in cooperation with STC s.r.l. (Mesagne, Italy). The prototype consists essentially of a tubular reactor, inside of which the titanium dioxide will be fluidized, supported on specific particles with good fluidization behavior, by the introduction of ethylene-enriched gaseous mixture flow. The structure consists of a metal square frame (side 40 cm), where the reactor and ultraviolet lamps are located. This part is closed and isolated, by means of reflecting panels to minimize the dispersion of the light. Supports for the UV lamps allow movement along the radial direction. The piping and valves are made of rigid PVC. A recirculation circuit is constituted by a pipe that collects the outgoing gas from the flange and conveys it to a compressor, which will impart to the gas the energy to overcome pressure losses due to the fluidized bed and to the recirculation line. Two branches on the discharge line allow the entry of the mixture to be treated, and the output of the gas during the washing procedure of the pipes. The return line has a sampling circuit, for gas chromatographic ethylene evaluation. The photocatalytic reactor is equipped with an electrical panel for managing the main utilities.

Features and major components of the reactor are the following:

- Compressor for air circulation (*VacuumDesign serie CS*, nominal flow 7.2 m³ h⁻¹, pressure 0.8 bar, power 300 W).
- Flowmeter (200 L min⁻¹)
- Differential Pressure Gauge (0 - 300 mbar)

- Pressure Gauge (0 - 400 mbar)
- UV Lamps (Osram FD T26 L18W-73 G13 BLB)
- Gas temperature sensor (0 - 100 °C)
- Maximum air-flow capacity (80 L min⁻¹)

In order to design the reactor several parameters were studied in order to maximize the degradation rate of ethylene in the atmosphere of cold room for storage of fresh products, such as gas flow-rate per unit of reactor volume and/or mass of the catalyst, the geometry of the reactor, and the location of the UV lamps.

Figure 7.1.2 shows the design and sizing of the tubular reactor in which the photooxidation of ethylene by titanium oxide-based material, activated by UV light, will take place. Reactor was manufactured in plexiglas because of its transparency to light. Internal volume of the cylinder is about 0.9 L. Gas flow of ethylene-contaminated air will cross the reactor containing photocatalytic material.

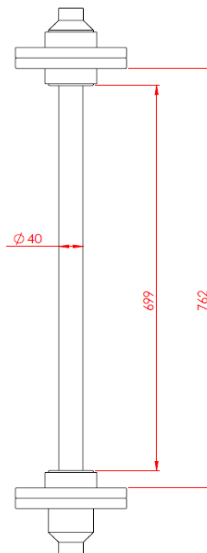


Figure 7.1.2. Rendering of the tubular plexiglas reactor for photocatalytic oxidation of ethylene (STC s.r.l.).

Piping system and instrumentation diagram (P&ID) is reported in Figure 7.1.3. Components, instrumentation and sensors previously described are positioned in the circuit according to this diagram.

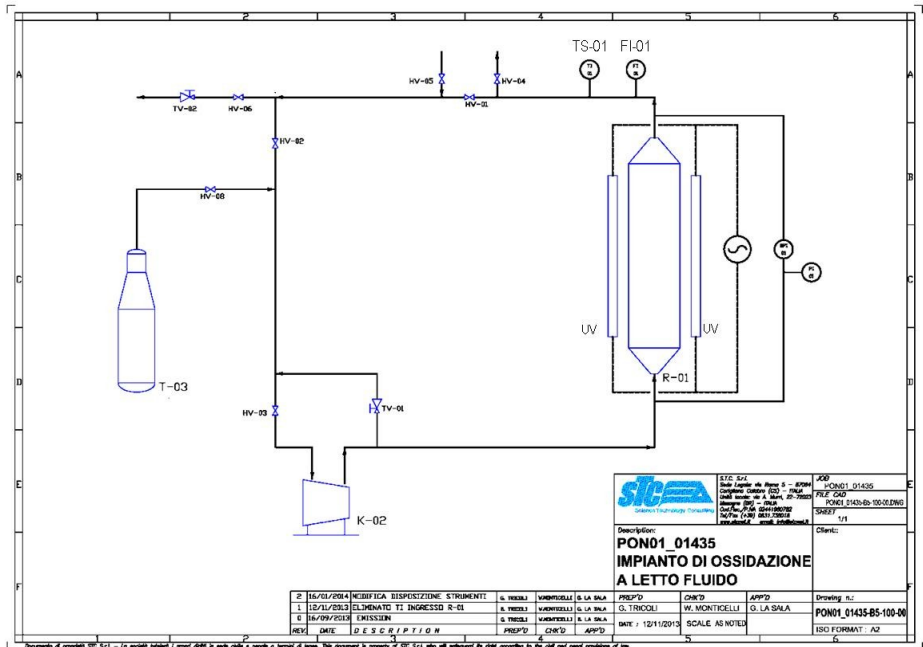


Figure 7.1.3. P&ID of fluidized bed photocatalytic reactor (STC s.r.l.).

Where:

- R-01: Photocatalytic reactor
- T-03: Gas cylinder
- K-02: Compressor
- TV 01-TV 02: Throttles
- HV-01/HV-08: Valves
- UV: UV lamps supports
- FI-01: Flowmeter
- TS-01: Temperature sensor

Some images of the reactor are shown in Figure 7.1.4.



Figure 7.1.4. Rendering (a and b) and a photo (c) of the fluidized bed photocatalytic reactor prototype (STC s.r.l.).

The photoreactor can be used in different action modes. Following, the steps to test the performance of the photoreactor with known concentration of ethylene mixture from gas cylinder (T-03) are reported. The compressor capacity will allow the mixture to drain from the tank or from the external atmosphere. The prototypal system is designed to work in continuous or batch mode. The throttle TV-01 allows to reach the optimal condition of the fluidized bed in the reactor. The flowmeter

provides the measurement of the flow actually circulating in the reactor. To start the reaction, it is sufficient to turn on the UV lamps. After the reaction time, the measurement of the content of residual ethylene allows to evaluate the level of reduction achieved. The degree of ethylene conversion can be varied increasing or decreasing the contact time between pollutant and photocatalytic surface (progressively closing or opening TV-02). In order to operate in batch mode, it is sufficient to close the exit valve before turning on the UV lamp. The system will lead to a pressure equal to the discharge pressure of the cylinder. The reaction progress can be assessed by measuring the residual ethylene content in the gas sampled at different times.

7.2.2. *Fluidization tests*

Fluidization tests were performed on tabular alumina (dimension range $0.425 \div 1$ mm), alumina microspheres (dimension range $0.75 \div 1.50$ mm), both provided by *Salentec* s.r.l. (Lecce, Italy), and glass beads (dimension 5 mm).

7.2.3. *Fluidized bed photoreactor activity evaluation*

Mixed $\text{SiO}_2/\text{TiO}_2$ -coated alumina microspheres with high porosity, were developed and tried within the FBP. Following, the coating process carried out by the Department of Engineering of University of Salento (Lecce, Italy) is described. To obtain T-SBA 73 (composed of 70% TiO_2 and 30% SiO_2), 10 g of F127 ($\text{EO}_{106}\text{PO}_{70}\text{EO}_{106}$), a nonionic triblock copolymer, was dissolved in 190 g of ethanol and 12.35 g concentrated HCl by stirring overnight. A quantity of 10.4 g of TEOS (tetraethoxysilane, Sigma-Aldrich) were added dropwise and were stirred for 1 hour. Then, 24.91 g of titanium isopropoxide (Sigma-Aldrich) were mixed to the above sol by adding slowly and stirred for 2 hours. This sol was used for coating the alumina beads in a desiccator under vacuum. After coating, the beads were annealed at $550\text{ }^\circ\text{C}$ for 1 hours.

About 360 g of coated material were inserted in the plexiglas reactor. To evaluate the FBP photocatalytic activity in decomposing ethylene, the photoreactor was used in batch mode. Exogenous ethylene was diluted within the air present in the system (about 3 L) to reach the desired initial concentration. Gaseous mixture was then treated by means of recirculating system under UV illumination. The catalytic efficiency of the photoreactor was monitored following ethylene concentration and its reduction percentage during the experiment time.

7.3. Results and Discussion

Aim of the tests was the identification of the best support for titanium dioxide powder, from the point of view of fluidization behavior. The first fluidization test was conducted on samples of tabular alumina. Within the fluidized bed compact zones occurred due to the irregularity of alumina microparticles, which hinder the gas passage. Because of this difficulty encountered by the gas, multiple beds were created. The beds ascended along the tube, collapsing when the gas pressure was no longer efficient to their sustenance. This type of fluidized bed is unstable. However, maintaining a constant flow rate of the inlet gas, the described phenomenon was attenuated, and disappeared when the redistribution of void volumes allowed a more uniform fluidization. Consequently, after a first phase of particles mixing, FBP could work in minimum fluidization conditions. On the other hand, because of the morphology of the tabular grains, a minimum change of void volume level caused the return to the previous behavior. A solution to this "multiple" behavior of the fluidized bed, could be represented by using a more uniform material. Therefore, the tabular alumina was sieved into 3 intervals defined as follows:

1. nominal size: $0.425 \div 0.85$ mm
2. nominal size: $0.85 \div 0.97$ mm
3. nominal size: $0.97 \div 1$ mm

In further tests, using the second and the third size intervals, it was possible to better fluidize the material. Creation of multiple bed still occurred, although in a less accentuated way. It was concluded that tabular alumina is not suitable as support for titanium oxide powders, given the irregularities in the size and the tendency to create multiple beds with non-uniform behavior.

To allow the maximum contact between photocatalyst and ethylene, is necessary that the fluid bed remains the most stable and uniform as possible.

Alumina microspheres, whose diameter ranged between 0.75 and 1.5 mm (Figure 7.3.1), were used for further trials, due to their more regular shape than tabular support. A minimum of 100 g of material were necessary in order to get the minimum fluidization, and the corresponding flow was about 40 L min^{-1} . In these conditions the measured pressure drops were low. Increasing the quantity of microspheres inside the reactor up to 1.8 kg and maintaining constant input flow rate, the pressure losses increased. Increasing the flow rate, pressure losses did not increase and the bed maintained the minimum fluidization condition. Due to the dispersed particle size, it was possible to observe that the void volume degree inside the bed was not uniform, and zones with different permeability characteristics occurred. This could affect the efficiency of the reactor, shielding the inner portions of the bed from UV light. Furthermore, it was clear from this test that the particle size of the material should be as least dispersed as possible in order to obtain uniform void volume degree and avoid occurrence of multiple beds when the minimum fluidization condition was respected. Two size intervals were then tested ($0.75 \div 0.97 \text{ mm}$ and $0.97 \text{ mm} \div 1.5 \text{ mm}$). The fluidization behavior of the two samples was substantially similar. The difference between the two beds was the void volume degree: material with diameters between 0.97 mm and 1.5 mm, showed a greater degree of voids, and this could represent an advantage for the optimal diffusion and distribution of ultraviolet light.



Figure 7.3.1. Alumina microspheres sample

Further tests on glass beads were also carried out. In this case the fluidization occurred with regular behavior, and no phenomena of redistribution of the voids were observed. Moreover the flow through the bed was uniform, without creating preferential channels for air passage. These characteristics are due to the high regularity of the particle size. This type of media, like the alumina microspheres, may be the most indicated for use in fluidized bed photoreactor. However, due to the results of the previous photocatalytic activity tests (reported in the section 4. *Comparison of photocatalytic properties of different titanium oxide-based materials*) TiO_2 -coated glass beads showed no ethylene reduction activity.

From the results described above alumina microspheres were finally chosen as support material for titanium oxide powders to be used in the FBP, both for their fluidization performance and for their ability to incorporate photocatalytic material. The microparticle cavities were coated with mesoporous mixed $\text{SiO}_2/\text{TiO}_2$ nanocomposite material (T-SBA 73) as previously described. A test was then carried out in order to verify potential FBP functioning and the photocatalytic activity of the developed material. The material were inserted in the tubular reactor inside the FBP. The system was closed in order to allow the continuous

recirculation of the ethylene-enriched gaseous mixture with a total flow of 80 L min⁻¹ and a pressure of 0.1 bar.

The photocatalytic material showed a “slugging” fluidization behavior, that allowed high contact time with ethylene and uniform irradiation by UV lamps.

Starting from an ethylene concentration of 40 ppm, it was observed a consistend reduction of ethylene concentration after 3 hours of treatment under UV light (47%). At the end of the experiment, after 270 minutes, it was possible to reach 11.3 ppm, with a maximum reduction percentage of about 72.5% (Figure 7.3.2).

It was possible to notice, however, that the fluidization regime caused strong collisions between the coated microspheres. As a consequence of this, the powdered coating material tended to separate from its support with a tendence of blocking reactor higher and lower filters with a progressive reduction of the flow rate and of the bed height.

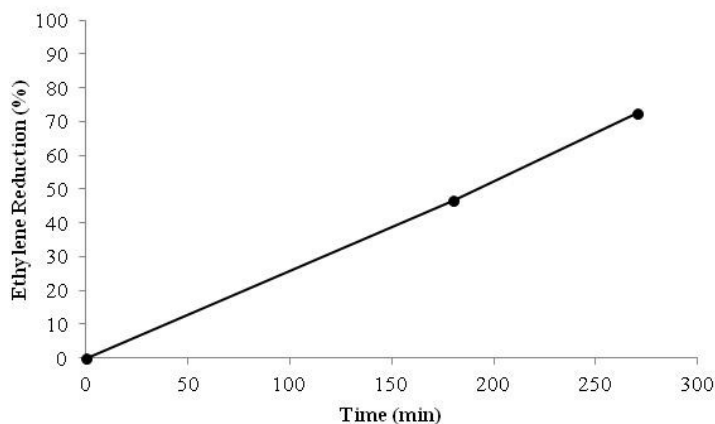


Figure 7.3.2. Rate of ethylene reduction percentage in the gaseous mixture within the fluidized bed photoreactor under UV light (2 X 18 W-lamps).

In order to carry out further, more exhaustive experiments using the FBP there is a need to better refine its efficacy, in order to make it suitable for use in presence of possibly high quantity of powder separating from its support due to unavoidable collisions during the fluidization state. On the other hand it is also important to

develop active photocatalytic material with suitable fluidization properties and minimal loss of active powder.

With the completion of FBP operation, its use will be useful for the companies to avoid the detrimental effects ethylene-related on fresh plant tissues. The technological transfer to the postharvest industry could be then carried out, with many advantages.

8. General conclusions

This work was included in the project “OFRALSER - *High-Convenience Fruits and Vegetables: New Technologies for Quality and New Products*” (PON01-01435). The general aim of this 3-years project was related to the development of new products and technologies to improve quality of fresh fruits and vegetables. Among the research activities carried out in “OFRALSER”, the use of photocatalytic activity of TiO₂-based materials, may represent an innovation in the postharvest field, due to its high oxidizing capacity, low cost, non-toxicity, chemical robustness and high photostability. Innovative aspects will be achieved throughout the development of TiO₂-based materials, able to prolong postharvest life of fresh products, and in the development of a fluidized bed reactor for the photocatalytic oxidation of ethylene in the atmosphere of cold storage rooms.

The application of TiO₂ as an innovative technique to preserve fresh produce from detrimental effects of ethylene, required preliminary stages to develop and study different materials, in order to select the most effective one. In the first part of this thesis, TiO₂-coated glass beads were developed and tested inside glass reactor at laboratory scale. Several trials were carried out using different ethylene concentrations in the treated gaseous mixture, and different flow-rate in the flow-through system. No reduction were observed, maybe due to the low amount of titanium oxide powder actually attached on the glass marbles. The spherical surface of the glass support did not allow to obtain an uniform layer of photocatalytic powder. Alumina-based TiO₂ material was then developed by the Dept. of Engineering at University of Salento (Lecce, Italy) and subsequently tested at University of Foggia. A maximum ethylene reduction percentage of 60% was evaluated in the closed system. It was possible to notice that the higher the contact time between the C₂H₄-enriched atmosphere and the photocatalytic material, the higher the degradation of the pollutant. However, in any case no differences were observed due to UV light exposure. For this reason it was concluded that this material was able to reduce ethylene by means of adsorption rather than photocatalysis. Mesoporous mixed SiO₂/TiO₂ nanocomposites with different TiO₂

content were synthesized and tested. This material showed a light-dependent oxidant activity in flow-through system as well as in closed one, and the silica, used as support for titanium oxide powder, exerted also its adsorption activity against C_2H_4 , enhancing the photocatalytic action of the material. Material composed by 80% of titanium oxide and 20% of silica (T-SBA 82) had the best activity against ethylene resulting in its complete elimination from the atmosphere. Also in this case the reduction rate increased when the contact time between C_2H_4 and the photocatalyst was prolonged. Moreover, when the photocatalytic nanocomposite were not irradiated with ultraviolet light, it did not show photooxidation activity. T-SBA 82 behavior was comparable with the adsorption capacity of silica alone. To test the mixed material efficacy, an *in vivo* test was performed on tomatoes. Mature green tomatoes were processed with ethylene-enriched mixture treated or not with SiO_2/TiO_2 and UV light. Ethylene photocatalytically destroyed by titanium oxide, reduced ripening trend of the fruits. Concluding, it could be stated that the developed material would be suitable for postharvest handling of whole or fresh-cut fruits and vegetables. In fact, reducing the ethylene surrounding the products, and within packages, it is possible to prolong their shelf-life. During the trials it was demonstrated that using this composite material in closed system, such could be a bag which contain the product, allowed to completely eliminate ethylene. Further studies concerning the effects of the new photocatalytic materials on plant tissues are therefore necessary to develop photooxidative packaging films. In the future, the technological transfer will make this materials suitable for postharvest handling of fresh produce. This innovation will allow to prolong their quality and reducing waste, without an excessive increase in costs.

The last part concerned the design and test of fluidized bed photocatalytic reactor. After the realization, carried out by STC s.r.l. (Mesagne, Italy), fluidization tests on different materials were carried out. Tabular alumina resulted to be not suitable for use as support for titanium oxide in fluidized bed, because of its multiple bed creation and poor propensity for fluidization. Glass beads showed a good fluidization behavior, however, its TiO_2 -coating was demonstrated to be not performant. A good choice seemed to be alumina microspheres, that showed good

fluidization ongoing and may be suitable for use as support for photocatalytic materials. TiO₂-coated microspheres were tested inside the photoreactor in a closed system. However, no reduction was observed during the treatment. The development of materials with high photocatalytic activity to be used in photocatalytic reactors may lead to the replacement of traditional, discontinuous and/or expensive techniques for removal or inhibition of ethylene action during postharvest storage. Using porous alumina microspheres as support and composite powder T-SBA 73 as photocatalytic coating it was possible to reach a maximum reduction percentage of about 72.5%. It was possible to notice, however, that the fluidization regime caused strong collisions between the coated microspheres. As a consequence of this, the powdered coating material tended to separate from its support and tended to block reactor filters with a progressive reduction of the bed height. However, further tests are necessary to develop this active composite material, in order to obtain continuous reduction of ethylene by means of air passage through the photocatalytic fluidized bed.

References

Abe K. and Watada A.E. (1991). Ethylene absorbent to maintain quality of lightly processed fruits and vegetables. *Journal of Food Science*, 56 (6): 1589–1592.

Abeles F.B., Morgan P.W., Saltveit M.E. (1992). Ethylene in Plant Biology, vol. 15, 2nd ed. Academic Press, San Diego, California.

Akiyama S. and Togeda H. (2000). *Hikari shokubai to kanrengijutsu: 21 seikikigyo no technology*. Tokyo, Japan: Nikkankogyo Shimbunsha.

Alberici R.M. and Jardim W.F. (1997). Photocatalytic destruction of VOCs in the gas-phase using titanium dioxide. *Applied Catalysis B: Environmental*, 14: 55.

Alexander L. and Grierson D. (2002) Ethylene biosynthesis and action in tomato: a model for climacteric fruit ripening. *Journal of Experimental Botany*, 53: 2039–2055.

Amodio M.L., Rinaldi R., Colelli G. (2005). Effects of controlled atmosphere and treatment with 1-methylcyclopropene (1-MCP) on ripening attributes of tomatoes. *Acta Horticulturae (ISHS)* 682:737-742.

An T., Chen J., Nie X., Li G., Zhang H., Liu X., Zhao H. (2012). Synthesis of carbon nanotube–anatase TiO₂ sub-micrometer-sized sphere composite photocatalyst for synergistic degradation of gaseous styrene. *ACS Applied Materials & Interfaces*, 4: 5988–5996.

Ao Y.H., Xu J.J., Fu D.G., Shen X.W., Yuan C.W. (2008). Low temperature preparation of anatase TiO₂-coated activated carbon, *Colloids and Surfaces A: Physicochemical and Engineering Aspects*, 312: 125–130.

Argueso C.T., Hansen M. and Kieber J.J. (2007). Regulation of Ethylene Biosynthesis. *Journal of Plant Growth Regulation*, 26:92–105.

Arvanitoyannis I.S. and Oikonomou G. (2012). Active and Intelligent Packaging. In: *Modified Atmosphere and Active Packaging Technologies*. Edited by Ioannis S. Arvanitoyannis. CRC Press Taylor&Francis Group.

Augugliaro V., Bellardita M., Loddo V., Palmisano G., Palmisano L., Yurdakal S. (2012). Overview on oxidation mechanisms of organic compounds by TiO₂ in heterogeneous photocatalysis. *Journal of Photochemistry and Photobiology C: Photochemistry Reviews*, 13: 224– 245.

Augugliaro V., Litter M., Palmisano L., Soria J. (2006). The combination of heterogeneous photocatalysis with chemical and physical operations: A tool for improving the photoprocess performance. *Journal of Photochemistry and Photobiology C: Photochemistry Reviews*, 7:127-144.

Baek M.-H., Yoon J.-W., Hong J.-S., Suh J.-K. (2013). Application of TiO₂-containing mesoporous spherical activated carbon in a fluidized bed photoreactor - Adsorption and photocatalytic activity. *Applied Catalysis A: General*, 450: 222–229.

Bai J.H., Baldwin E.A., Goodner K.L., Mattheis J.P., Brecht J.K. (2005). Response of four apple cultivars to 1-methylcyclopropene treatment and controlled atmosphere storage. *HortScience*, 40: 1534–1538.

Bapat V.A., Trivedi P.K., Ghosh A., Sane V.A., Ganapathi T.R., Nath P. (2010). Ripening of fleshy fruit: Molecular insight and the role of ethylene. *Biotechnology Advances*, 28: 94–107.

Barry C.S., Llop-Tous M.I., Grierson D. (2000). The regulation of 1-aminocyclopropane-1-carboxylic acid synthase gene expression during the transition from system-1 to system-2 ethylene synthesis in tomato. *Plant Physiology*, 123:979–986.

Bathgate, B., Purton, M.E., Grierson, D., Goodenough, P.W. (1985). Plastid changes during the conversion of chloroplasts to chromoplasts in ripening tomatoes. *Planta*, 165: 197–204.

Biard P.F., Bouzaza A., Wolbert D. (2007). Photocatalytic degradation of two volatile fatty acids in an annular plug-flow reactor; kinetic modeling and contribution of mass transfer rate. *Environmental Science and Technology*, 41: 2908.

Bisswanger H. (2002). *Enzyme kinetics: principles and methods*. Wiley-VCH, Weinheim, Germany.

Blankenship S.M., Dole J.M. (2003). 1-Methylcyclopropene: a review. *Postharvest Biol. Technol.* 28: 1–25.

Bodaghi H., Mostofi Y., Oromiehie A., Zamani Z., Ghanbarzadeh B., Costa C., Conte A., Del Nobile M.A. (2013). Evaluation of the photocatalytic antimicrobial effects of a TiO₂ nanocomposite food packaging film by in vitro and in vivo tests. *LWT - Food Science and Technology*, 50: 702-706.

Booth H. S. and Campbell M. B. (1926). Studies of Anesthetic Ethylene: I. The Odor of Ethylene. *Anesthesia and Analgesia*, July–August 1929, pages 221-226.

Bouzayen M., Latché A., Nath P., Pech J.C. (2009). Mechanisms of fruit ripening. In: Pua EC, Davey MR, editors. *Plant Developmental Biology–Biotechnological Perspectives: Vol 1*. Berlin Heidelberg: Springer-Verlag.

Breck D.W. Zeolite Molecular Sieves, Wiley, New York, 1984.

Broun R. and Mayak S. (1981). Aminoxyacetic acid as an inhibitor of ethylenesynthesis and senescence in carnation flowers. *Scientia Horticulturae*, 15(3): 277–282.

Buda A.S., Joyce D.C. (2003). Effect of 1-methylcyclopropene on the quality of minimally processed pineapple fruit. *Australian Journal of Experimental Agriculture*, 43: 177–184.

Burg, S.P., Apelbaum, A., Eisinger, W., Kang, B.G. (1971). Physiology and mode of action of ethylene. *HortScience*, 6: 359-364.

Busca G., Porcile G., Lorenzelli V. (1986). FT-IR studies of unsaturated and aromatic hydrocarbons adsorbed on metal oxide catalysts. *Journal of Molecular Structure*. 141: 395.

Cai C., Xu C., Shan L., Li X., Zhou C., Zhang W., *et al.* (2006). Low temperature conditioning reduces postharvest chilling injury in loquat fruit. *Postharvest Biology and Technology*, 41(3): 252-259.

Cameron, A.C. and Reid M.S. (2001). 1-MCP blocks ethylene-induced petal abscission of *Pelargonium peltatum* but the effect is transient. *Postharvest Biology and Technology*, 22: 169-177.

Candan A.P., Graell J., Larrigaudière C. (2008). Roles of climacteric ethylene in the development of chilling injury in plums. *Postharvest Biology and Technology*, 47: 107–1

Capitani G., Hohenester E., Feng L., Storici P., Kirsch J.F., Jansonius J.N. (1999). Structure of 1-aminocyclopropane-1-carboxylate synthase, a key enzyme in the biosynthesis of the plant hormone ethylene. *Journal of Molecular Biology*, 294(3): 745–56.

Cefola M., Amodio M.L., Rinaldi R., Vanadia S., Colelli G. (2010). Exposure to 1-methylcyclopropene (1-MCP) delays the effects of ethylene on fresh-cut broccoli raab (*Brassica rapa* L.). *Postharvest Biology and Technology*, 58: 29–35.

Çelikel, F. G. and Dodge L.L., Reid M.S. (2002). Efficacy of 1-MCP (1-methylcyclopropene) and Promalin for extending the post-harvest life of Oriental lilies (*Lilium* × ‘Mona Lisa’ and ‘Stargazer’). *Scientia Horticulturae*, 93: 149-155.

Chawengkijwanich C. and Hayata Y. (2008). Development of TiO₂ powder-coated food packaging film and its ability to inactivate *Escherichia coli* in vitro and in actual tests. *International Journal of Food Microbiology* 123: 288–292.

Chen X. and Mao S.S. (2006). Synthesis of titanium dioxide (TiO₂) nanomaterials. *Journal of Nanoscience and Nanotechnology*, 6: 906–925.

Cheng J., Hu P., Ellis P., French S., Kelly G., Lok C.M. (2009). A DFT study of the transition metal promotion effect on ethylene chemisorption on Co(0 0 0 1). *Surface Science*, 603: 2752.

Cho M., Chung H., Choi W., Yoon J. (2004). Linear correlation between inactivation of *E. coli* and OH radical concentration in TiO₂ photocatalytic disinfection. *Water Research*, 38 (4): 1069–1077.

Choi Y.S. and Kim B.W. (2000). Photocatalytic disinfection of *E. coli* in a UV/TiO₂-immobilised optical-fibre reactor. *Journal of Chemical Technology and Biotechnology*, 75 (12): 1145–1150.

Colelli G., Sánchez M.T., Torralbo F.J. (2003). Effects of treatment with 1-methylcyclopropene (1-MCP) on tomato. *Alimentaria* n. 342:67-70.

Cornacchia R., Rinaldi R., Mahjoub M., Colelli G. (2007). The effect of 1-methylcyclopropene (1-MCP) application before and after cutting on the shelf life extension of fresh-cut tomatoes. Proc. V Congreso Iberoamericano de Tecnología Postcosecha y Agroexportaciones, Cartagena (Spain). Pp. 826-834.

Crowe C. T. (2006). *Multiphase flow handbook*. Boca Raton, FL, CRC Press.

Daneshvar N., Salari, D., Khataee A.R. (2004). Photocatalytic degradation of azo dye acid red 14 in water on ZnO as an alternative catalyst to TiO₂. *Journal of Photochemistry and Photobiology A: Chemistry*, 162 (2–3): 317.

Dashliborun A.M., Sotudeh-Gharebagh R., Hajaghazadeh M., Kakooei H., Afshar S. (2013). Modeling of the photocatalytic degradation of methyl ethyl ketone in a fluidized bed reactor of nano-TiO₂/γ-Al₂O₃ particles. *Chemical Engineering Journal*, 226: 59–67.

de Wild J.P.J., Otma E.C., Peppelenbos H.W. (2003). Carbon dioxide action on ethylene biosynthesis of preclimacteric and climacteric pear fruit. *J. Exp. Bot.* 54: 1537–1544.

Dhall R.K. (2013). Ethylene in Post-harvest Quality Management of Horticultural Crops: A Review. *Journal of Crop Science and Technology*, Vol 2, No 2.

Doodeve C. F. and Kitchener J. A. (1938). The mechanism of photosensitisation by solids. *Transactions of the Faraday Society*, 34: 902.

Drahl C. (2008). Palladium's Hidden Talent. *Chemical & Engineering News*, 86(35): 53–56.

Dyer A. (1988). *An Introduction to Zeolite Molecular Sieves*, John Wiley and Sons Press.

Elgar H.J., Woolf A.B. and Bielecki R.L. (1999). Ethylene production by three lily species and their response to ethylene exposure. *Postharvest Biology and Technology*, 16: 257-267.

Elridge R.B. (1993). Olefin/paraffin separation technology: a review. *Industrial & Engineering Chemistry Research*, 32: 2208.

Esguerra E.B., Mendoza J.R., Pantastico E.B. (1978). Regulation of fruit ripening. II. Use of perlite-KMnO₄ insert as an ethylene absorbent. *Philippine Journal of Science*, 107: 23-31.

Fan X., Blankenship S.M., Mattheis J.P., (1999). 1-Methylcyclopropene inhibits apple ripening. *Journal of American Society of Horticultural Science*, 124: 690–695.

Faubion D. and Kader A. (1996). *Perishables Handling Newsletters*, 86: 27–28.

Flores F., El-Yahyaoui F., de Billerbeck G., Romojaro F., Latchè A., Bouzayen M., Pech J.C., Ambid C. (2002). Role of ethylene in the biosynthetic pathway of aliphatic ester aroma volatiles in Charentais Cantaloupe melons. *Journal of Experimental Botany*, 53: 201–206.

Fogler H.S. and Gürmen M.N. (2008). Chapter 12 - Diffusion and Reaction in Porous Catalysts. Professional Reference Shelf. Fogler & Gurmen[©] - University of Michigan. (2008). <http://www.umich.edu/~elements/12chap/html/12prof2a.htm>

Forney C.F., Mattheis J.P., Baldwin E.A. (2009). Effects on flavor. In: Modified and Controlled Atmospheres for the Storage, Transportation, and Packaging of Horticultural Commodities. Edited by Elhadi M. Yahia. CRC Press, Taylor&Francis Group.

Forsyth F.R., Eaves C.A., and Lockhard C.L. (1967). Controlling ethylene levels in the atmosphere of small containers of apples. *Canadian Journal of Plant Science*, 47: 717-718.

Fox M. A. and Dulay M. T. (1993). Heterogeneous photocatalysis. *Chemical Reviews*, 93: 341.

Fujishima A. and Honda K. (1972). Electrochemical photolysis of water at a semiconductor electrode, *Nature*, 238: 37.

Fujishima A. and Zhang X. (2006). Titanium dioxide photocatalysis: present situation and future approaches. *Comptes rendus Chimie*. 9: 750–760.

Fujishima A., Hashimoto K., Watanabe T. (1999). *TiO₂ Photocatalysis Fundamentals and Applications*. Best Knowledge Center (BKC), Tokyo, Japan.

Fujishima A., Honda K. and Kikuchi S. (1969). Photosensitized electrolytic oxidation on semiconducting n-type TiO₂ electrode. *Kogyo Kagaku Zasshi*, 72: 108.

Fujishima A., Rao T.N., Tryk D.A. (2000a). Titanium dioxide photocatalysis. *Journal of Photochemistry and Photobiology C*, 1: 1-21.

Fujishima A., Rao T.N., Tryk D.A. (2000b). TiO₂ photocatalysts and diamond electrodes. *Electrochim. Acta* 45: 4683–4690.

Fujishima A., Zhang X., Tryk D.A. (2007). Heterogeneous photocatalysis: from water photolysis to applications in environmental cleanup. *International Journal of Hydrogen Energy*, 32: 2664–2672.

Fujishima A., Zhang X., Tryk D.A. (2008). TiO₂ photocatalysis and related surface phenomena. *Surface Science Reports*, 63: 515–582.

Garcia-Lopez E., Marci G., Serpone N., Hidaka H. (2007). Photoassisted oxidation of the recalcitrant cyanuric acid substrate in aqueous ZnO suspensions. *Journal of Physical Chemistry C*, 111: 18025–18032.

Giovannoni J. (2001). Molecular biology of fruit maturation and ripening. *Annual Review of Plant Physiology and Plant Molecular Biology*, 52:725– 749.

Gross K.C., Wang C.Y., Saltveit. (2004). The commercial storage of fruits, vegetables and florist and nursery stocks. *USDA Agricultural Handbook 66*. <http://www.ba.ars.usda.gov/hb66/contents.html>

Gulyas H., Bockelmann D., Hemmerling L., Bahnemann D., Sekoulov I. (1994). Treatment of Recalcitrant Organic Compounds in Oil Reclaiming Wastewater by Ozone/Hydrogen Peroxide and UV/Titanium Dioxide *Water Science and Technology*, 29: 129–132.

Haji T., Yaegaki H., Yamaguchi M. (2003). Softening of stony hard peach by ethylene and the induction of endogenous ethylene by 1-aminocyclopropane-1-carboxylic acid (ACC). *Journal of the Japanese Society for Horticultural Science*, 72: 212–217.

Hamilton A.J., Bouzayen, M., Grierson D. (1991). Identification of a tomato gene for the ethylene-forming enzyme by expression in yeast. *Proceedings of the National Academy of Sciences, USA* 88: 7434–7437.

Han, S.S. and Miller J.A. (2003). Role of ethylene in postharvest quality of cut oriental lily 'Stargazer'. *Plant Growth Regulation*, 40: 213-222.

Hashimoto K., Irie H. and Fujishima A. (2005). TiO₂ Photocatalysis: A Historical Overview and Future Prospects. *Japanese Journal of Applied Physics*, Vol. 44, No. 12 pp. 8269–8285.

Hatton T.T. and Reeder W.F. (1972). Quality of 'Lula avocados stored in controlled atmospheres with or without ethylene. *Journal of the American Society for Horticultural Science*, 97: 339-343.

Hegg E.L., Que L.J. (1997). The 2-His-1-carboxylate facial triad. *European Journal of Biochemistry*, 250:625–629.

Herney-Ramirez J., Vicente M.A., Madeira L.M. (2010). Heterogeneous photo-Fenton oxidation with pillared clay-based catalysts for wastewater treatment: A review. *Applied Catalysis B: Environmental*, 98: 10–26.

Hertog M.G., Hollman P.C.H., Katan M. (1992). Content of potentially anticarcinogenic flavonoids of 28 vegetables of 9 fruits commonly consumed in the Netherlands. *Journal of Agricultural and Food Chemistry*, 40: 2379–2383.

Hiwasa K., Kinugasa Y., Amano S., Hashimoto A., Nakano R., Inaba A., Kubo Y. (2003). Ethylene is required for both the initiation and progression of softening in pear (*Pyrus communis* L.) fruit. *Journal of Experimental Botany*, 54: 771–779.

Hoehn E., Prange R.K., Vigneault C. (2009). Storage technology and Application. In: *Modified and Controlled Atmospheres for the Storage, Transportation, and Packaging of Horticultural Commodities*. Edited by Elhadi M. Yahia. CRC Press, Taylor&Francis Group.

Hoffmann M.R., Martin S.T., Choi W., Bahnemann D.W. (1995). Environmental Applications of Semiconductor Photocatalysis. *Chemical Reviews*, 95: 69–96.

Horie Y., Taya M., Tone A. (1998). Evaluation of photocatalytic sterilization rates of *Escherichia coli* cells in titanium dioxide slurry irradiated with various light sources. *Journal of Chemical Engineering of Japan*, 31(4): 577-584.

Hu Q., Fang Y., Yang Y., Ma N., Zhao L. (2011). Effect of nanocomposite-based packaging on postharvest quality of ethylene-treated kiwifruit (*Actinidia deliciosa*) during cold storage. *Food Research International*, 44: 1589–1596.

Huai Q., Xia Y., Chen Y., Callahan B., Li N., Ke H. (2001). Crystal structures of 1-aminocyclopropane-1-carboxylate (ACC) synthase in complex with aminoethoxyvinylglycine and pyridoxal-5'-phosphate provide new insight into catalytic mechanisms. *Journal of Biological Chemistry*, 276(41): 38210–6.

Huang Z., Maness P.C., Blake D.M., Wolfrum E.J., Smolinski S.L., Jacoby W.A. (2000). Bactericidal mode of titanium dioxide photocatalysis. *Journal of Photochemistry and Photobiology. A, Chemistry*, 130 (2–3): 163–170.

Huber D.J. (2008). Suppression of ethylene responses through application of 1-methylcyclopropene: a powerful tool for elucidating ripening and senescence mechanisms in climacteric and nonclimacteric fruits and vegetables. *HortScience*, 43: 106–111.

Hunter D.A., Yi M., Xu X. and Reid M.S. (2004). Role of ethylene in perianth senescence of daffodil (*Narcissus pseudonarcissus* L. 'Dutch Master'). *Postharvest Biology and Technology*, 32: 269- 280.

Hur J.S., Oh S.O., Lim K.M., Jung J.S., Kim J.W., Koh Y.J. (2005). Novel effects of TiO₂ photocatalytic ozonation on control of postharvest fungal spoilage of kiwifruit. *Postharvest Biology and Technology*, 35 (1): 109–113.

Ikeda K., Sakai H., Baba R., Hashimoto K., Fujishima A. (1997) Photocatalytic reactions involving radical chain reactions using microelectrodes, *Journal of Physical Chemistry B*, 101: 2617–2620.

Ilkenhans T., Poulston S. and Smith A. W. J. (2007). Johnson Matthey PLC, *World Appl.* 052, 074.

Inoue T., Fujishima A., Konishi S., Honda K. (1979). Photoelectrocatalytic reduction of carbon dioxide in aqueous suspensions of semiconductor powders. *Nature*, 277: 637–638.

Jańczyk A., Krakowska E., Stochel G., Macyk W. (2006). Singlet oxygen photogeneration at surface modified titanium dioxide. *Journal of the American Chemical Society*, 128: 15574–15575.

Jaymaran K.S., Raju P.S. (1992). Development and evaluation of a permanganate-based ethylene scrubber for extending the shelf-life of fresh fruits and vegetables. *Journal of Food Science and Technology*. 29: 77-83.

Johnson P.R. and Ecker J.R. (1998). The ethylene gas signal transduction pathway: A molecular perspective. *Annual Review of Genetics*, 32: 227–254.

Joyce D.C. and Poole M.C. (1993). Effects of ethylene and dehydration on cut flowering stems of *Verticordia* spp. *Australian Journal of Experimental Agriculture*, 33: 489-493.

Kader A.A. (1995). Regulation of fruit physiology by controlled/modified atmospheres. *Acta Horticulturae*, 398: 59–70.

Kader A.A. (2002). Postharvest Biology and Technology: An Overview. In Kader AA (Ed) *Postharvest Technology of Horticultural Crops*, Pub. 3311, Oakland, CA. pp. 39-47.

Kat S. and Masuo F. (1964). *Kogyo Kagaku Zasshi*, 67: 1136.

Kato S. and Mashio F. (1956). Abtr. Book Annu. Meet. Chemical Society of Japan, p. 223.

Keidel E. (1929). “Die Beeinflussung der Lichtechtheit von Teerfarblacken durch Titanweiss [Influence of titanium white on the fastness to light of coal-tar dyes], *Farben-Zeitung*, vol. 34, pp. 1242–1243.

Kende H. (1993). Ethylene biosynthesis. *Annual Review of Plant Physiology. Plant Molecular Biology*, 44: 283–307.

Kikuchi Y., Sunada K., Iyoda T., Hashimoto K., Fujishima A. (1997). Photocatalytic bactericidal effect of TiO₂ thin films: dynamic view of the active oxygen species responsible for the effect. *Journal of Photochemistry and Photobiology. A, Chemistry*, 106 (1–3): 51– 56.

Kim B., Kim D., Cho D., Cho S. (2003). Bactericidal effect of TiO₂ photocatalyst on selected food-borne pathogenic bacteria. *Chemosphere*, 52 (1): 277–281.

Kim G.H. and Wills R.B.H. (1995). Effect of ethylene on storage life of lettuce. *Journal of the Science of Food and Agriculture*, 69: 197-201.

Kitinoja L. and Kader A.A (2002). Small-Scale Postharvest Handling Practices: A Manual for Horticultural Crops (4th Edition). Post-harvest Horticulture Series No. 8 July 2002, Slightly Revised in November 2003. <http://www.fao.org/docrep/009/ae075e/ae075e21.htm>.

Kudo A., Miseki Y. (2009). Heterogeneous photocatalyst materials for water splitting, *Chemical Society Reviews*, 38: 253–278.

Kuhn K.P., Chaberny I.F., Massholder K., Stickler M., Benz V.W., Sonntag H.G. Erdinger L. (2003). Disinfection of surfaces by photocatalytic oxidation with titanium dioxide and UVA light. *Chemosphere*, 53 (1): 71–77.

Kumar S., Fedorov A.G., Gole J.L. (2005). Photodegradation of ethylene using visible light responsive surfaces prepared from titania nanoparticle slurries. *Applied Catalysis B: Environmental* 57: 93-107.

Li H., Bian Z., Zhu J., Zhang D., Li G., Huo Y., Li H., Lu Y. (2007). Mesoporous titania spheres with tunable chamber structure and enhanced photocatalytic activity. *Journal of the American Chemical Society*, 129: 8406–8407.

Li J., Qu L., Li N (2005). Tyr152 plays a central role in the catalysis of 1-aminocyclopropane-1-carboxylate synthase. *Journal of Experimental Botany*, 56:2203–2210.

Lim T.H. and Kim S.D. (2002). Photocatalytic degradation of trichloroethylene over TiO₂/SiO₂ in an annulus fluidized bed reactor. *Korean Journal of Chemical Engineering*, 19: 1072-1077.

Lim T.H. and Kim S.D. (2004). Trichloroethylene (TCE) degradation by photocatalysis in annular flow and annulus fluidized bed photoreactors. *Chemosphere*, 54: 305-311.

Linsebigler, A.L., Lu G., Yates J.T. (1995). Photocatalysis on TiO₂ Surfaces: Principles, Mechanisms, and Selected Results. *Chemical Reviews*, 95 (3): 735.

Liu B., Nakata K., Sakai M., Saito H., Ochiai T., Murakami T., Takagi K., Fujishima A. (2011). Mesoporous TiO₂ core shell spheres composed of nanocrystals with exposed high-energy facets: facile synthesis and formation mechanism. *Langmuir*, 27: 8500–8508.

Liu M., Piao L., Lu W., Ju S., Zhao L., Zhou C., Li H., Wang W. (2010a). Flower-like TiO₂ nanostructures with exposed {001} facets: facile synthesis and enhanced photocatalysis. *Nanoscale*, 2: 1115–1117.

Liu S., Yu J., Jaroniec M. (2010b). Tunable photocatalytic selectivity of hollow TiO₂ microspheres composed of anatase polyhedra with exposed {001} facets. *Journal of the American Chemical Society*, 132: 11914–11916.

Lougheed E.C. (1987). Interactions of oxygen, carbon dioxide, temperature and ethylene that may induce injuries in vegetables. *HortScience* 22: 791–794.

Maeda K. (2011). Photocatalytic water splitting using semiconductor particles: history and recent developments, *Journal Photochemistry and. Photobiology, C* 12: 237–268.

Maneerat C. and Hayata Y. (2006). Antifungal activity of TiO₂ photocatalysis against *Penicillium expansum* in vitro and in fruit tests. *International Journal of Food Microbiology* 107: 99 – 103.

Maneerat C., Hayata Y., Egashira N., Sakamoto K., Hamai Z., Kuroyanagi M. (2003). Photocatalytic reaction of TiO₂ to decompose ethylene in fruit and vegetable storage. *Transactions of the ASABE*, Vol. 46(3): 725–730.

Maness P.C., Smolinski S., Blake D.M., Huang Z., Wolfrum E.J., Jacoby W.A. (1999). Bactericidal activity of photocatalytic TiO₂ reaction: toward an understanding of its killing mechanism. *Applied Environmental Microbiology*, 65 (9): 4094–4098.

Martínez-Romero D., Guillén F., Castillo S., Zapata P.J., Valero D., Serrano M. (2009). Effect of ethylene concentration on quality parameters of fresh tomatoes stored using a carbon-heat hybrid ethylene scrubber. *Postharvest Biology and Technology*, 51: 206–211.

Matos J., Laine J., Hermann J.M. (2001). Effect of the type of activated carbons on the photocatalytic degradation of aqueous organic pollutants by UV-irradiated titania, *Journal of Catalysis*, 200: 10–20.

Matsunaga T., Tomada R., Nakajima T., Wake H. (1985). Photoelectrochemical sterilization of microbial cells by semiconductor. *FEMS Microbiology Letters*, 29 (1–2): 211–214.

Matsunaga T., Tomada R., Nakajima Y., Nakamura N., Komine T. (1988). Continuous sterilization system that uses photosemiconductor powders. *Applied and Environmental Microbiology*, 54 (6): 1330–1333.

Mattheis J.P., (2008). How 1-methylcyclopropene has altered the Washington State apple industry. *HortScience*, 43: 99–101.

Matthews R. W. (1987). Photooxidation of organic impurities in water using thin films of titanium dioxide. *Journal of Physical Chemistry*, 91: 3328.

Megías Z., Martínez C., Manzano S., Barrera A., Rosales R., Valenzuela J.L., Garrido D., Jamilena M. (2014). Cold-induced ethylene in relation to chilling injury

and chilling sensitivity in the non-climacteric fruit of zucchini (*Cucurbita pepo* L.). *LWT - Food Science and Technology* 57: 194-199.

Moa J., Zhang Y., Xu Q., Lamson J.J., Zhao R. (2009). Photocatalytic purification of volatile organic compounds in indoor air: a literature review, *Atmospheric Environment*, 43: 2229–2246.

Muggli D.S. and Ding L. (2001). Photocatalytic performance of sulfated TiO₂ and Degussa P-25 TiO₂ during oxidation of organics. *Applied Catalysis B: Environmental*, 32(3): 181-194.

Nakata K., Fujishima A. (2012). TiO₂ photocatalysis: Design and applications. *Journal of Photochemistry and Photobiology C*, 13: 169-189.

Nath P., Sane A.P., Trivedi P.K., Sane V.A., Asif M. (2007). Role of transcription factors in regulating ripening, senescence and organ abscission in plants. *Steward Postharvest Review*, 2:1-14.

Nelson R.J., Flakker C.L., Muggli D.S. (2007). Photocatalytic oxidation of methanol using titania-based fluidized beds. *Applied Catalysis B*, 69: 189–195.

Noguchi T., Fujishima A., Sawunyama P., Hashimoto K. (1998). Photocatalytic degradation of gaseous formaldehyde using TiO₂ film. *Environmental Science and Technology*, 32: 3831.

Nosaka A.Y., Kojima E., Fujiwara T., Yagi H., Akutsu H., Nosaka Y. (2003b). Photoinduced changes of adsorbed water on a TiO₂ photocatalytic film as studied by 1H NMR spectroscopy. *Journal of Physical Chemistry B*, 107: 12042–12044.

Nosaka Y., Daimon T., Nosaka A.Y., Murakami Y. (2004). Singlet oxygen formation in photocatalytic TiO₂ aqueous suspension. *Physical Chemistry Chemical Physics*, 6: 2917–2918.

Nosaka Y., Komori S., Yawata K., Hirakawa T., Nosaka A.Y. (2003a). Photocatalytic [radical dot]OH radical formation in TiO₂ aqueous suspension studied by several detection methods. *Physical Chemistry Chemical Physics*, 5: 4731–4735.

Nosaka Y., Nakamura M., Hirakawa T. (2002). Behavior of superoxide radicals formed on TiO₂ powder photocatalysts studied by a chemiluminescent probe method. *Physical Chemistry Chemical Physics*, 4: 1088–1092.

Obee T.N. and Hay S.O. (1997). Effect of moisture and temperature on the photooxidation of ethylene on titania. *Environmental Science and Technology*, 31: 2034–2038.

Obuchi E., Sakamoto T., Nakano K., Shiraishi F. (1999). Photocatalytic decomposition of acetaldehyde over TiO₂/SiO₂ catalyst. *Chemical Engineering Science*, 54: 1525.

Ochiai T. and Fujishima A. (2012). Photoelectrochemical properties of TiO₂ photocatalyst and its applications for environmental purification. *Journal of Photochemistry and Photobiology C: Photochemistry Reviews*, 13: 247– 262.

Oh S.Y., Shin S.S., Kim C.C., Lim Y.J. (1996). Effect of packaging films and freshness keeping agents on fruit quality of ‘Yumyung’ peaches during MA storage. *Journal of Korean Society for Horticultural Sciences*, 37: 781-786.

Park D.-R., Zhang J., Ikeue K., Yamashita H., Anpo M. (1999). Photocatalytic Oxidation of Ethylene to CO₂ and H₂O on Ultrafine Powdered TiO₂ Photocatalysts in the Presence of O₂ and H₂O. *Journal of Catalysis*, 185: 114–119.

Patdhanagul N., Srithanratana T., Rangsiwatananon K., Hengrasmee S. (2010). Ethylene adsorption on cationic surfactant modified zeolite NaY. *Microporous and Mesoporous Materials*, 131: 97–102.

Peiser G. and Suslow T.V. (1998). Factors Affecting Ethylene Adsorption by Zeolite: The Last Word (from us). *Perishables Handling Quarterly Issue No. 95*.

Peiser G.D., Wang T., Hoffman N.E., Yang S.F., Liu H. et al. (1984). Formation of cyanide from carbon 1 of 1-aminocyclopropane-1-carboxylic acid during its conversion to ethylene. *Proceedings of the National Academy of Sciences USA* 81:3059–3063.

Pelayo C., Vilas-Boas E.V. de B., Benichou M., Kader A.A. (2003). Variability in responses of partially ripe bananas to 1-methylcyclopropene. *Postharvest Biology and Technology*, 28: 75–85.

Peral J. and Ollis D.F. (1992). Heterogeneous photocatalytic oxidation of gas-phase organics for air purification: Acetone, 1-butanol, butyraldehyde, formaldehyde, and *m*-xylene oxidation *Journal of Catalysis*, 136: 554.

Pesis E., Ackerman M., Ben-Arie R., Feygenberg O., Feng X.Q., Apelbaum A., et al. (2002). Ethylene involvement in chilling injury symptoms of avocado during cold storage. *Postharvest Biology and Technology*, 24(2): 171-181.

Peternel I.T., Koprivanac N., Bozić A.M., Kusić H.M. (2007). Comparative study of UV/TiO₂, UV/ZnO and photo-Fenton processes for the organic reactive dye

degradation in aqueous solution. *Journal of hazardous materials*, 148(1–2): 477–484.

Picon A., Martinez-Javega J.M., Cuquerella J., Rio M.A.D., Navaroo P. (1993). Effects of precooling, packaging film, modified atmosphere and ethylene absorber on the quality of refrigerated Chandler and Douglas strawberries. *Food Chemistry*, 48: 189-193.

Ponec V., Knor Z., Cerny S. (1974). *Adsorption on solids*. London, England: Butterworth Group.

Redman P.B., Dole J.M., Maness N.O., Anderson J.A. (2002). Postharvest handling of nine specialty cut flower species. *Scientia Horticulturae*, 92: 293-303

Reid M.S. (2002). Ethylene in Postharvest Technology. In Kader AA (Ed) *Postharvest Technology of Horticultural Crops*, Pub. 3311, Oakland, CA. pp. 149-162.

Rupasinghe H.P.V., Murr D.P., Paliyath G., Skog L. (2000). Inhibitory effect of 1-MCP on ripening and superficial scald development in ‘McIntosh’ and ‘Delicious’ apples. *Journal of Horticultural Science and Biotechnology*, 75: 271–276.

Ryu A. (2010). Recent progress on photocatalytic and photoelectrochemical water splitting under visible light irradiation, *Journal of Photochemistry and Photobiology C*, 11: 179–209.

Saito T., Iwase T., Morioka T. (1992). Mode of photocatalytic bactericidal action of powdered semiconductor TiO₂ on mutans streptococci. *Journal of Photochemistry and Photobiology. B, Biology*, 14 (4): 369–379.

Sakai H., Baba R., Hashimoto K., Fujishima A., Heller A. (1995). Local detection of photoelectrochemically produced H₂O₂ with a “Wired” horseradish peroxidase microsensor, *Journal of Physical Chemistry*, 99: 11896–11900.

Saltveit M. E. (1999). Effect of ethylene on quality of fresh fruits and vegetables. *Postharvest Biology and Technology*, 15: 279–292.

Saltveit M.E. (2005). Aminoethoxyvinylglycine (AVG) reduces ethylene and protein biosynthesis in excised discs of mature-green tomato pericarp tissue. *Postharvest Biology and Technology*, 35: 183-190.

Sauer M.L. and Ollis D.F. (1994), Acetone Oxidation in a Photocatalytic Monolith Reactor *Journal of Catalysis*, 149; 81.

Schaller G.E. (2012). Ethylene and the regulation of plant development. *BMC Biology*, 10: 9.

Schotsmans W.C., DeLong J.M., Larrigaudière C., Prange R. (2009). Effects on Physiological disorders. In: *Modified and Controlled Atmospheres for the Storage, Transportation, and Packaging of Horticultural Commodities*. Edited by Elhadi M. Yahia. CRC Press, Taylor&Francis Group.

Scott K.J., Guigni J., Bailey W. (1984). The use of polyethylene bags and ethylene absorbent to extend the life of kiwifruit (*Actinidia chinensis* Planch) during cool storage. *Journal of Horticultural Science*, 50: 563-566.

Scott K.J., McGlasson W.B., Roberts E.A. (1970). Potassium permanganate as an ethylene absorbent in polyethylene bags to delay ripening of bananas during storage. *Australian journal of experimental agriculture and animal husbandry*. 10: 237-240.

Selvarajah S., Bauchot A.D. and John P. (2001). Internal browning in cold-stored pineapples is suppressed by a postharvest application of 1-methylcyclopropene. *Postharvest Biology and Technology*, 23(2): 167-170.

Serek, M. and Trolle L. (2000). Factors affecting quality and postproduction life of *Exacum affine*. *Scientia Horticulturae*, 86: 49-55.

Shiraishi F., Nomura T., Yamaguchi S., Ohbuchi Y. (2007). Rapid removal of trace HCHO from indoor air by an air purifier consisting of a continuous concentrator and photocatalytic reactor and its computer simulation *Chemical Engineering Journal*, 127: 157.

Shukri G. and Kasai H. (2014). Density functional theory study of ethylene adsorption on clean anatase TiO₂ (001) surface. *Surface Science*, 619: 59–66.

Sirisuk A., Hill C.G., Anderson M.A. (1999). Photocatalytic degradation of ethylene over thin films of titania supported on glass rings. *Catalysis Today* 54: 159–164.

Sisler E.C., Blankenship S.M. *Methods of counteracting an ethylene response in plants*, U.S; 1996.

Sisler E.C., Serek M. (1997). Inhibitors of ethylene responses in plants at the receptor level: recent developments. *Physiology Plant*, 100:577–82.

Sisler E.C., Serek M. (2003). Compounds interacting with the ethylene receptor in plants. *Plant Biology*, 5: 473–480.

Sisler, E.C. (2006). The discovery and development of compounds counteracting ethylene at the receptor level. *Biotechnology Advances*, 24: 357–367.

Sisler, E.C., Serek, M. (1999). Compounds controlling the ethylene receptor. *Botanical Bulletin of Academia Sinica*, 40: 1–7.

Smith A.W.J., Poulston S., Rowsell L., Terry L.A., Anderson J.A. (2009). A New Palladium-Based Ethylene Scavenger to Control Ethylene-Induced Ripening of Climacteric Fruit. *Platinum Metals Review*, 53(3): 112–122.

Solano R., Ecker J.R. (1998). Review Ethylene gas: perception, signaling and response. *Current Opinion in Plant Biology*, 1(5):393-8.

Spanu P., Grosskopf D.G., Felix G., Boller T. (1994). The apparent turnover of 1-aminocyclopropane-1-carboxylate synthase in tomato cells is regulated by protein-phosphorylation and dephosphorylation. *Plant Physiology*, 106: 529–535.

Srivastava N.C. and Eames I.W. (1998). A review of adsorbents and adsorbates in solid vapour adsorption heat pump systems. *Applied Thermal Engineering* 18: 707-714.

Stepanova A.N., Alonso J.M. (2009). Ethylene signaling and response: where different regulatory modules meet. *Current Opinion in Plant Biology*, 12, 548–555.

Stepanova A.N., Ecker J.R. (2000). Review Ethylene signaling: from mutants to molecules. *Current Opinion in Plant Biology*, 3(5):353-60.

Sunada K., Kikuchi Y., Hashimoto K. and Fujishima A. (1998). Bactericidal and detoxification effects of TiO₂ thin film photocatalysts. *Environmental Science & Technology*, 32: 726.

Sunada K., Watanabe T. and Hashimoto K. (2003). Bactericidal activity of copper deposited TiO₂ thin film under weak UV light illumination. *Environmental Science & Technology*, 37: 4785.

Surajit K., Andrei G.F., James L.G. (2005). Photodegradation of ethylene using visible light responsive surfaces prepared from titania nanoparticle slurries. *Applied Catalysis B: Environment*, 57: 93–107.

Suslow T. (1997). *Perishables Handling Quart.* 92 (1997) 32–33.

Suzuki K.I. (1993). Photocatalytic air purification on TiO₂-coated honeycomb support. In *Photocatalytic Purification and Treatment of Water and Air*, 421-434. D.F. Ollis and H. Al-Ekabi, eds. Oxford, U.K.: Elsevier Science.

Terry L.A., Ilkenhans T., Poulston S., Rowsell L., Smith A.W.J. (2007). Development of new palladium-promoted ethylene scavenger. *Postharvest Biology and Technology*, 45: 214–220.

Tiaz, L. and E. Zeiger (2002). *Plant Physiology: Third Edition*. Sinauer Associates Inc. Sunderland, MA.

Tibbitts T.W., Cushman K.E., Fu X., Anderson M.A., Bula R.J. (1998). Factors controlling activity of zirconia–titania for photocatalytic oxidation of ethylene. *Advances in Space Research*, 22: 1443–1451.

Tsuji J. (2004). Palladium reagents and catalysts: new perspectives for the 21st century. John Wiley and Sons. p. 90.

U.S. EPA, Argonne National Laboratory, and the U.S. Army Corps of Engineers. The Brownfields and Land Revitalization Technology Support Center. "Glossary". Retrieved 2009-12-21.

USDA. 1991. U.S. Standards for Grades of Fresh Tomatoes. USDA, Agr. Mktg. Serv., Washington, DC.

Veen H. (1979). Effects of silver on Ethylene synthesis and action in cut carnations, *PLANTA*, 145: 467-470.

Vilas-Boas E.V. de B., Kader A.A. (2006). Effect of atmospheric modification, 1-MCP and chemicals on quality of fresh-cut banana. *Postharvest Biology and Technology*, 39: 155–162.

Vilas-Boas E.V. de B., Kader A.A. (2007). Effect of 1-methylcyclopropene (1-MCP) on softening of fresh-cut kiwifruit, mango and persimmon slices. *Postharvest Biology and Technology*, 43: 238–244.

Vincent G., Queffeuilou A., Marquaire P., Zahraa O. (2007). Remediation of olfactory pollution by photocatalytic degradation process: study of methyl ethyl ketone (MEK). *Journal of Photochemistry and Photobiology A*, 191: 42–50.

Wang K.L.C., Li H., Ecker J.R. (2002). Ethylene Biosynthesis and Signaling Networks. *The Plant Cell*, S131–S151, Supplement 2002, www.plantcell.org © 2002 American Society of Plant Biologists.

Wang L.W., Wang R.Z., Oliveira R.G. (2009). A review on adsorption working pairs for refrigeration. *Renewable and Sustainable Energy Reviews*, 13: 518–534.

Wang R., Hashimoto K., Fujishima A., Chikuni M., Kojima E., Kitamura A., Shimohigoshi M., Watanabe T. (1997). Light-induced amphiphilic surfaces. *Nature* 388: 431–432.

Wang W.C. (1990). *Chilling Injury in Horticultural Crops*. CRC Press, Boca Raton, FL.

Wang X., Liu Y., Hu Z., Chen Y., Liu W., Zhao G. (2009). Degradation of methyl orange by composite photocatalysts nano-TiO₂ immobilized on activated carbons of different porosities. *Journal of Hazardous Materials*, 169: 1061–1067.

Warton M.A., Ku V.V.V., Wills R.B.H. (2001). Ethylene levels associated with fruit and vegetables during marketing. *Australian Journal of Experimental Agriculture*, 40: 460–465.

Watanabe N., Horikoshi S., Hidaka H., Serpone N. (2005). On the recalcitrant nature of the triazinic ring species, cyanuric acid, to degradation in Fenton solutions and in UV-illuminated TiO₂ (naked) and fluorinated TiO₂ aqueous dispersions. *Journal of Photochemistry and Photobiology A: Chemistry*. 174: 229–238.

Watkins C.B. (2002). Ethylene synthesis, mode of action, consequences and control. In: Knee M, editor. *Fruit quality and its biological basis*. Boca Raton, Florida: Sheffield Academic Press, p. 180-224.

Watkins C.B. (2006). The use of 1-methylcyclopropene (1-MCP) on fruits and vegetables. *Biotechnology Advances*, 24: 389–409.

Watkins C.B. (2008). Overview of 1-methylcyclopropene trials and uses for edible horticultural crops. *HortScience* 43: 86–94.

Watkins C.B., Nock J.F., Whitaker B.D. (2000). Responses of early, mid and late season apple cultivars to postharvest application of 1-methylcyclopropene (1-MCP) under air and controlled atmosphere storage conditions. *Postharvest Biology and Technology*, 19: 17–32.

Wawrzyńczak A. and Goszczyńska D.M. (2003). Effect of ethylene inhibitors on longevity of cut carnations (*Dianthus caryophyllus* L.) and ethylene production by flowers. *Journal of Fruit and Ornamental Plant Research*, 11: 89-98.

Wei C., Lin W.Y., Zaina Z., Williams N.E., Zhu K., Kruzic A.P., Smith R.L., Rajeshwar K. (1994). Bactericidal activity of TiO₂ photocatalyst in aqueous media: toward a solar-assisted water disinfection system. *Environmental Science and Technology*, 28 (5): 934– 938.

Wild B.L., McGlasson W.B., Lee T.H. (1976). Effect of reduced ethylene levels in storage atmospheres on lemon keeping quality. *Hort-Science*, 11: 114-115.

Wills R.B.H. and Kim G.H. (1995). Effect of ethylene on postharvest life of strawberries. *Postharvest Biology and Technology*, 6: 249-255.

Wills R.B.H. and Warton M.A. (2004). Efficacy of Potassium Permanganate Impregnate into Alumina Beads to Reduce Atmospheric Ethylene. *Journal of American Society of Horticultural Science*, 129(3): 433-438.

Wills R.B.H., Warton M.A., Mussa D.M.D.N., Chew L.P. (2001). Ripening of climacteric fruits initiated at low ethylene levels. *Australian Journal of Experimental Agriculture*, 41: 89–92.

Wist J., Sanabria J., Dierolf J., Torres C., Pulgarin W. (2002). Evaluation of photocatalytic disinfection of crude water for drinking-water production. *Journal of Photochemistry and Photobiology. A, Chemistry*, 147 (3): 241– 246.

Wu C.H., Chang C.L. (2006). Decolorization of Reactive Red 2 by advanced oxidation processes: Comparative studies of homogeneous and heterogeneous systems. *Journal of hazardous materials*, 128(2–3): 265–272.

Xiang Q., Yu J., Jaroniec M. (2011). Tunable photocatalytic selectivity of TiO₂ films consisted of flower-like microspheres with exposed {001} facets. *Chemical Communications*, 47: 4532–4534.

Xing Y., Li X., Zhang L., Xu Q., Che Z., Li W., Bai Y., Li K. (2012). Effect of TiO₂ nanoparticles on the antibacterial and physical properties of polyethylene-based film. *Progress in Organic Coatings*, 73: 219– 224.

Yamazaki S., Tsukamoto H., Araki K., Tanimura T., Tejedor-Tejedor I., Anderson M.A. (2001). Photocatalytic degradation of gaseous tetrachloroethylene on porous TiO₂ pellets. *Applied Catalysis B: Environmental*, 33: 109.

Yang R., Zhang Y., Xu Q., Mo J. (2007). A mass transfer based method for measuring the reaction coefficients of a photocatalyst. *Atmospheric Environment*, 41: 1221.

Yang S.F. (1987). The role of ethylene and ethylene synthesis in fruit ripening. In: Thomson, W.W., Nothnagel,

Yang W. C. (Ed.). (2003). *Handbook of fluidization and fluid-particle systems*. CRC Press.

Yang S.F. and Hoffman N.E. (1984). Ethylene biosynthesis and its regulation in higher-plants. *Annual Review of Plant Physiology. Plant Molecular Biology*, 35: 155–189.

Ye S.-Y., Fang Y.-C., Song X.-L., Luo S.-C., Ye L.-M. (2013). Decomposition of ethylene in cold storage by plasma-assisted photocatalyst process with TiO₂/ACF-based photocatalyst prepared by gamma irradiation. *Chemical Engineering Journal*, 225: 499–508.

Ye S.-Y., Tian Q.-M., Song X.-L., Luo S.-C. (2009). Photoelectrocatalytic degradation of ethylene by a combination of TiO₂ and activated carbon felts. *Journal of Photochemistry and Photobiology A: Chemistry* 208: 27–35.

Yue P.L. and Khan F. (1983). Photocatalytic ammonia synthesis in a fluidized bed reactor. *Chemical Science and Engineering*, 38: 1893-1900.

Zhang Y.H. (1989). Adsorption function. Shanghai, China: Publishing House of Scientific and Technological Literature in Shanghai.

Zhang Y.P., Yang R., Xu Q.J., Mo J.H. (2007). Characteristics of photocatalytic oxidation of toluene, benzene, and their mixture. *Journal of the Air & Waste Management Association*, 57: 94.

Zhang Z., Ren J.S., Clifton I.J., Schofield C.J. (2004). Crystal structure and mechanistic implications of 1-aminocyclopropane-1-carboxylic acid oxidase--the ethylene-forming enzyme. *Chemistry and Biology*, 11(10): 1383–94.

Zheng Z., Huang B., Qin X., Zhang X., Dai Y. (2010). Strategic synthesis of hierarchical TiO₂ microspheres with enhanced photocatalytic activity. *Chemistry - A European Journal*, 16: 11266–11270.

Zheng Z., Huang B., Qin X., Zhang X., Dai Y., Jiang M., Wang P., Whangbo M.-H. (2009). Highly efficient photocatalyst: TiO₂ microspheres produced from TiO₂ nanosheets with a high percentage of reactive {001} facets. *Chemistry - A European Journal*, 15: 12576–12579.

Zhong J., Wang J., Tao L., Gong M., Zhimin L., Chen Y. (2007). Photocatalytic degradation of gaseous benzene over TiO₂/Sr₂CeO₄: Preparation and photocatalytic behavior of TiO₂/Sr₂CeO₄. *Journal of Hazardous Materials*, 139: 323.

Zorn M.E., Tompkins D.T., Zeltner W.A., Anderson M.A. (1999) Photocatalytic oxidation of acetone vapor on TiO₂/ZrO₂ thin films. *Applied Catalysis B: Environmental*, 23: 1.

Zuliana R., Boyce A.N., Nair H., Chandran S. (2008). Effects of aminooxyacetic acid and sugar on the longevity of pollinated *Dendrobium* Pompadour. *Asian Journal of Plant Sciences*, 7(7): 654–659. Retrieved 2011-05-18.